Chapter 4

Sedimentary Basin Analysis

by

John M. Armentrout

John M. Armentrout

John Armentrout is involved in integrated stratigraphic interpretation at Mobil Oil Corp.'s Dallas Technology Center. He received his BS in biology (1964) and MS in geology (1967) from the University of Oregon. He later attended the University of Washington where he received his Ph.D. in geology. After earning his doctorate, John joined Mobil's Alaskan Exploration Group. Subsequent assignments have included production geology, global basin analysis, deepwater clastics, and new exploration ventures. He is also actively involved in professional societies and has served as vice-president of the Dallas Geological Society, president of the Gulf Coast Section SEPM, president of the Society of Sedimentary Geology, 1991 SEPM technical program chair, and 1997 SEPM vice-chair for the AAPG annual meeting hosted by the Dallas Geological Society. His teaching/lecturing experience includes offering an SEPM course on integrated stratigraphic analysis, being named an AAPG Distinguished Lecturer, and being appointed a National Research Council Post-Doctoral Research Associate with the USGS. John's recent publications include papers on Gulf of Mexico Neogene sequence stratigraphy and hydrocarbon geochemistry; sequence stratigraphy of active margin basins in Oregon, Washington, Trinidad, China, and India; and Neogene biostratigraphy and petroleum systems of the Niger Delta.

Overview

Introduction

Sedimentary basin analysis involves studying the history of sediment accumulation within depocenters and the tectonic processes that create the basin depression, influence the distribution of sediments, and deform the contained rocks. Aspects of basin analysis, as presented in this chapter, focus on several scales:

- Plate tectonic/basin—geographic area of crustal subsidence and its sedimentary fill
- Subbasin depocenter—locus of sediment accumulation
- Depositional sequence—sediment accumulated during one depositional cycle
- Local basins—local structural and stratigraphic compartments within a depocenter

Understanding the local basin—achieved through integrating stratigraphic, structural, biostratigraphic, and geochemical data—is the critical scale of basin analysis for petroleum system identification. Reconstructing a basin's history, from regional tectonic setting to a single local basin, provides the geologic framework for defining exploration plays and prospects.

Example: Gulf of Mexico basin

Throughout this chapter, the Gulf of Mexico (GOM) basin is used as the example of sedimentary basin analysis and the relationship of basin analysis to defining essential elements and processes of the petroleum system. By using only one example, the reader should be better able to focus on the process of data integration, which can be adapted or modified for other basin types. Aspects of plate tectonics and depositional history are used to define several scales of subbasinal entities and their relationship to petroleum source and reservoir rocks. A history of progressive growth faulting and salt mobility controls the formation of potential traps, the locus of sediment transport and accumulation, and potential avenues of hydrocarbon migration and accumulation.

The chapter progresses from largest scale to smallest scale (Figure 4–1). It begins with the entire GOM basin and concludes with a case history of the East Breaks minibasin petroleum system. The East Breaks minibasin is an example of play and prospect definition within the context of a subregional petroleum system within one subprovince of the GOM Tertiary basin.

In this chapter

This chapter contains the following sections.

Index maps for GOM example

The figure below is a series of index maps for the GOM basin analysis example used in this chapter. Each map represents a different scale of sedimentary basin analysis, beginning with the largest (the GOM basin) and progressing to the smallest (the East Breaks minibasin).

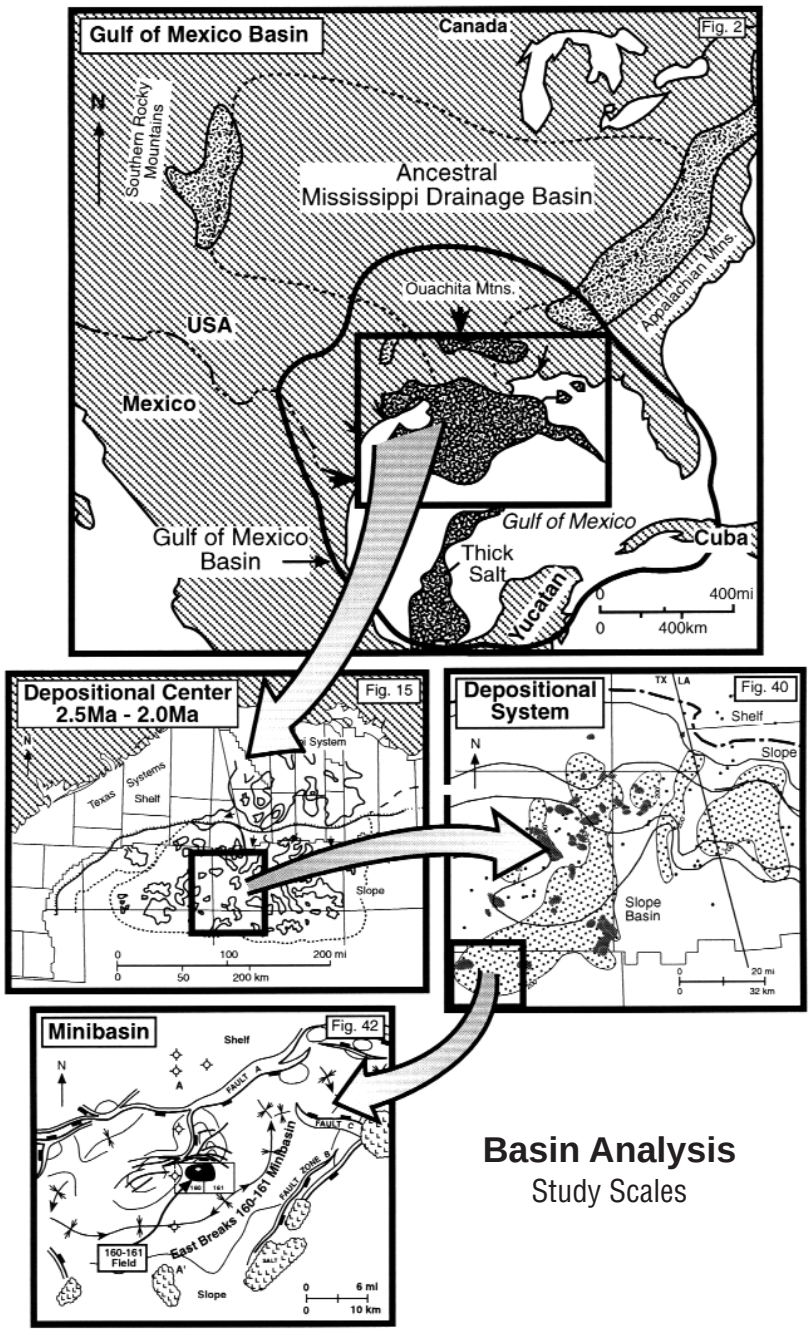

Figure 4–1.

Section A
Basin Framework

Introduction

A sedimentary basin consists of a geographic area of crustal subsidence in which sediment accumulates. A basin may have several episodes of subsidence, sediment accumulation, and deformation, and each episode may have a slightly different geographic extent. Thus, the area of the basin referred to in present-day terms may have a different context at specific times in the geologic past.

This section explains how to analyze the basin from the large-scale perspective. In subsequent sections, the GOM basin will be examined by stepping down through three levels to arrive at individual fields and prospects.

Development of basin history results from integrating bits and pieces of knowledge gathered over decades of study. The GOM basin example presented here evolved along that pathway from the study of local elements gathered together in ever-larger areas of analysis until basinwide and plate tectonic models had been constructed. The presentation of a relatively complete basin interpretation glosses over this historical pathway. In studying this overview of the present-day understanding of the GOM Tertiary basin's history, you may be able to more quickly assemble the essential elements of less-well-understood basins.

In this section

This section contains the following topics.

Subsection A1

Defining the Basin Framework

Introduction

Defining the basin framework is a process that includes the following:

- Outlining a basin's boundaries
- Characterizing its tectonostratigraphic evolution
- Mapping total sediment thickness
- Identifying sand-prone depocenters
- Locating age and location of oil and gas fields
- Establishing their geologic age and hydrocarbon types
- Delineating the occurrence of probable hydrocarbon source rocks

The resulting maps serve as the foundation for subsequent, more detailed analyses of the basin. Depending on the basin in question, this information may be available from the literature, from commercially available petroleum studies, and from oil company files. In some basins the data may be lacking. The first step in basin analysis is to gather all of the information available for the area of study, carefully identifying observation vs. interpretation.

In this subsection

This subsection contains the following topics.

How to Define the Framework of a Basin

The term "basin"

The term "basin" has different meanings in different disciplines. Stratigraphers refer to a basin as the location of sedimentary fill deposited in the geologic past. Structural geologists think of a basin as a container created by tectonic processes, such as rifting. Often the term is used to name and locate a geographic province, such as the Williston basin, which in turn is separate from the genetic use of basin to mean a sedimentary basin—the focus of this chapter.

Defining the basin framework

To define a basin, we follow the steps listed in the table below.

Step	Action
1	Define the outline of the basin and important regional structural features.
2	Map total sediment thickness.
3	Identify subbasins (depocenters and minibasins).
4	Map age and location of oil and gas fields.
5	Map age and location of source rocks.

Basin outline and structural features

The particular study area, whether only a part of a basin or an entire basin itself, should be identified on a large-scale geographic map using total sediment thickness as the primary control. We then map major regional structural features. If postdepositional deformation has resulted in erosion, we construct a paleogeographic restoration to approximate the original depositional basin outline (see section D2, Paleogeography).

Basins, depocenters, and minibasins

The interaction of the eustatic cycles of sediment accumulation within geographically shifting regional depocenters results in a complex stratigraphic architecture later deformed by tectonic movement. This deformation results in the formation of subbasins, depocenters, and minibasins. Minibasins in the GOM basin are relatively small areas of sedimentary thicks bounded by faults and salt-cored highs. We subdivide the basin into depocenters by identifying age-specific sediment thicks. We then subdivide depocenters into minibasins by identifying areas within the depocenter isolated by structure.

Subbasin sediment thickness, location

Each basin consists of a number of subbasin elements that have significant impact on exploration for hydrocarbons within each of these subbasins. We can prepare (or locate) a map showing total sediment thickness and the distribution of hydrocarbon occurrences within each subbasin element.

Source age, location

Hydrocarbon types reflect the composition of the kerogens from which they were generated and provide an estimate of the potential number of source-rock intervals or variations of kerogen facies within a source rock. We can prepare or locate a map showing the distribution of hydrocarbon types.

Example: Defining a Basin Outline

Discussion

The GOM basin includes strata beneath the present-day Gulf of Mexico and extends onshore beneath the Gulf coastal plain of Mexico and the United States. Sediment is supplied primarily by fluvial systems draining the ancestral Mississippi River system and smaller river systems draining the Rocky, Ouachita, and Appalachian mountain ranges. Lesser amounts of carbonate sediments are produced locally by biochemical processes. Critical to the understanding of the GOM basin history and the associated petroleum systems of the northern Gulf of Mexico is the interaction of the Cretaceous–Holocene Mississippi drainage basin and thick salt deposited during the Jurassic.

The figure below shows the geographic distribution of the Neogene Mississippi River drainage basin and distribution of the primary fluvial input systems (arrows). It also shows the interpreted limits of thick Jurassic salt (>1.5 km). The geographic shifts of primary fluvial input have resulted in depocenters of different ages across the GOM Tertiary basin.

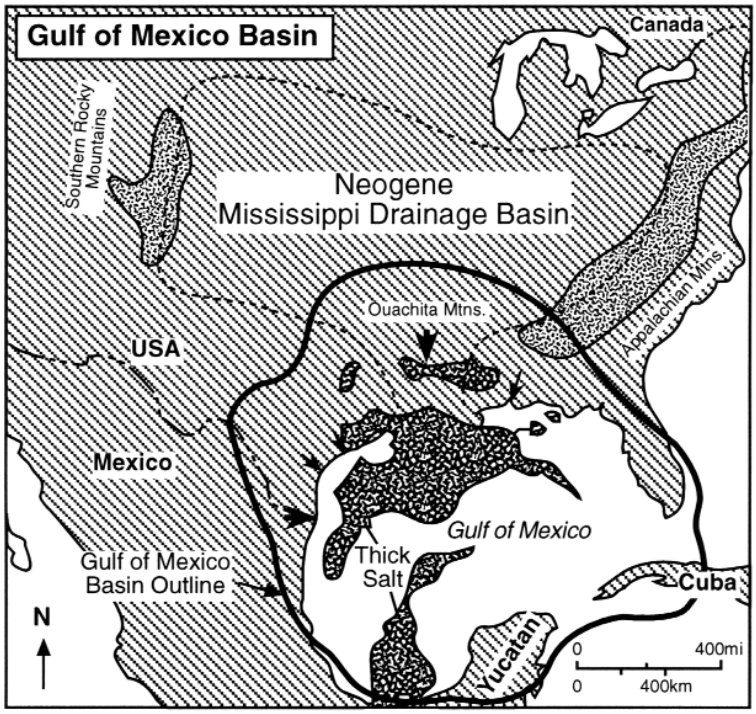

Figure 4–2. Modified after Winker and Buffler (1988); courtesy AAPG.

Example: Mapping Sediment Thickness and Field Location

Discussion

A map of the sediment thickness (isopach) and occurrence of hydrocarbons is an initial step in identifying the petroleum system(s) of a basin. The figure below shows the total Jurassic to Recent sediment thickness and hydrocarbon occurrences in the GOM basin The hydrocarbon occurrences are concentrated in reservoir rocks that range in age from Jurassic to Pleistocene along the northern margin of the basin in the area over transitional crust and thick salt accumulations. Identification of specific subbasinal depocenters within the area of hydrocarbon occurrences is shown in Figure 4–4. Hydrocarbon types reflect the composition of the kerogens from which they were generated and provide an estimate of the potential number of source rocks within the area (see Figure 4–5).

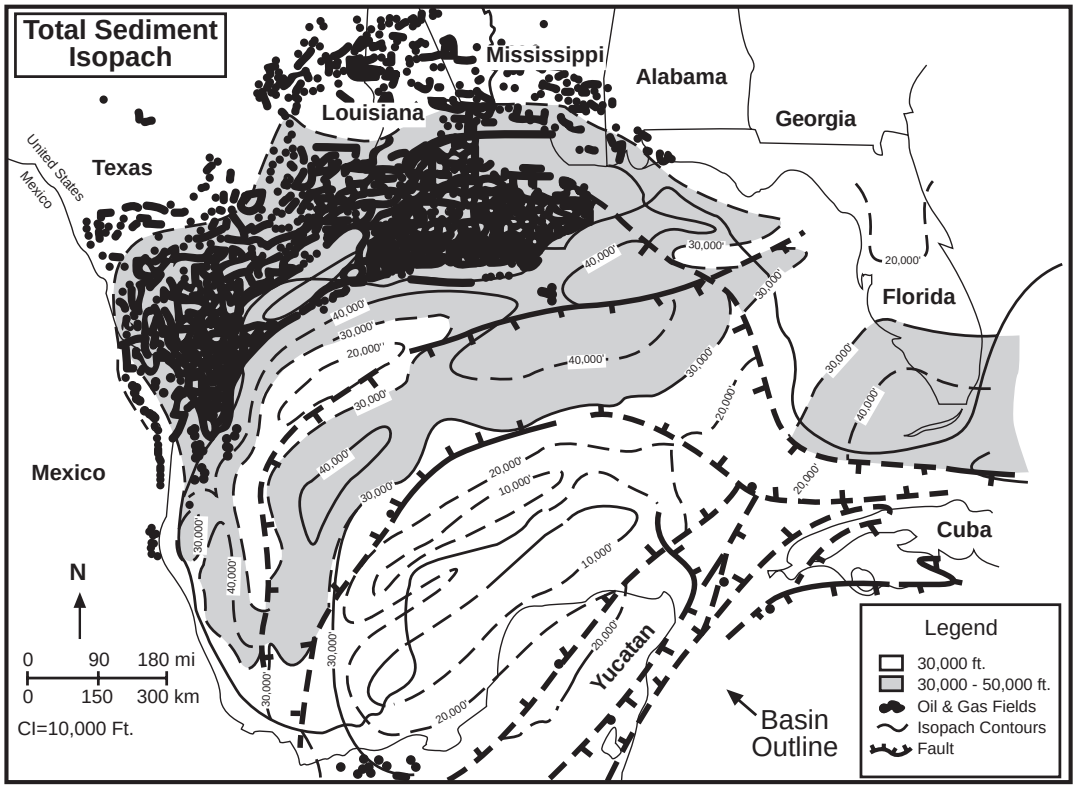

Figure 4–3. From Winker and Buffler (1988); courtesy AAPG.

Example: Mapping Sediment Thickness and Field Location, continued

Map of major sand influxes

Major influxes of sand into the northern GOM margin have shifted laterally from the Late Cretaceous to Recent (Winker, 1982). Each of these depocenters is related to the progressive filling of the basin margin, shifting the accommodation space basinward. Accommodation space refers to the volume of space available for sediment accumulation—the space resulting from the interaction of tectonic subsidence or uplift, sea level change, and compaction of the underlying sediment. Additionally, the lateral shift of the fluvial systems is recorded by sand-prone facies that document both the primary input area and the lateral shift of the depocenter through time.

Many of these lateral shifts result from tectonic events along the basin margin or within the drainage basins themselves (Galloway, 1989a). The lateral shift of the fluvial-deltaic systems is also reflected in the lateral shift of the gravity-flow depositional systems on the slope and basin floor (see Feng and Buffler, 1994).

The map below shows major sand influxes into the northern Gulf of Mexico from Late Cretaceous to Recent. Each area of sand-prone sediment provides age-specific potential reservoirs within these fluvial-deltaic depositional systems.

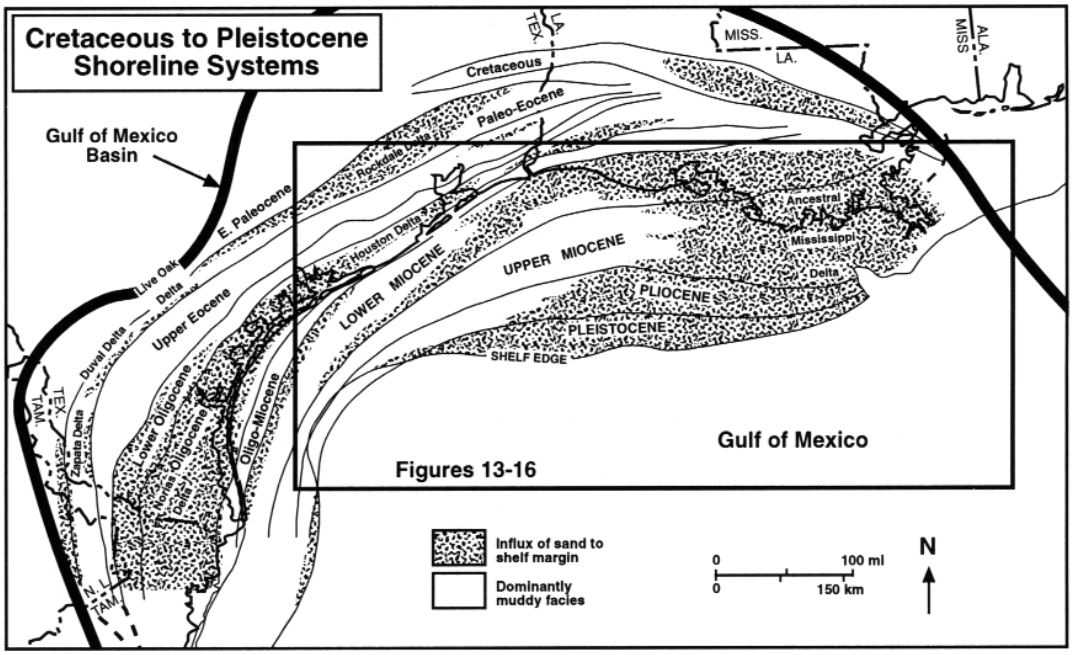

Figure 4–4. After Winker (1982); courtesy Gulf Coast Association of Geological Societies.

Example: Mapping Hydrocarbon Types

Discussion

Hydrocarbon types reflect the composition of the kerogens from which they were generated. Kerogens are the insoluble organic matter in sedimentary rocks. Maps of hydrocarbon types estimate the number and distribution of mature generating source rocks. The following map of hydrocarbon types is based on analyses of more than 2000 oil, 600 gas, and 1200 seep samples correlated to specific source rocks. Nine oil–source-rock families have been identified (labeled 1–9; see table on following page), each having a specific geographic distribution related to mature source-rock location and migration paths. We will focus on the High Island–East Breaks area, where families 1 and 6 overlap (bold arrow).

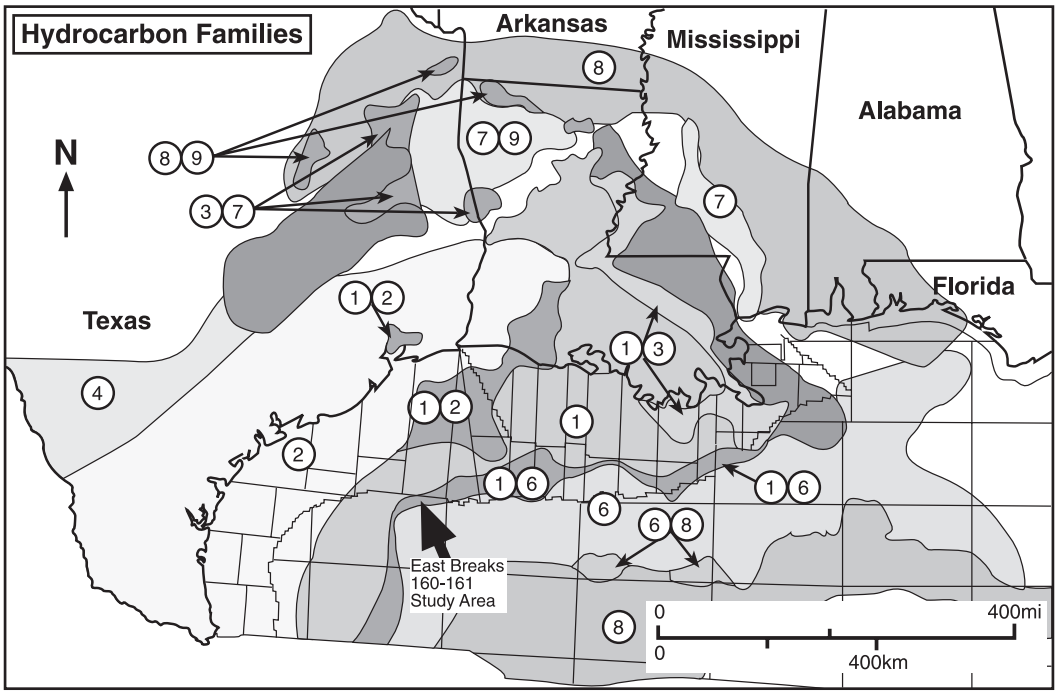

Figure 4–5. Modified from Gross et al. (1995).

Example: Mapping Hydrocarbon Types, continued

Source table

The table below, modified from Gross et al. (1995), lists source-rock ages, oil types, and map numbers for Figure 4–5.

Source-Rock Age	Oil Type	Map #
Lower Tertiary (centered on Eocene, ~50–40 Ma)	Tertiary marine[1] Tertiary intermediate[1] Tertiary terrestrial	① ① ②
Upper Cretaceous (centered on Turonian, ~85–95 Ma)	Marine; low sulfur; no Tertiary influence Calcareous; moderate sulfur; no Tertiary influence[2]	③ ④
Lower Cretaceous (centered on Aptian, ~115–105 Ma)	Carbonate; elevated salinity; Lower Cretaceous Calcareous; moderate sulfur; Lower Cretaceous[2]	⑤ ④
Uppermost Jurassic (centered on Tithonian, ~140–130 Ma)	Marine; high sulfur; Jurassic[3] Marine; moderately high sulfur; Jurassic[3] Marine; moderate sulfur; Jurassic[3] Calcareous; Upper Jurassic or Lower Cretaceous?	⑥ ⑥ ⑥ ⑦
Upper Jurassic (Oxfordian, ~ 152–145 Ma)	Carbonate; elevated salinity; Jurassic[4]	⑧
Triassic (Eagle Mills, > 210 Ma)	Triassic; lacustrine	⑨

[1]Tertiary marine and Tertiary intermediate are mapped together.

[2]Calcareous–Moderate Sulfur–No Tertiary Influence and Calcareous–Moderate Sulfur–Lower Cretaceous are mapped as an undifferentiated unit.

[3]Oil subtypes related to variations in sulfur content and associated geochemical parameters have not been subdivided on Figure 4–5.

[4]Oil subtypes reflecting differences in salinity and clastic input to source facies are known but are not delineated on Figure 4–5.

Summary

By overlaying maps of total overburden thickness above major source-rock intervals, thermally mature source-rock distribution, hydrocarbon occurrences, and major structural features, the regional elements of the petroleum system(s) begin to emerge.

Subsection A2

Assessing the Impact of Tectonics

Introduction

Plate tectonics provides an excellent starting point from which to analyze a basin because plate interactions probably created the basin. Global processes and previous plate positions are understood well enough to place almost any basin into its relative geographic position during the 570 m.y. of the Phanerozoic (Golonka et al., 1993).

Procedure

To unravel tectonostratigraphic phases of a basin, follow the steps listed in the table below and detailed in this section.

Step	Action
1	Assemble a regional tectonic map of the basin and surrounding area.
2	Make regional structure cross sections.
3	Determine plate tectonic evolution and history.
4	Develop a model of tectonostratigraphic phases of the basin that incorporates important tectonic and stratigraphic features.
5	Develop a model of the tectonic history of the basin.
6	Illustrate the tectonostratigraphic phases of the model using a series of cross sections restored to critical stages in the basin's history.
7	Determine the impact of tectonic evolution on petroleum system evolution.

In this subsection

The following topics are covered in this subsection.

Making Regional Tectonic Maps

Introduction

Tectonic maps of a basin and surrounding areas, in combination with regional structure cross sections, give an overall impression of the geologic architecture of the basin and form the base from which other interpretations are made. A large-scale map shows the depth to the basement in the basin and the distribution of crustal types. Always be sure important tectonic elements are shown, such as specific fold belts and major faults.

Tectonic map

The figure below is a tectonic map of the GOM basin. It shows the following:

- Generalized depth to basement (approximately the base of Jurassic sedimentary rock)
- Distribution of four crustal types—continental, thick transitional, thin transitional, and oceanic
- Known distribution of mid-Jurassic evaporites (pre-marine evaporites)
- Several major structural features

The thickest sediments occur over the thin transitional crust, which has subsided beneath the load of more than 14 km (>45,000 ft) of sedimentary rock. (For additional discussion of the structural framework, see Jones and Freed, 1996.)

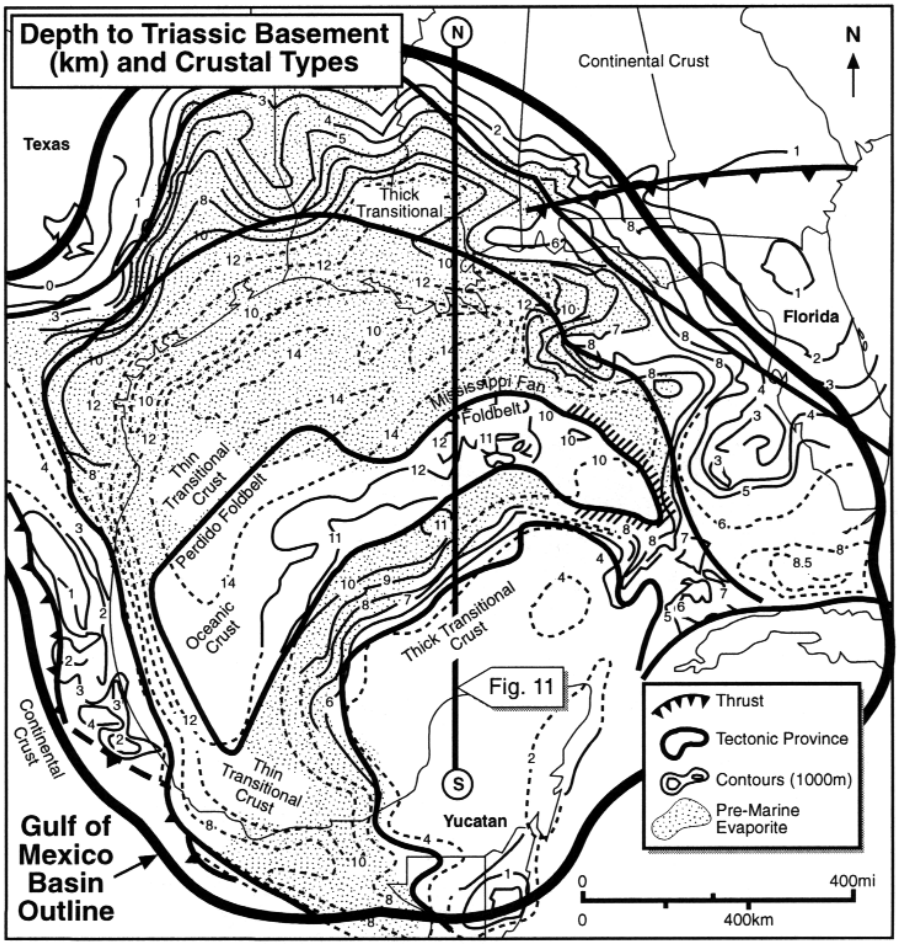

Figure 4–6. Modified from Buffler (1991); courtesy New Orleans Geological Society.

Salt tectonic map

The stratigraphic and tectonic history of the GOM basin is strongly affected by salt tectonics. As a consequence of differential loading of salt by sediment sourced from the North American craton, the distribution of salt-cored structures is oldest in the onshore northern margin of the basin where Late Cretaceous and early Cenozoic progradation resulted in salt-structure growth.

Offshore beneath GOM waters, evacuation of salt structures is oldest in the north and is progressively younger toward the south. However, there are Late Jurassic and Early Cretaceous salt-cored structures along the Sigsbee Escarpment. Pliocene and Pleistocene depositional loading has displaced salt basinward and differentially loaded detached salt sills into salt-cored massifs and salt-cored diapirs.

The salt-withdrawal synclines formed by sediment loading result in bathymetric lows that serve as sediment transport pathways down the slope (Bouma, 1982). The present-day sea-floor bathymetry of the northern Gulf of Mexico slope reflects this transport-pathway lineation of salt-withdrawal synclines bordered by salt-cored anticlines (see Figure 4–41). The distribution of the sediment-thick synclines and salt-core anticlines persists through time, resulting in predictability of sediment transport avenues, depositional areas of potential reservoir sands, and conduits from deeply buried source rocks upward to the hydrocarbon traps (see Figures 4–54 and 4–55).

McGuinness and Hossack (1993) present an excellent discussion of palinspastic reconstruction of the stratigraphic record disrupted by salt tectonics. Jackson et al. (1995) and Simmons et al. (1996) present a good discussion of salt distribution and tectonics.

The figure below shows salt structures in the northwestern Gulf of Mexico and adjacent interior basins.

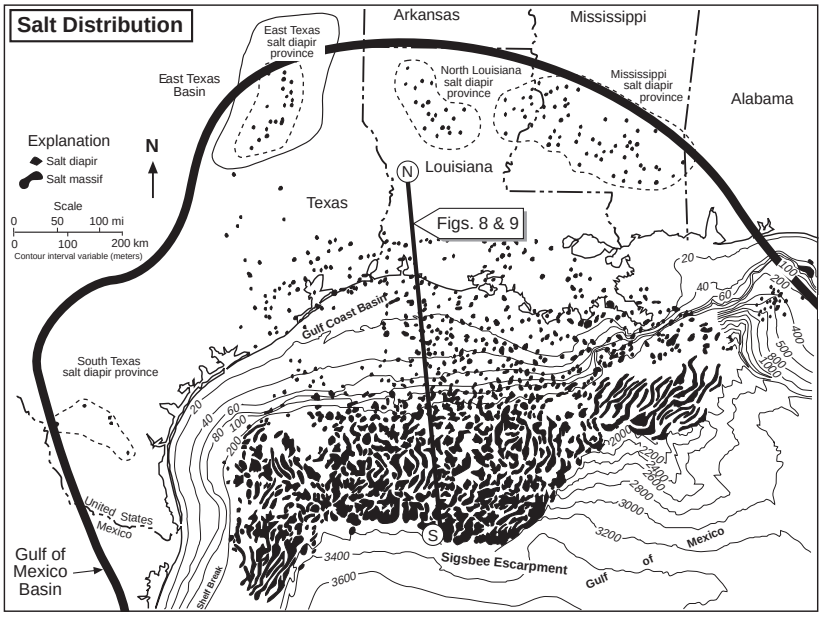

Figure 4–7. Modified from Jackson and Galloway (1984); courtesy AAPG.

Making Regional Structural Cross Sections

Cross section utility

Regional structural cross sections show interpretations of the present-day geology of a basin. They illustrate the relationship between structure and stratigraphy. Modeling the tectonic history and tectonostratigraphic phases begins with regional structural cross sections and works backward, disclosing important events.

Discussion of GOM basin

Much of the petroleum discovered within the northern GOM basin is in Neogene anticlinal and stratigraphic traps developed as a consequence of interaction between Jurassic salt and Cenozoic siliciclastic progradation. The basic model consists of sediment prograding into the basin and differentially loading the plastic salt, causing diapirs and growth faults to develop (Trippet, 1981; Ingram, 1991). Two different interpretations of the present-day geology are presented below in two different structural cross sections. Migration of hydrocarbons from Mesozoic and early Tertiary organic-rich rocks are significantly affected by the selection of either of these two interpretations of salt deformation.

Traditional structure cross section

Traditional regional cross sections, such as in the figure below, have shown highly deformed salt rooted within the in-place Middle Jurassic mother salt. Such cross sections have been used to suggest that successive progradation of siliciclastics loaded and displaced the salt as each sedimentary cycle's depocenter stepped progressively basinward. Differential loading of the salt formed deeply rooted diapirs and shallow growth faults as a result of sediment downbuilding and consequent displacement of salt. Mature source rocks occurring between the deeply rooted diapirs could yield hydrocarbons able to migrate within each salt-walled compartment of each depocenter.

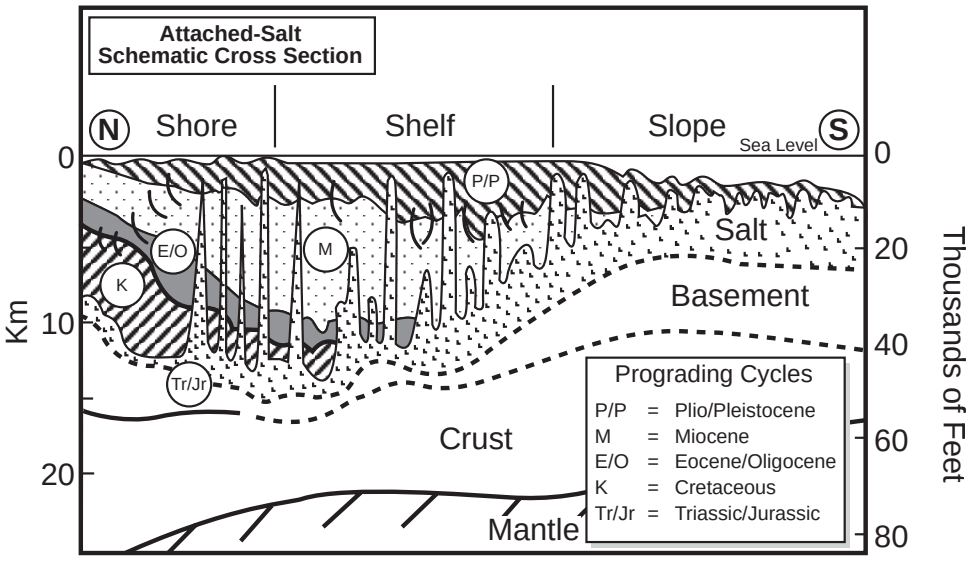

Figure 4–8. Modified after Antoine et al. (1974); courtesy Springer-Verlag.

Making Regional Structural Cross Sections, continued

Recent structure cross section

More recent models of salt deformation recognize both the in-place Middle Jurassic mother salt and displaced sheets of Middle Jurassic salt that have become detached from the mother salt as shown in the figure below. The detached salt is emplaced progressively over younger sediments because of the passive response to differential loading by sediment and gravitational forces. Basinward gravitational slope failure forms major growth fault systems on the upper slope and toe-thrust structures downslope (Bruce, 1973). Each "pulse" of salt displacement evolves through a new generation of deformation (Fiduk et al., 1989; West, 1989; Koyi, 1993; and McGuinness and Hossack, 1993). Maturing source rocks of Mesozoic and early Tertiary age can yield hydrocarbons that may migrate vertically along growth faults and salt walls, through holes in salt canopies, laterally below salt, or within sandstones between salt sheets.

Basin evolution

The contrast between the cross sections of Figures 4–8 and 4–9 illustrate changing concepts of basin evolution. When constructing a basin's history, we must understand the concepts underlying each previous study so we can fully appreciate the subtle changes in geologic models and take into account their consequences as the basin model evolves.

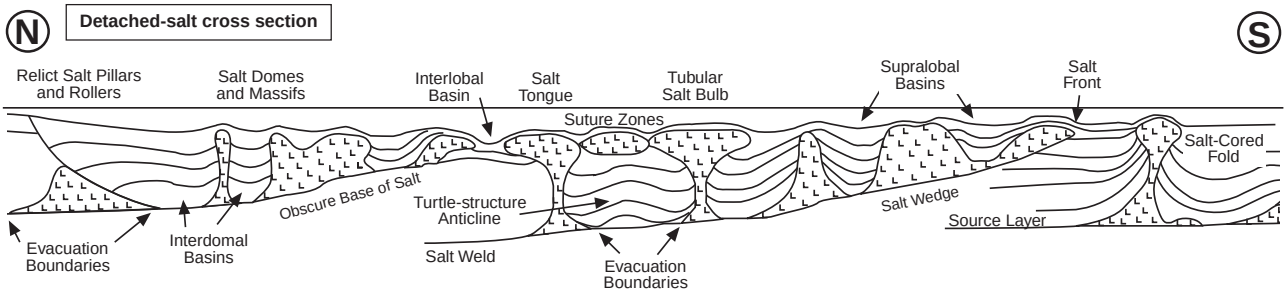

Figure 4–9. From Hall et al. (1993); courtesy Gulf Coast SEPM.

Determining Plate Tectonic Setting and History

Introduction

By understanding the present structural and stratigraphic configuration of a basin, we can interpret its plate tectonic history within the context of global plate reconstructions. Starting with the present configuration of the basin, we can move back in time and map the basin at critical periods in its plate tectonic development. Maps should show features such as spreading centers, contractional areas, extensional areas, crustal types, and mobile belts.

Critical period map

Tectonically, the Gulf of Mexico is a Mesozoic–Cenozoic rift basin formed along a southwest–northeast-spreading center on the southern margin of the North American craton (Buffler, 1991). The basic tectonic architecture developed as a consequence of the Jurassic breakup of Pangea as Africa and South America separated from North America (Pindell, 1993). The GOM basin is underlain by oceanic and transitional crust (Buffler, 1991) deformed along a set of north–northwest-trending faults (Marton and Buffler, 1993).

The figure below shows the Gulf of Mexico region as it looked approximately 130 Ma. Note the spreading and transform fault systems separating the North American, Atlantic, Farallon, and Caribbean plates. Striped areas are cratonic basement; shading is transitional to oceanic basement; and arc-related volcanics are noted by a "∧" pattern east of the Farallon/Caribbean trench.

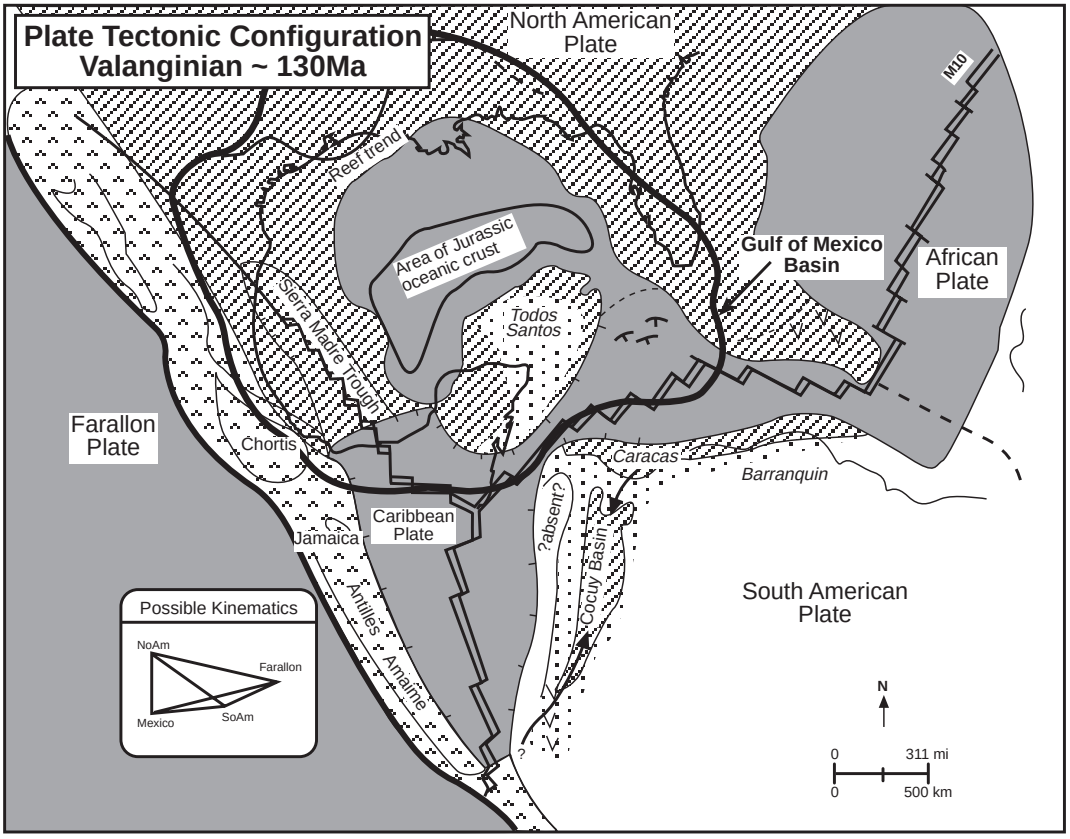

Figure 4–10. Modified from Pindell (1993); courtesy Gulf Coast SEPM.

Determining Tectonostratigraphic History

Introduction

Models of tectonic history provide a framework for understanding the history of each phase of basin development. A tectonostratigraphic phase is a period of basin evolution during which tectonic and stratigraphic elements resulted in a specific configuration of depositional and deformational elements, many of which were critical to the evolution of the basin's petroleum system. The tectonostratigraphic history for a basin is usually portrayed in a time series of cross sections, showing the geologic elements of each phase. Because all basins are three dimensional, care must be taken to assemble enough cross sections to depict basin history accurately.

Tectonostratigraphic phases

Tectonic evolution of the GOM basin has resulted in five primary tectonostratigraphic phases (A–E), each with a different sediment accumulation and deformation history. Figure 4–11 is a schematic diagram showing a series of cross sections representing the four phases of Late Triassic to Early Cretaceous evolution of the GOM basin (see Figure 4–6 for the location).

- **Phase A** (Figure 4–11A) consists of Late Triassic to Early Jurassic rifting along linear zones within brittle crust with deposition of synrift nonmarine sediments and volcanics within half-grabens.
- **Phase B** (Figure 4–11B) of Middle Jurassic age is characterized by rifting and attenuation of the crust, with formation of transitional crust and the associated basement highs and lows that form the basic architecture. The outer periphery of the basin underwent moderate stretching and the crust remained thick, forming broad arches and basins. The central basin underwent considerable stretching and subsidence to form a large area of thin transitional crust over which thick salt was deposited. Nonmarine terrigenous sediments continued to be deposited within the peripheral grabens.
- **Phase C** (Figure 4–11C) of Late Jurassic age consists of emplacement of oceanic crust as mantle upwelling concentrated along the generally east–west-trending weakness in the continental crust. As the crust underlying the basin began to cool, subsidence resulted in the relative rise of sea level. The basin margins were transgressed by broad shallow-to-deep shelfal marine environments with deposition of thick carbonate successions. Locally, thick, terrigenous clastic prisms prograded into the basin. Potential and known reservoirs occur within both the carbonate and clastic depositional systems of this tectonostratigraphic phase. During the Late Jurassic maximum transgression, the deep basin was sediment starved, and thick, organic-rich shales accumulated in low-oxygen environments (source-rock types 6 and 7).
- **Phase D** (Figure 4–11D) of Early Cretaceous age is characterized by broad carbonate platforms rimmed by reef buildups along the margins established at the boundary of differential subsidence between thin and thick crust. Fine-grained carbonates were deposited in the adjacent deep basin. Terrigenous clastics continued to be input at local points along the northern margin. Known and potential reservoirs occur within both carbonate and clastic depositional systems of these early Cretaceous rocks.

Tectonostratigraphic phases (continued)

- **Phase E** (Figure 4–9) began during the mid-Cenomanian with a rapid fall and rise of sea level superimposed on a long-term rise that terminally drowned the outer margins of the carbonate platforms, causing the margins to retreat landward. Widespread submarine erosion created a prominent mid-Cretaceous unconformity. Subsequent deposition was dominated by terrigenous sedimentation as large clastic prisms prograded first from the west and northwest in the Late Cretaceous and early Cenozoic and then from the north (Mississippi River drainage) during the late Cenozoic. Most of the offshore and many onshore reservoirs occur within these Late Cretaceous and Cenozoic siliciclastic deposits. The prograding prisms of siliciclastic sediment differentially loaded the underlying salt, resulting in deformation by both salt mobility and down-to-the-basin growth faulting along the shelf-slope break (Bruce, 1973; Winker and Edwards, 1983).

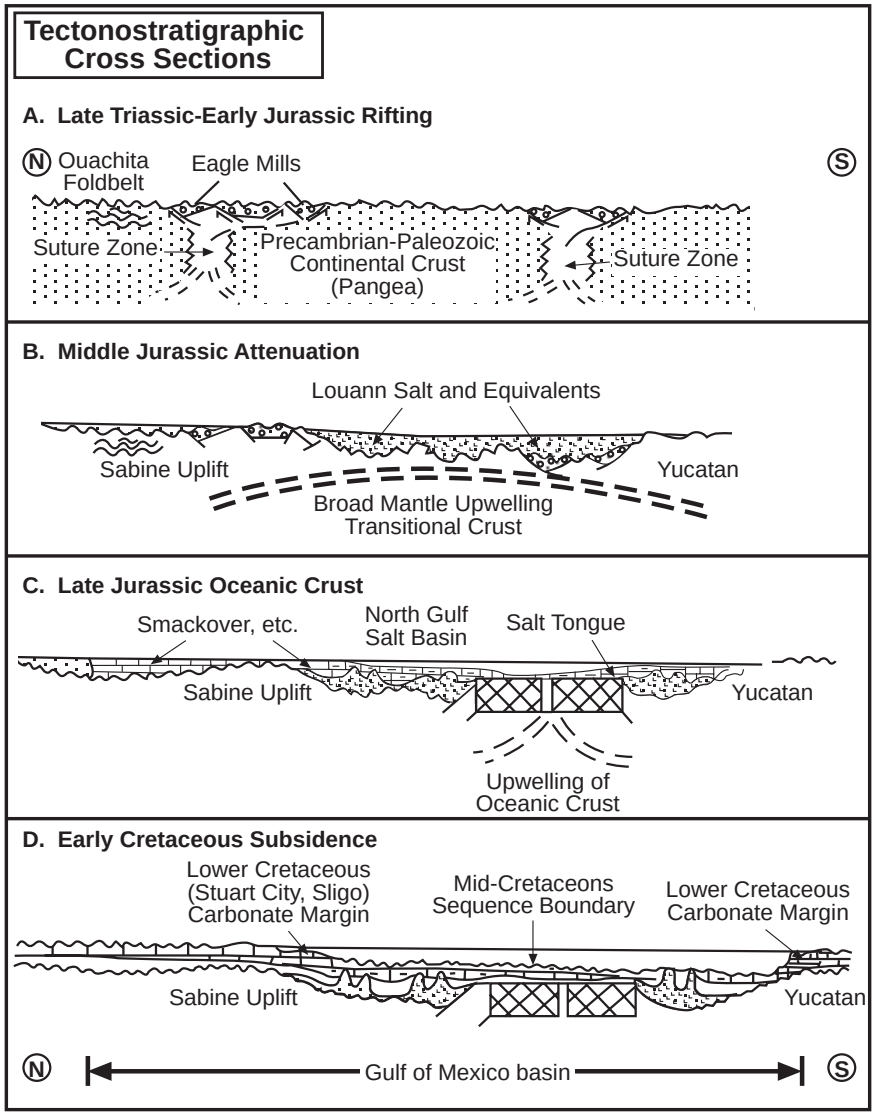

Figure 4–11. Modified from Buffler (1991); courtesy New Orleans Geological Society.

Using a Tectonic History Model for Petroleum System Analysis

Introduction

A model of the tectonic history of a basin provides a regional framework for understanding the development of essential elements and processes of the petroleum systems in a basin. A basin such as the Gulf of Mexico can have more than one petroleum system; therefore, the evolution of elements and processes can have an impact on different petroleum systems at the same time or at different times, depending on the events of each tectonostratigraphic phase.

Example from GOM basin

The tectonic history of the GOM basin provides the regional framework for mapping elements and processes of the petroleum systems within the High Island–East Breaks area. Following is a summary of the tectonic history of the basin.

1. Within the GOM rift basin, major areas of transitional crust formed between continental crust and Late Jurassic oceanic crust. Middle Jurassic crustal attenuation associated with the transitional crust formed sags in which evaporites were deposited.
2. During the Late Jurassic and Early Cretaceous, thermal subsidence of the basin center and relatively high sea level formed extensive carbonate platforms along the basin margin and sediment starvation of the basin center. Organic-rich, oil-prone marine sediments were deposited within low-oxygen environments of this sediment-starved basin. These rocks later became the primary source of oil and gas—some of which migrated to and is stored within porous zones of the carbonate platforms.
3. Late Cretaceous and Cenozoic siliciclastic sedimentation formed thick, prograding prisms over the transitional crust and differentially loaded the Late Jurassic salt. The deformed salt created anticlinal highs bordering sediment-filled synclinal lows, which continued to subside and provide sediment transport pathways downslope. The deformation of the salt and associated sediments formed both structural and stratigraphic traps within the siliciclastic section. Sedimentary burial and salt-thickness/mobility patterns affect hydrocarbon generation due to variations in the thermal conductivity of salt. Intersecting fault trends, one paralleling northwest–southeast-trending basement faults and a second associated with depositional strike-oriented growth faults, provide vertical avenues for migration of hydrocarbons from deeply buried mature Mesozoic source rocks upward into reservoir rocks of Jurassic, Cretaceous, and Cenozoic age.

Areas of maximum sediment accumulation and consequent salt deformation were controlled by areas of maximum sediment input and sea-floor subsidence.

Section B
Depocenters

Introduction

Within a basin, different areas receive different amounts of sediment through time, resulting in numerous depocenters. Each depocenter is an area containing a thick stratigraphic succession. These different depocenters have unique histories of sediment accumulation, compaction, subsidence, deformation, and thermal maturation of potential hydrocarbon source rocks. Delineation of these depocenters is the second step in basin analysis. Subdividing a depocenter into age-significant units and depositional cycles is the topic of section C.

In this section

This section contains the following topics.

Mapping and Analysis of Depocenters

What is a depocenter?

"Depocenter" refers to an area or site of maximum deposition, or the geographic location of the thickest part of any specific geographic unit in a depositional basin (Gary et al., 1974).

Sediment supply rate and facies patterns

Within each depocenter, facies do one of the following:

- Prograde if the rate of sediment supply exceeds the rate of accommodation space formation
- Aggrade if the rate of sediment supply equals the rate of accommodation space formation
- Retrograde if the rate of sediment supply is less than the rate of accommodation space created (Van Wagoner et al., 1988)

Siliciclastic vs. carbonate supply

Most siliciclastic basins have sediment supplied from drainage areas outside of the boundary of the depositional basin. Lateral changes in sediment input locations can result in lateral shifts in the depocenter if enough space exists to accommodate the sediment near each input location. In carbonate basins, organisms near the site of accumulation produce most sediment, and facies tend to extend over large platform areas.

The figure below is a map of the drainage basin of the modern Mississippi River, illustrating the network of rivers feeding into one sediment input point. The Holocene depocenter of the Mississippi River is immediately offshore and west of the river mouth. Smaller drainage basins also supply terrigenous sediment to the western and central Gulf of Mexico, while in situ carbonate factories supply most of the sediment to the Florida peninsula.

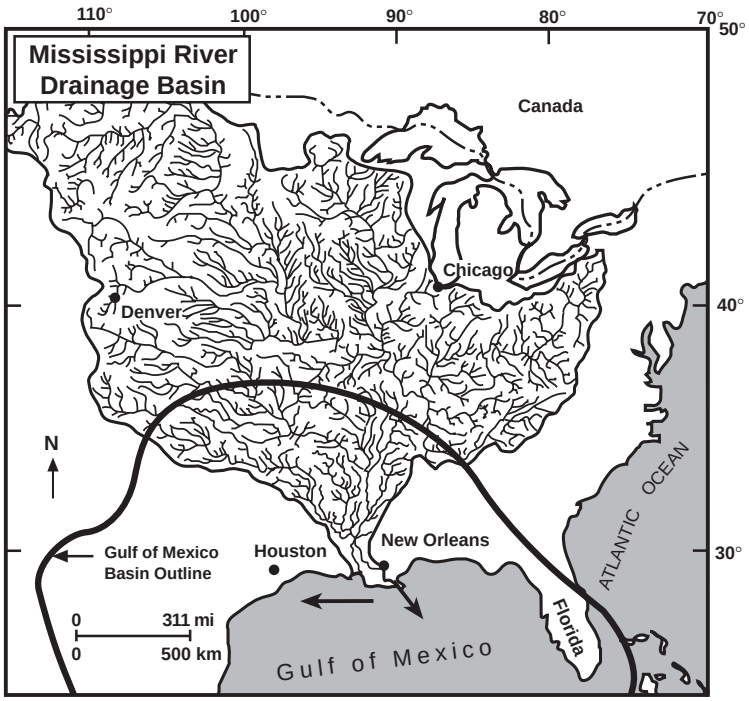

Figure 4–12. Modified from Coleman and Roberts (1991); courtesy New Orleans Geological Society.

Mapping and Analysis of Depocenters, continued

Depocenter complexes

In basins with relatively rapid subsidence and multiple sediment supply systems, a complex set of depocenters occurs. Each depocenter has a unique history of accumulation, based on

- variations in source rock maturation,
- manner and timing of hydrocarbons expulsion and migration, and
- style of fluid entrapment and preservation.

Recognizing the temporal and spatial distribution of each depocenter is critical to understanding basin history and petroleum system formation. Along the basin margin, depocenters may be dominated by deltaic complexes. On the slope and basin floor, depocenters are related to transport systems of gravity-flow processes.

Mapping age of thicks

Mapping age-specific isopach thicks defines laterally shifting sites of maximum deposition along the margin of a basin. Each depocenter has a unique history of accumulation with consequent variations in maturation, migration, and entrapment history of associated petroleum systems.

Mapping depocenters

Follow the procedure detailed in the table below to map depocenters. **Note:** Isopach maps (step 1) are shown in this section. Steps 2–5 are detailed in sections C and D.

Step	Action
1	Make isopach maps of individual depocenters using well data and high-quality seismic profiles calibrated to well data.
2	Establish correlation of surfaces bounding each tectonostratigraphic phase and construct isopach maps or relative thickness maps.
3	Map deltaic/shelf depocenters by mapping net sand distribution from well data.
4	Identify shelf margins using biostratigraphic and seismic facies analysis.
5	Identify deepwater intraslope basins from isochron mapping and calibration to stratigraphy in wells.

Example: Mapping Fluvial Input

Introduction

The late Cretaceous to Recent depositional history of the northern Gulf of Mexico continental margin has been influenced by several factors (Coleman and Roberts, 1991):

- Fluvial supply system and delta formation
- Subsidence
- Diapiric and tectonic movement
- Fluctuation in sea level

Summary of GOM fluvial history

Mesozoic and Cenozoic fluvial systems have filled in the northern margins of the GOM rift basin, prograding the continental margin of one area until sediment input shifts to another area (Figure 4–4). Subsidence is related to basement cooling or differential response of basement types to loading (Figure 4–6). Formation of diapirs and tectonic movement of growth fault systems has already being discussed as it relates to sediment loading. Fluctuation in sea level is discussed in section D.

Example: Mapping Depocenters Through Time

Introduction

Mapping age-specific isopach thicks in the northern GOM basin defines laterally shifting sites of maximum deposition (Figure 4–4). Methods of mapping are clearly presented in Tearpock and Bischke (1991).

GOM basin depocenter time intervals

In the northern GOM basin, depocenters prograde (Figure 4–4) over the transitional crust (Figure 4–6) and deform the underlying salt into a complex network of salt-cored anticlines and salt-withdrawal synclines (Figures 4–8, 9). Late Neogene depocenters of the Mississippi River, the largest source of sediment to the northern Gulf of Mexico, developed during five time periods from the latest Miocene through Holocene (from Piggott and Pulham, 1993; see also Goldthwaite, 1991). Following are the five depocenter intervals and their time periods.

Interval	Time Period, Ma
A	6–4
B	4–3
C	3–2.5
D	2.5–1
E	1–Present

Figures 4–13 to 4–16 are maps of depocenters and paleogeography for intervals A, B, D, and E. These were constructed by correlating wells using fossil extinction events and grids of interpreted seismic reflection profiles. The High Island–East Breaks study area is shown on each map.

Formation of High Island–East Breaks depocenter

Between 2.5 and 2.0 Ma, the major northern GOM basin depocenter was focused offshore of western Louisiana and eastern Texas. The westernmost part of this depocenter appears to have been the input area for the ancestral Mississippi River system. The resulting depocenter, the High Island–East Breaks depocenter, has more than 16,000 ft (4875 m) of late Pliocene and early Pleistocene sediments deposited during a succession of high-amplitude sea level cycles.

Timing of petroleum generation

Each of the isopach maps in this section is annotated with the area of active petroleum generation and migration. These comments are based on the modeling of Piggott and Pulham (1993), illustrated and discussed along with Figures 4–32 and 4–33.

Example: Mapping Depocenters Through Time, continued

Interval A paleogeography

The figure below shows the paleogeography of the Mississippi River depositional system from approximately 6 Ma to 4 Ma (interval A). Deposition consists of net sand isopach thicks on the shelf and intraslope basins that are interpreted to be deepwater "fan" complexes.

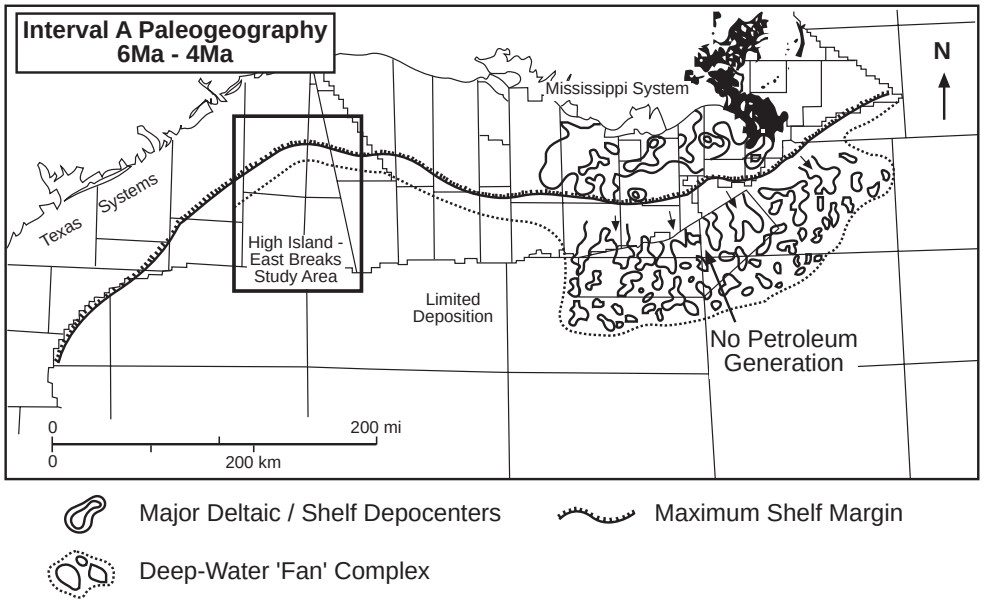

Figure 4–13. After Piggott and Pulham (1993); courtesy Gulf Coast Section SEPM.

Interval B paleogeography

This figure shows paleogeography from approximately 4 Ma to 3 Ma (interval B). Shelf and intraslope basin thicks are potentially sand prone. (Note the shift westward from the previous depocenter location.)

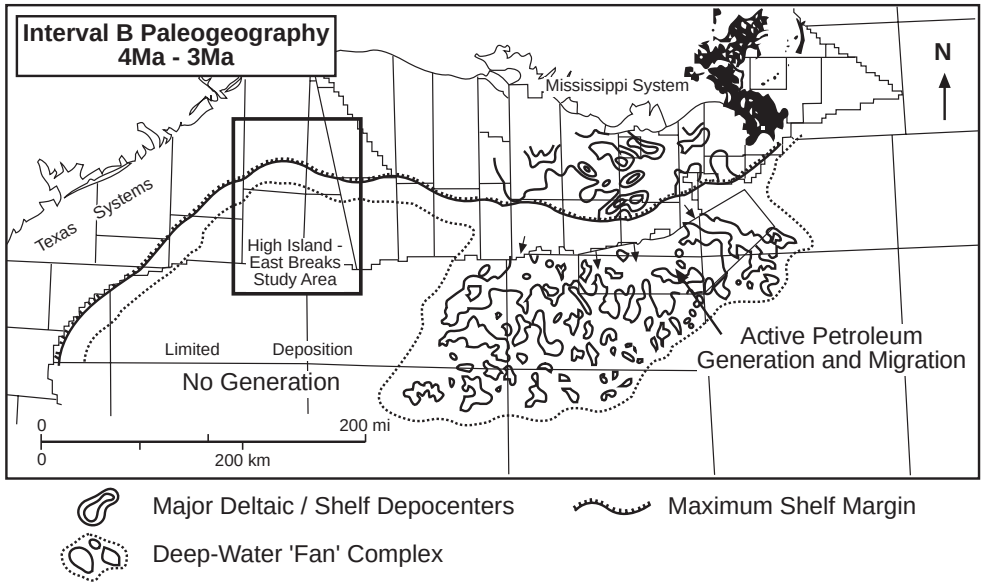

Figure 4–14. After Piggott and Pulham (1993); courtesy Gulf Coast Section SEPM.

Example: Mapping Depocenters Through Time, continued

Interval D paleogeography

The following figure shows paleogeography from approximately 2.5 Ma to 2 Ma (interval D). Again, shelfal net sand thicks and intraslope basin isopach thicks interpreted to be deepwater "fan" complexes are the dominant depositional environments. Note the depocenter has shifted to offshore western Louisiana and Texas. The High Island–East Breaks study area occurs within the western part of this depocenter.

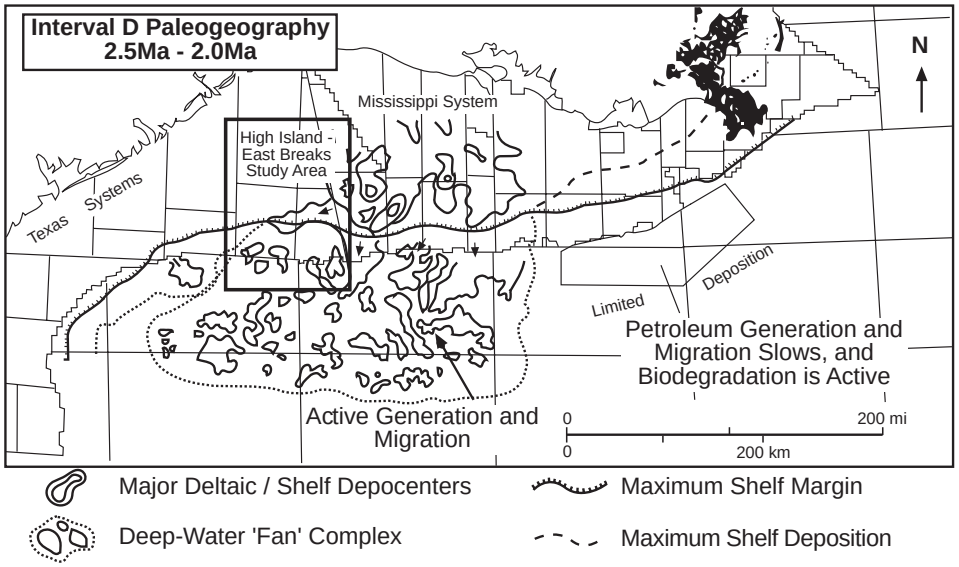

Figure 4–15. After Piggott and Pulham (1993); courtesy Gulf Coast Section SEPM.

Interval E paleogeography

The paleogeographic map below represents time from about 1 Ma to the present (interval E). Canyons are interpreted from incised and back-filled geometries on seismic reflection profiles. Note the depocenter has shifted back to offshore eastern Louisiana from the preceding location offshore eastern Texas/western Louisiana.

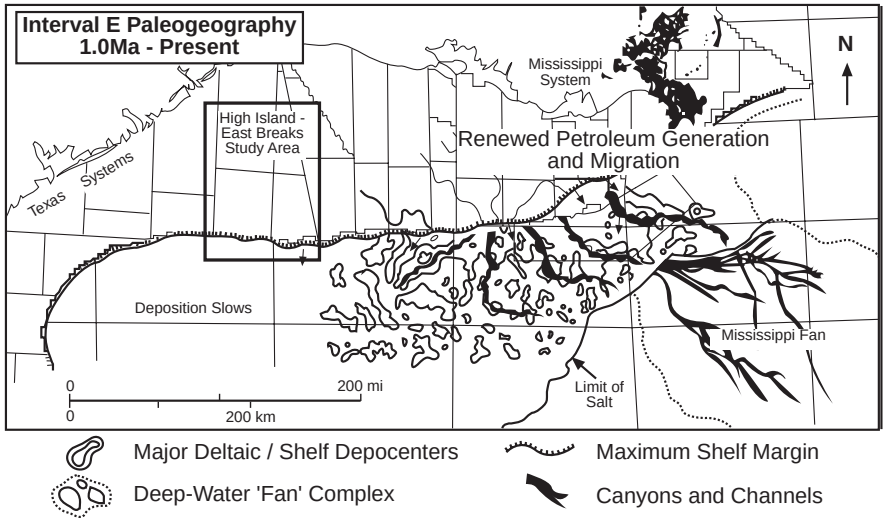

Figure 4–16. After Piggott and Pulham (1993); courtesy Gulf Coast Section SEPM. Also after Weimer (1990); courtesy AAPG.

Example: Mapping Depocenters Through Time, continued

Depocenter summary

Mapping age-specific isopach thicks defines laterally shifting sites of maximum deposition along the margin of the basin. Each of these depocenters has a unique history of accumulation with consequent variations in maturation, migration, and entrapment histories. Evaluation of depocenter maps should include comparison of the results with the larger-scale isopach maps (Figures 4–3, 4–4).

GOM depocenter summary

In the case of the northern Gulf of Mexico, the depocenters prograde over the transitional crust and deform the underlying salt, forming a complex network of salt-cored anticlines and salt-withdrawal synclines. Between 2.5 and 2.0 Ma, the major northern Gulf of Mexico depocenter was focused offshore western Louisiana and eastern Texas. The westernmost part of this depocenter area, the High Island–East Breaks depocenter, appears to have been the input area for the ancestral Mississippi River system. The resulting depocenter has more than 16,000 ft (4875 m) of late Pliocene and early Pleistocene sediments deposited during a succession of high-amplitude sea level cycles (see section C, Depositional Sequences).

Section C
Depositional Sequences

Introduction

Each depocenter has a unique depositional history that reflects the integration of all responses to depositional processes and environmental factors, including tectonics, climate, sediment supply, and sea level variation. These factors result in cycles of deposition: the sediments accumulated during each cycle are the depositional sequence. Integration of multiple data sets, including (1) seismic reflection profiles, (2) biostratigraphic analyses, (3) wireline logs, (4) cores, and (5) detailed measured sections, helps us define the depositional sequences and interpret primary factors affecting formation of each cycle. Precise mapping of each depositional sequence within each depocenter requires careful data integration.

This section discusses the concept of depositional sequences and how to identify them, using a data set from the High Island–East Breaks area. The location of this study area is shown on the depocenter maps of Figures 4–13 through 4–16.

In this section

This section contains the following topics.

Examples in this section

The following figure is a map of the study area, showing the named offshore exploration areas and bathymetry. It also shows the locations of the East Breaks 160-161 field, illustrated seismic profiles and a reference well.

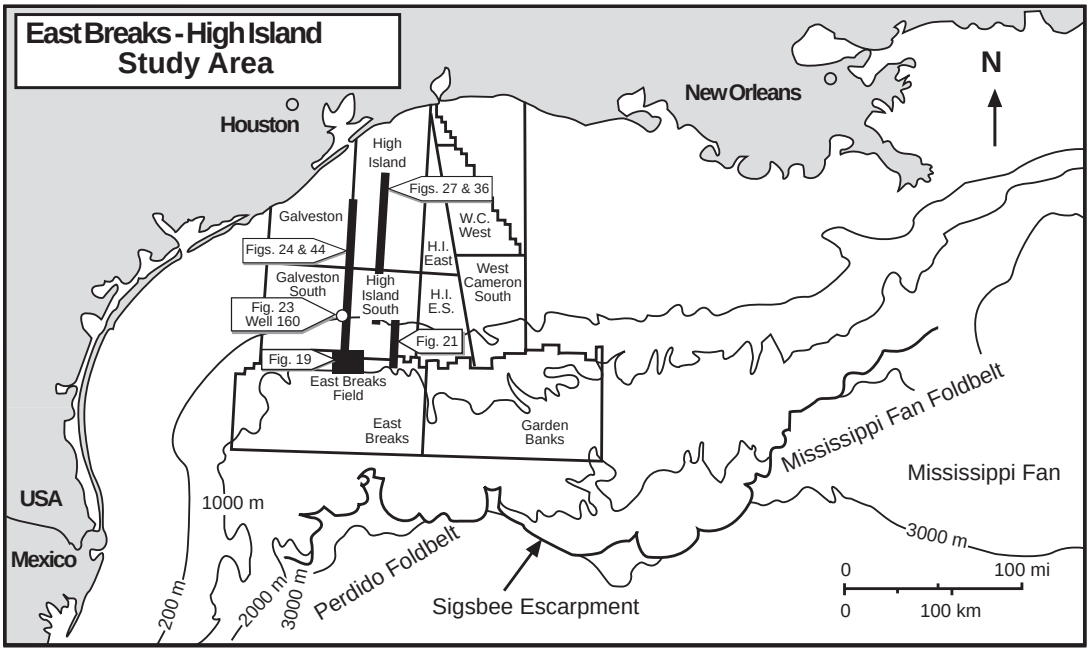

Figure 4–17.

Definitions of Depositional System Elements

Depositional cycle vs. sequence

The term *depositional cycle* refers to time through which one complete cycle of relative sea level change occurs. The sediments deposited during one such cycle are called a *depositional sequence.*

Sequence boundaries

A depositional sequence is bounded by unconformities or the correlative conformities and is subdivided by internal surfaces of transgression and maximum flooding (Mitchum, 1977; see also Vail, 1987; Posamentier et al., 1988; Van Wagoner et al., 1990). Each of these surfaces is chronostratigraphically significant, separating consistently older strata from younger strata.

An alternative concept of defining a depositional sequence is that of Galloway (1989a,b). Galloway uses the maximum flooding surface and correlative condensed section as the bounding surface of the "genetic" depositional sequence. Both sequence concepts use the erosional unconformities, maximum flooding surface, and transgressive surface as interpretation horizons for partitioning each sequence. Sequence surfaces are often best recognized on seismic reflection profiles by stratal terminations called *lapouts,* such as downlap and onlap.

Maximum flooding surface

The maximum flooding surface represents the greatest transgression of shallow marine facies within a sequence (Mitchum, 1977). This is typically associated with a downlap surface formed by the progradation of the overlying highstand systems tract. Not all downlap surfaces are associated with maximum flooding surfaces.

Transgressive surface

The transgressive surface is the first significant marine flooding surface across the shelf (Mitchum, 1977). Above this surface, shallow marine facies shift landward dramatically.

Systems tracts

Systems tracts are composed of all deposits accumulating during one phase of relative sea level cycle, such as lowstand systems tract or highstand systems tract. Attributes of each systems tract are discussed in section D.

Age model

An age model is the chronostratigraphic relationship of different depositional sequences.

Biofacies

A biofacies is an assemblage of organisms (living or fossil) found together because they responded to similar environmental conditions.

Microfossil abundance patterns

Microfossil abundance patterns are relative high and low peaks in the number of microfossils found in a sample or set of samples. They most often indicate sedimentation rates (Armentrout et al., 1990). Intervals with slow rates of sediment accumulation have consequent concentrations of abundant fossils and are associated with maximum flooding and transgressive surfaces. Intervals with high rates of sedimentation usually have low fossil abundances due to dilution and are often associated with sequence boundaries.

Definitions of Depositional System Elements, continued

Illustration of sequence boundaries

The following figure illustrates the bounding surfaces for sequences. The GOM basin analysis example in this chapter is based primarily on well log and seismic data interpretation using this passive margin sequence stratigraphic model. Different models are necessary for different settings, such as a foreland basin (see Van Wagoner and Bertram, 1995) or a rift basin (Prosser, 1993).

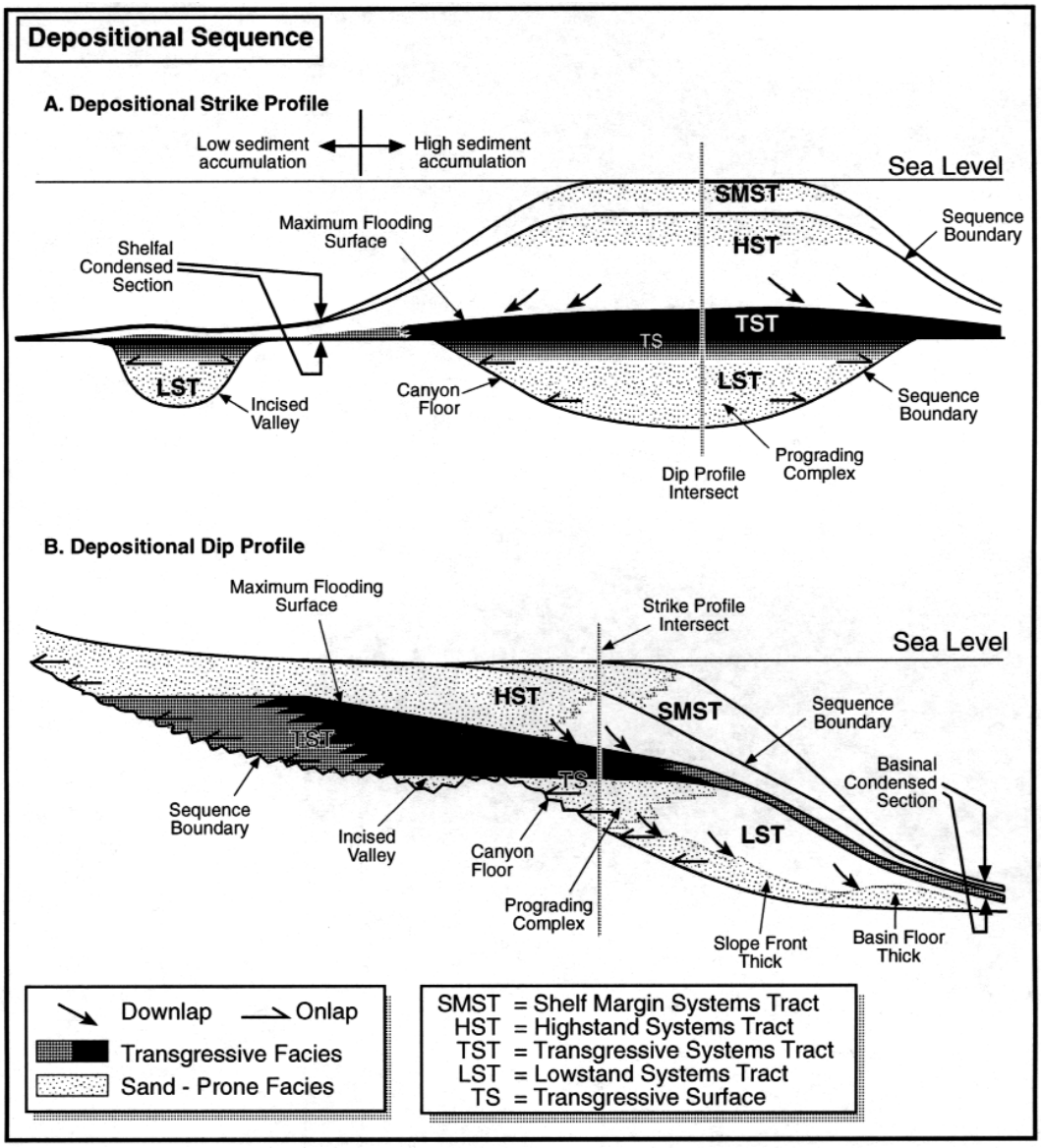

Figure 4–18. After Vail (1987) and Loutit et al. (1988); courtesy AAPG and SEPM.

Identifying Depositional Sequences

Introduction

A depositional sequence is bounded by unconformities or the correlative conformity. It is subdivided by internal surfaces of transgression and maximum flooding (Vail, 1987; Van Wagoner et al., 1990). Each of these surfaces is chronostratigraphically significant, consistently separating older strata from younger strata.

Identifying data

To identify depositional sequences, we use the following:

- Seismic record sections
- Biostratigraphic histograms
- Wireline logs
- Detailed measured stratigraphic sections
- Combinations of the above items

Procedure

Use the table below to identify depositional sequences.

Step	Action
1	Identify depositional sequences in seismic reflection profiles, correlating sequence boundaries throughout a data grid of seismic reflection profiles.
2	Analyze biostratigraphic data for age-significant bioevents and abundance patterns that may suggest depositional sequences.
3	Analyze the depositional patterns from wireline logs, integrate the biostratigraphic data with correlated well log and seismic data, and select candidate depositional sequences.
4	Make regional stratigraphic sections by integrating seismic profile interpretations, biostratigraphic analyses, and regional well log cross sections.
5	Identify depositional sequences based on the fully integrated data set.

Identifying Depositional Sequences in Seismic Sections

Analyzing seismic sections

We identify depositional sequences in seismic sections by finding repetitive patterns of seismic reflections. To test the validity of the sequences identified from seismic reflection profiles, we compare the seismic sequences with sequences identified from biostratigraphic and well log data to see if they make geologic sense. Identifying depositional sequences can be complicated by postdepositional erosion and deformation. It is often helpful to begin a seismic sequence analysis using a grid of relatively few profiles with an area of relatively undeformed rocks.

GOM basin example

In the shelf-margin facies of the East Breaks study area of the GOM basin, a depositional sequence in its simplest form is identified in seismic sections as a couplet consisting of two patterns:

- Sigmoidal clinoform packages
- Regionally extensive parallel reflections

Each clinoform package defines a locally thick progradational unit interpreted as a relative sea level lowstand delta (Sutter and Berryhill, 1985). They are lateral to other clinoform packages and are bounded above and below by regionally extensive, parallel, often uniformly high-amplitude seismic reflections. The regionally extensive parallel reflections correlate across faults and have the same relative thickness on both sides of most outer-shelf and upper-slope faults.

The seismic reflection profile of the figure below, from the East Breaks field area, illustrates both clinoform and parallel reflection patterns in late Pleistocene sediments immediately below the sea floor (between two sets of bold arrows). Three listric growth faults (down arrows) cut through the clinoforms. These growth faults are part of the regional fault system bounding the shelf edge and upper slope salt-withdrawal basins in the High Island and East Breaks areas.

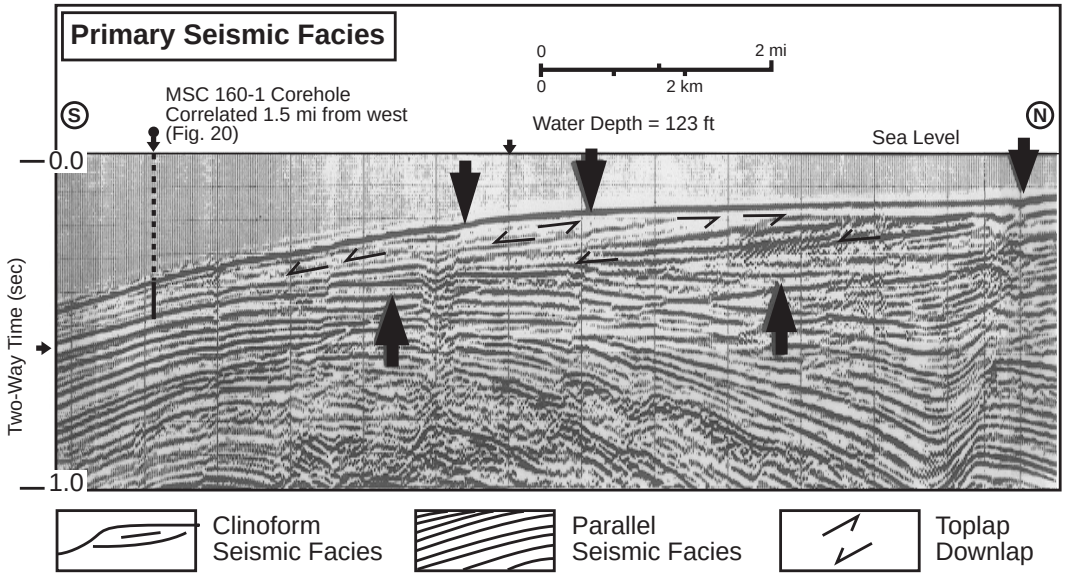

Figure 4–19. Modified from Armentrout (1993); courtesy Gulf Coast SEPM.

Identifying Depositional Sequences in Seismic Sections, continued

GOM basin example (continued)

The arrow at the far left edge of Figure 4–19 marks the trough (white) between parallel, high-amplitude, continuous reflections (black) that underlie the clinoforms (best expressed toward the left side of the figure). Two up arrows show the correlation of this trough across the faults. The clinoforms toplap to the right (north) against the sea floor reflection, defining the overlying transgressive surface above the clinoform tops and below the regionally extensive sea floor reflection. Additionally, the clinoform downlaps basinward, defining a downlap surface. In this case, the downlap surface coincides with the underlying sequence boundary (see Armentrout, 1991).

Depositional cycle

The data from the High Island–East Breaks shelf-margin delta suggest that regionally extensive and uniform layers of mud occur above and below locally shingled clinoform packages. Couplets of these two depositional facies constitute a sequence of one depositional cycle. The position of the sequence at the shelf edge suggests that it is composed of a shelf margin systems tract and a condensed section. For criteria for recognizing depositional cycles in other settings, see Loucks and Sarg (1993), Steel et al. (1995), Van Wagoner and Bertram (1995), and Weimer and Posamentier (1993).

Type 1 vs. type 2 sequences

The sequence stratigraphic model includes type 1 and type 2 sequences (Vail, 1987; Posamentier and Vail, 1988). A type 1 sequence boundary is interpreted to form when the rate of eustatic fall exceeds the rate of subsidence at the depositional break, producing a relative fall in sea level at that position. This usually results in an extensive erosional surface with stream incision landward of the depositional break. In contrast, a type 2 sequence boundary forms when the rate of eustatic fall is slightly less than or equal to the rate of basin subsidence at the depositional break. There is no relative fall in sea level at the depositional break, and erosion and stream incision is less than at type 1 boundaries.

Depositional break

In early publications the depositional break is referred to as the *shelf break,* often uniquely imaged on seismic reflection profiles (Vail and Todd, 1981; Vail et al., 1984). More recently, the depositional break was referred to as the *shoreline break,* a position coincident with the seaward end of a stream-mouth bar in a delta or the upper shoreface in a beach environment (Van Wagoner et al., 1990). Shoreline breaks are well imaged on high-resolution seismic profiles and in well-exposed outcrop belts but are usually below resolution scale of most industry seismic reflection profiles.

Nomenclature problems

These scale differences result in nomenclature problems. The High Island–East Breaks shelf-margin delta (Figures 4–19, 4–21) fits a type 2 sequence criterion of Vail and Todd (1981) because it represents a lowstand prograding complex at the same position as preceding shelf-edge depositional breaks. As such, this lowstand is part of a type 2 depositional sequence and would be called a shelf-margin systems tract. If the criteria of Van Wagoner et al. (1990) are used, the High Island–East Breaks shelf-margin delta would be called a type 1 lowstand prograding complex because the preceding shoreline break is tens of miles further north on the Texas shelf. Clarification of such scale-dependent reference points is critical to effective communication through the careful selection of precise labels for elements of depositional sequences.

Identifying Depositional Sequences from Biostratigraphic Data

Introduction

Biostratigraphic data can aid in identifying individual depositional sequences and stacked depositional sequences, especially when integrated with lithofacies and seismic facies. Biostratigraphic data include the following:

- Microfossil abundance patterns
- Extinction events
- Biofacies

Microfossil abundance patterns

Microfossil abundance patterns derived from examining well cuttings may provide high-resolution observations for identifying depositional sequences. Total microfossil abundance patterns reflect changes in sediment accumulation rates, provided the biogenic productivity varies less than the sediment accumulation rate. For example, during the reduced rate of sediment accumulation associated with transgression, the middle-shelf and deeper transgressive-phase deposits may be characterized by an increase in fossil abundance due to relative terrigenous sediment starvation and consequent concentration of fossil material. If the same conditions of biotic productivity hold during the increased rate of sediment accumulation associated with a prograding system, the accumulated sediments may be characterized by a decrease in fossil abundance due to dilution and environmental stress (Shaffer, 1987a; Armentrout et al., 1990).

Applying abundance patterns

In the Texas offshore Pliocene and Pleistocene depocenter, patterns of fossil abundance are often the most widely applicable observational criteria for identifying the surfaces that define sequences (Armentrout, 1987, 1991, 1996). Sequence boundaries are associated with intervals of few or no in situ fossils and often abundance peaks of reworked fossils in the overlying lowstand systems tract. The transgressive surface is characterized by the stratigraphic upward change from decreasing fossil abundance to increasing abundance. The maximum flooding surface is marked by the maximum fossil abundance interval due to sediment starvation (Loutit et al., 1988; Armentrout et al., 1990).

Example abundance pattern

The figure on the following page is an abundance histogram for the planktonic foraminiferal microfossils *Globorotalia menardii* (s = sinistral) and *Globorotalia inflata* from the MSC 160-1 core hole, East Breaks area (data provided by Gerry Ragan, Mobil Exploration and Producing US). The core hole is 0.3 mi to the west of the seismic reflection profile shown in Figure 4–19. Data on sediment type and biostratigraphy from core hole MSC 160-1 permits geologic characterizations of both the regionally parallel and locally shingled-clinoform seismic facies.

Example abundance pattern (continued)

The figure below contrasts the abundance of sinistral (s) *Globorotalia menardii (G. menardii)* with that of *Globorotalia inflata (G. inflata)* in each sample. Note the alternating pattern of abundance.

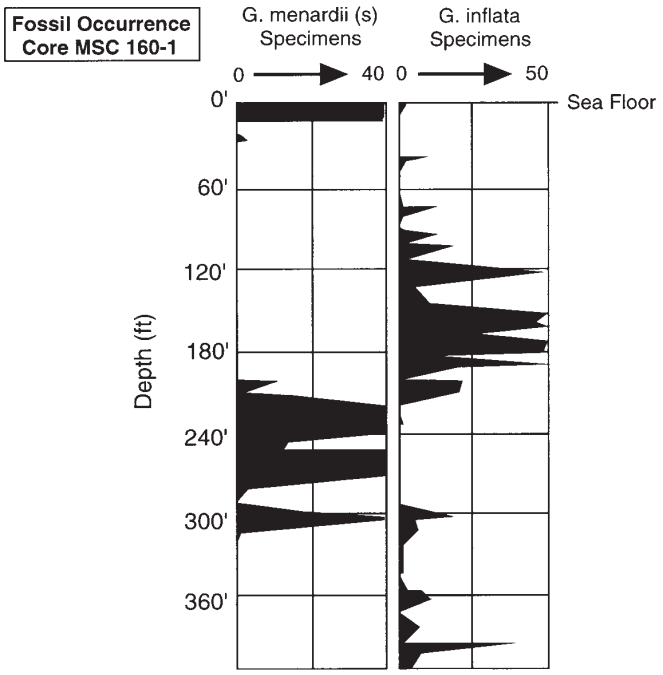

Figure 4–20. From Armentrout (1993, 1996); courtesy Gulf Coast SEPM and Geological Society of London.

Pattern interpretation

The high abundance of *G. menardii* at depths of 0–20 ft (0–7 m) shown in Figure 4–20 correlates with the interval at the sea floor that is part of the regionally extensive transgressive mud of the Holocene. The arrow on the seismic section, shown on Figure 4–19, at about 0.6 sec (two-way time) marks a trough between two high-amplitude continuous reflections that also correlate with the high-abundance interval of *G. menardii* between 190 and 320 ft (58 and 98 m). In contrast, the stratigraphic intervals of *G. menardii* low abundance and *G. inflata* high abundance correlate with the shingled-clinoform seismic facies.

Stratigraphic intervals with abundant *G. menardii* are interpreted to indicate warm-water interglacial conditions, and abundant *G. inflata* are interpreted as temperate-water glacial indicators (Kennett et al., 1985; Martin et al., 1990). The correlation of abundant *G. menardii* with the regionally extensive transgressive mud of the Holocene provides local confirmation of the warm-water interglacial interpretation. The regionally continuous reflections at 0.6 sec also indicate a transgressive interglacial interval. The shingled-clinoform facies correlates with the *G. inflata* abundance peak, suggesting deposition during temperate-water glacial conditions.

Note that the intervals of abundant *G. menardii* are thicker than intervals with abundant *G. inflata.* This suggests that more sediment accumulates associated with glacial lowstand progradation. Deposition of the thick clinoform packages necessitates some fault movement to accommodate the sediment accumulation (Armentrout, 1993).

Recognizing Stacked Depositional Sequences in Seismic Profiles

Introduction

Depositional sequences can stack into successions of sequences if accommodation space permits preservation of successive sequences. Seismically, stacked sequences are expressed as repetitious reflection patterns.

GOM basin example

The seismic reflection profile below is from the High Island South Addition area, GOM basin, 20 mi east of the East Breaks shelf-margin delta. It illustrates the vertical stacking of seven depositional sequences within a fault-bounded salt-withdrawal basin. Down arrows at the inflection point of each clinoform identify the top of the clinoform of each sequence. In general, each cycle consists of (1) a thick basinal package of relatively discontinuous, variable-amplitude, hummocky reflections that grade upward into (2) parallel, continuous, uniform amplitude reflections, overlain by (3) a prograding clinoform that downlaps the underlying facies. Each clinoform is interpreted as a shelf-margin delta prograding into this outer-shelf to upper-slope fault-bounded basin as shown by the present-day sea floor profile. The seven prograding clinoforms are mapped into a nearby well and are correlated with two-cycle charts (Figure 4–25). Cycle 1 of this figure correlates with the clinoform package of Figure 4–19.

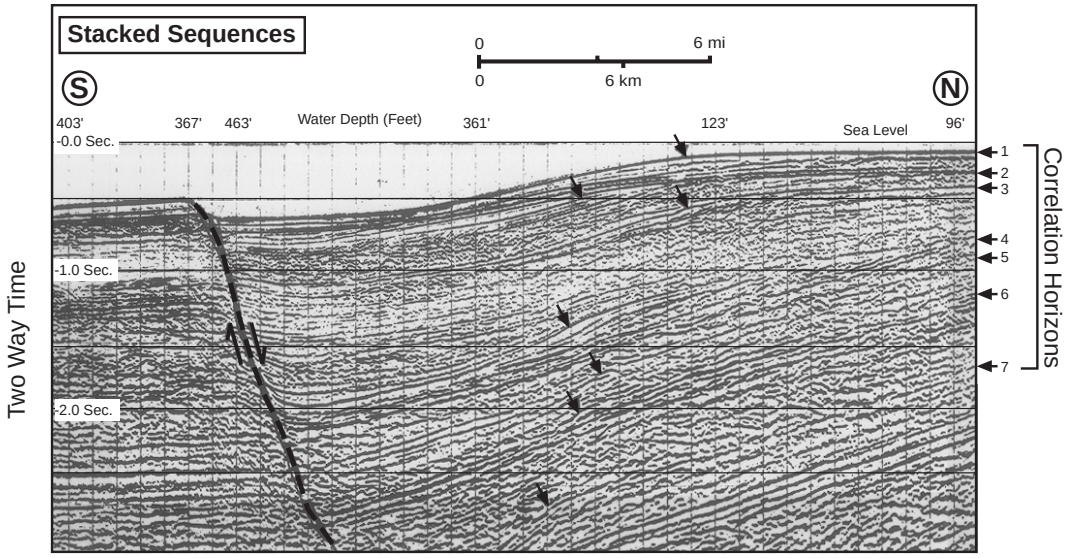

Figure 4–21. From Armentrout (1993, 1996); courtesy Gulf Coast SEPM and Geological Society of London.

Interpretation of example

The nearly vertical stacking of seven shelf-margin clinoforms suggests that accommodation space was created in the same area during seven cycles of progradation. The accommodation space is formed by down-to-the-north movement on the fault. This fault is part of a counter-regional listric growth fault that soles out into salt layers at depth. Movement on the fault occurred at a rate permitting the vertical stacking of shelf-margin clinoforms during each glacial/interglacial sea level cycle rather than progressive basinward progradation of successive clinoforms across a stable shelf-slope profile. This pattern clearly demonstrates the interplay of sediment supply, tectonics, climate, and sea level (see Beard et al., 1982; Anderson et al., 1996).

Recognizing Stacked Depositional Sequences from Well Data

Introduction

Stacked depositional sequences can be recognized in well data using

- variations in well log response
- biostratigraphic data such as microfossil abundance patterns and biofacies distribution

Armentrout (1996) discusses integration of these data sets.

Building regional log cross sections

Regional stratigraphic well-log cross sections form the foundation for many basin studies. They give a regional view of basin stratigraphy and can be integrated with seismic and biostratigraphic data. The table below outlines the steps for building regional well-log cross sections.

Step	Action
1	Build a grid of well-log sections that crosses the entire basin, either along depositional dip or depositional strike. Use as many wells as practical. Where available, add measured sections and core descriptions to the grid.
2	Correlate cross sections. Look for unconformities and flooding surfaces.
3	Tie the correlations from depositional-dip sections to depositional-strike sections.
4	Confirm correlations on seismic reflection profiles.

Biostratigraphic patterns

Using chronostratigraphically significant bioevents as defined by microfossil extinction events and abundance patterns, local cycles of transgression and regression can be correlated from well to well, providing a high-resolution calibration of depositional cyclicity. Patterns of relative dilution vs. concentration of fossils that correlate over a significant geographic area, such as a large portion of a basin margin, can be interpreted as reflecting cycles of regional transgression and regression rather than local lateral shifting of sediment input points.

Stratigraphic intervals rich in calcareous nannoplankton and foraminiferal fossils and having maximum gamma-ray values are interpreted to correlate with condensed depositional intervals deposited during relative sediment starvation related to transgression (Loutit et al., 1988). Intervals devoid of fossils or having low abundance values, often associated with sandy lithofacies, can be interpreted as deposited during relative high rates of accumulation related to progradation of the sediment supply into the area of the well, marking a phase of regression. Biofacies are interpreted using benthic foraminiferal assemblages indicative of water mass conditions (Tipsword et al., 1966; Culver, 1988; Armentrout, 1991).

GOM basin example

In the GOM basin, variations in well-log response and biofacies distribution are analyzed for recognition of stacked depositional sequences. The gamma-ray log display provides a measure of sediment type, with curve deflections to the left suggesting increased sand content while high values to the right indicate increases in clay content. Use of multiple logs, especially spontaneous potential, resistivity, density, and velocity logs calibrated by well-cutting descriptions and formation microscanner displays, provides a data set for reliable rock type identification. The figure below illustrates an interpretation template for log motif analysis.

Patterns of forestepping vs. backstepping log-motif funnels can define transgressive vs. regressive depositional trends and candidate systems tracts and sequences. Vail and Wornardt (1990) and Armentrout et al. (1993) detail the process.

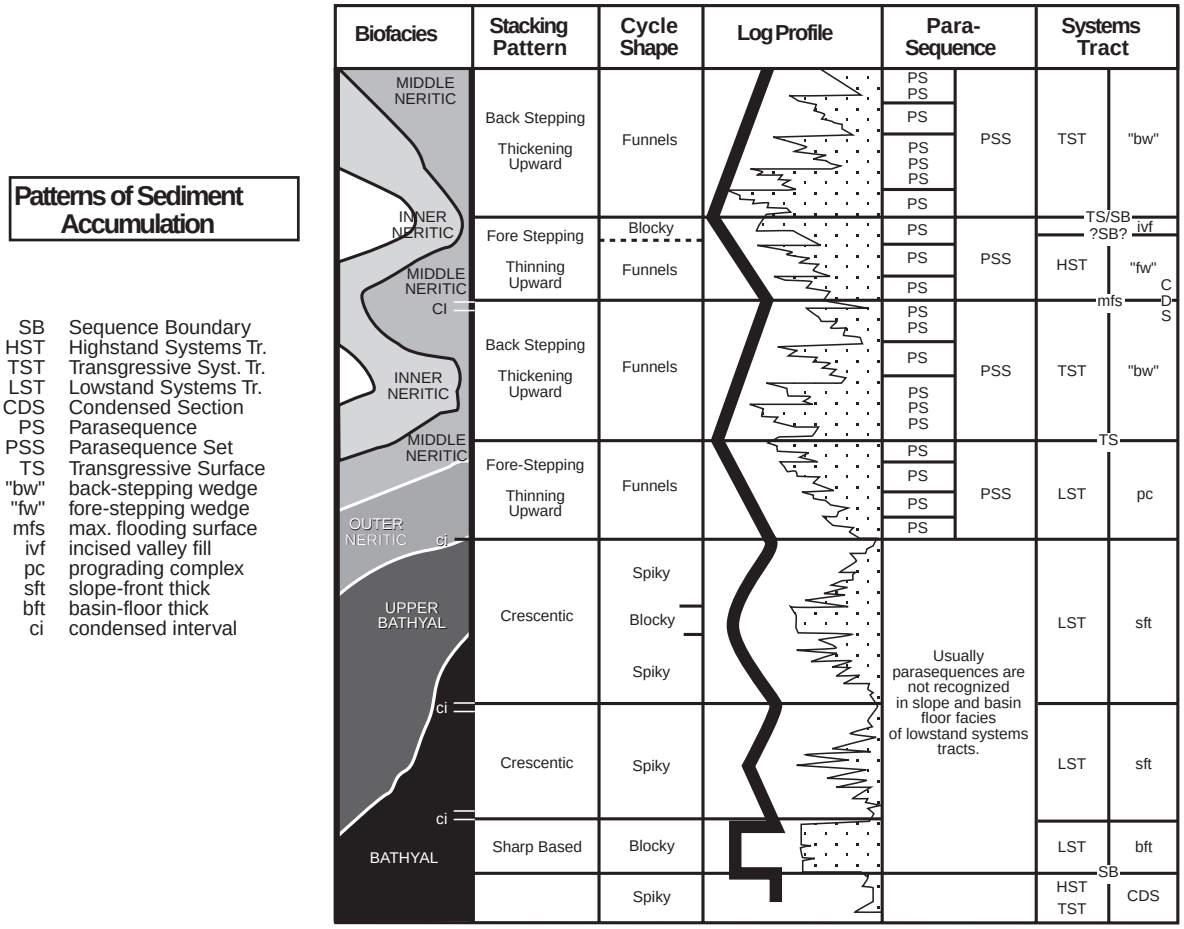

Figure 4–22. From Armentrout et al. (1993); courtesy The Geological Society of London.

GOM basin example chart

The histogram patterns of foraminiferal and calcareous nannoplankton abundance are shown on the next page for the South Galveston Mobil A-158 #3 well. The histogram is based on a detailed checklist of the relative abundance of each species of fossil in each well-cutting sample (Armentrout et al., 1990). Display of this data in two-way time facilitates integration with seismic reflection profiles using the synthetic seismogram to match

GOM basin example chart (continued)

the well data with the seismic reflection profile at the well site. Patterns of shallow vs. deep biofacies and fossil abundance (i.e., concentration vs. dilution) can be correlated with progradation of sandstone vs. mudstone interpreted from wireline log patterns. Bioevents (abbreviated acronyms such as 2B and SG) and faunal discontinuity events (abbreviated FDA-3 and FDA-4) provide correlation horizons between which the abundance patterns provide additional events for correlation (Armentrout, 1991).

In the histogram below (see Figure 4–17 for well location), the foraminiferal abundance scale is 0–1000 specimens and the nannoplankton abundance scale is 0–800 specimens. Biofacies include inner neritic (IN, 0–50 m), middle neritic (MN, 50–100 m), outer neritic (ON, 100–200 m), upper bathyal (UPPB, 200–500 m), middle bathyal (MDLB, 500–1000 m), and lower bathyal (LOWB, 1000–2000 m). This figure is the leftmost (southern) well panel in Figure 4–24. The wireline log (gamma ray) motif patterns (Figure 4–22), biostratigraphic abundance events, and extinction datums provide correlation events.

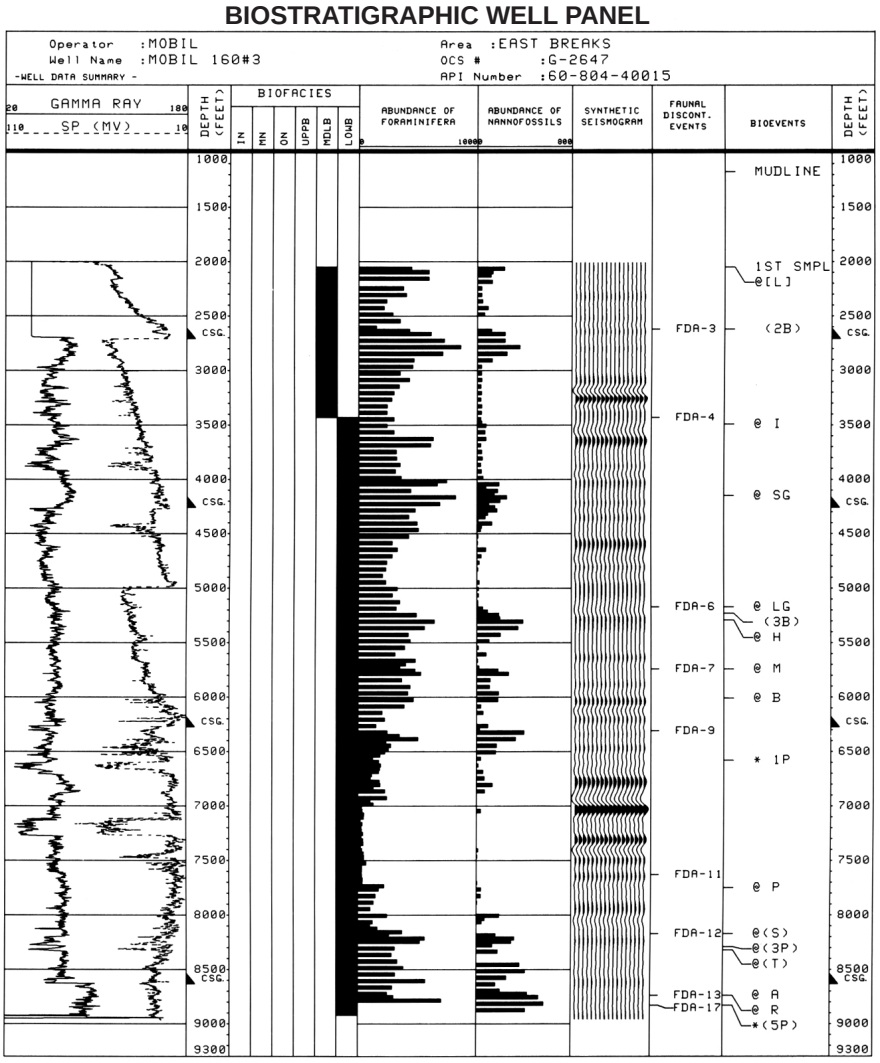

Figure 4–23. From Armentrout (1991, 1996); courtesy Springer-Verlag, Geological Society of London.

Recognizing Stacked Depositional Sequences from Well Data, continued

Biostratigraphic correlation of stacked sequences

The well correlation section on the next page is an example of using high-resolution biostratigraphic correlation to recognize depositional successions within stacked depositional sequences. In some basins containing nondescript fill that lacks unique marker beds, like the Gulf of Mexico, high-resolution biostratigraphic correlation is the best method for subdividing basin fill into sequences and systems tracts (Armentrout, 1987; Galloway, 1989a,b).

The four wells in the cross section are in a depositionally dip-oriented transect (Armentrout, 1996). The correlation horizons, based on seven chronostratigraphically significant bioevents (mostly extinction events), partition the strata into age-correlative intervals (Armentrout and Clement, 1990). Most of the chronostratigraphically significant bioevents occur in association with maximum fossil abundance, resulting in the interpretation of these correlation horizons as maximum flooding surface-condensed section data (Galloway, 1989a,b; Armentrout et al., 1990; Schaffer, 1987a,b, 1990; Armentrout, 1996).

Each well panel is formatted the same as Figure 4–23. The foraminiferal (left histogram) and calcareous nannoplankton (right histogram) abundance patterns of each well are very similar. Biostratigraphic correlation horizons (horizontal lines) provide ties between the wells, facilitating comparison between the abundance patterns and biofacies variations within each chronostratigraphic interval. Each correlation was checked against correlations independently constructed using a regional grid of seismic reflection profiles.

Identifying sequence in the GOB basin example

In Figure 4–24, candidates for maximum flooding surfaces are identified by abundance peaks in both foraminifera and nannoplankton and by extinction events known to be associated with regionally significant maximum transgressions (Armentrout and Clement, 1990; Schaffer, 1987a,b, 1990). Sequence boundary candidates occur between the maximum flooding surfaces and are identified by low abundance of fossils and by wireline log patterns. The northern wells (right) are rich in sand deposited in shallow water (neritic biofacies); sequence boundaries are likely to occur at the top of forestepping parasequence sets. The southern wells (left) are sand-poor shale deposited in deep water (bathyal biofacies); sequence boundaries are likely to occur at or slightly below flat-based blocky sands and at faunal abundance minima.

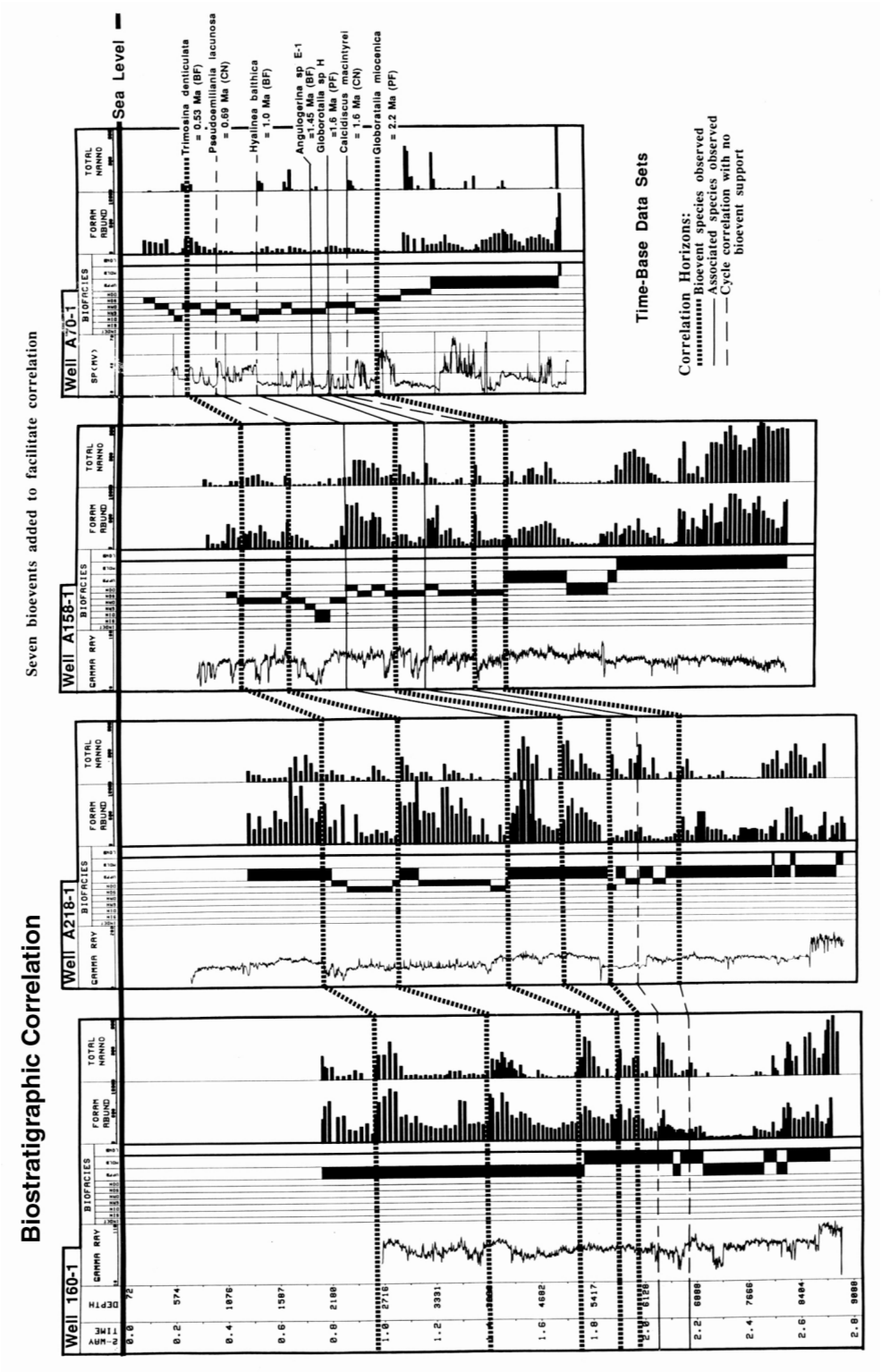

Figure 4–24. From Armentrout (1991, 1996); courtesy Springer-Verlag and The Geological Society of London.

Section D
Depositional Systems Tracts

Introduction

Subdivision of each sea level cycle into its depositional phases helps us construct high-frequency paleogeographic maps, one or more for each depositional systems tract. These maps help us predict reservoir and seal rock as well as delineate probable migration avenues. From integrated data sets, a high-resolution age model can be constructed and used to correlate and calibrate depositional sequences. Using the age model and stratigraphic thicknesses, rock accumulation rates of each cycle can be calculated and the thermal history for each depocenter reconstructed.

Subsection 1 of this section focuses on sea level cycle phase. Subsection 2 focuses on the use of paleogeography in petroleum exploration.

In this section

This section contains the following subsections.

Subsection D1
Sea Level Cycle Phase

Introduction

Depositional cycles can be subdivided into systems tracts, each representing a specific phase of relative sea level, e.g., highstand, falling (regressive), lowstand, and rising (transgressive). Nonmarine systems tracts can be related to rise and fall in lake level or water table level, which may or may not be synchronized with sea level change. [See Wheeler (1964) for a discussion of base level.] Identifying each cycle phase of a depositional sequence and mapping the contained facies provides a paleogeographic map for a relatively short time interval. Such high-resolution maps provide useful predictions for hydrocarbon prospecting. This subsection discusses the concept of sea level cycle phase, identification of cycle phase, construction of a cycle chart, and how sea level cycles of different duration interact.

In this subsection

This subsection contains the following topics.

Determining Sea Level Cycle Order

Introduction

One aspect of basin analysis focuses on mapping specific systems tracts of third-, fourth-, or fifth-order sea level cycles and the relationship that stacked depositional sequences deposited during those cycles have to each other. Knowing the order of a cycle or the phase of a cycle represented by a rock sequence is important for predicting the location and type of reservoir and seal and the location of potential source rocks.

Procedure

To determine cycle order of a sequence of sediments, we use biostratigraphic data, stratigraphic context (i.e., what part of a systems tract the interval is from), oxygen isotope curves, and published sea level curves. The table below suggests a procedure for determining cycle order of a rock sequence.

Step	Action
1	Determine the time span during which the sequence was deposited and compare to age ranges for cycle orders (see table below).
2	Determine the stratigraphic context of the sequence. What are the cycle orders for similar sequences above or below it?
3	Determine the age of the sequence and compare it to published sea level cycle curves (e.g., Haq et al., 1988).

Cycle order from thickness and areal extent

Because rates of sediment accumulation and areas of accommodation space vary, thickness and areal extent are of little use in establishing the order of depositional cycles. Most cycle hierarchies are based on duration. Establishing the duration of a sequence is difficult because of problems in high-resolution dating of rocks. However, with careful work an estimate can be made (see Miall, 1994; Armentrout, 1991, 1996).

Table of cycle order

Use the table below to help assess the sea level cycle order of a rock interval after Van Wagoner et al., 1990.

Cycle Order	Nomenclature	Thickness Range (ft)	Aerial Extent (mi^2)	Duration (Ma)	
				Range	Mode
1st	Megasequence	1000+	Global	50–100+	80
2nd	Supersequence	500–5000+	Regional	5–50	10
3rd	Sequence	500–1500	500–50,000	0.5–5	1
4th	Parasequence Set	20–800	20–2000	0.1–0.5	0.45
5th	Parasequence	10–200	20–2000	0.01–0.1	0.04

Determining Sea Level Cycle Order, continued

GOM basin example

The figure below shows the correlation of the third-order eustatic curve of Haq et al. (1988) and the oxygen isotope curve of Williams and Trainor (1987) with seven prograding clinoform intervals from the High Island South Addition in the GOM basin (see Figure 4–21). The correlations were established using the extinction events of the benthic foraminifera *Hyalinea balthica (Hyal B)* and *Trimosina denticulata (Trim A)* and the present-day sea floor as chronostratigraphic data. Six of the observed depositional cycles occur during the Tejas supersequence B 3.10 (0.8–0.0 Ma) third-order cycle of Haq et al. (1988). This correlation suggests that the local cycles are fourth-order depositional cycles with a duration of approximately 130,000 years each (see Mitchum and Van Wagoner, 1990).

The seven fourth-order cycles occur at approximately the same frequency as the oxygen isotope warm and cold cycles. The oxygen isotope cycles are interpreted as glacial-interglacial cycles corresponding with relative high- and lowstands of sea level (Williams and Trainor, 1987). The clinoforms generally correlate with trends in upward enrichment in isotope values, suggesting progradation during onset of glacial climates as a consequence of lowering sea level as continental ice formed.

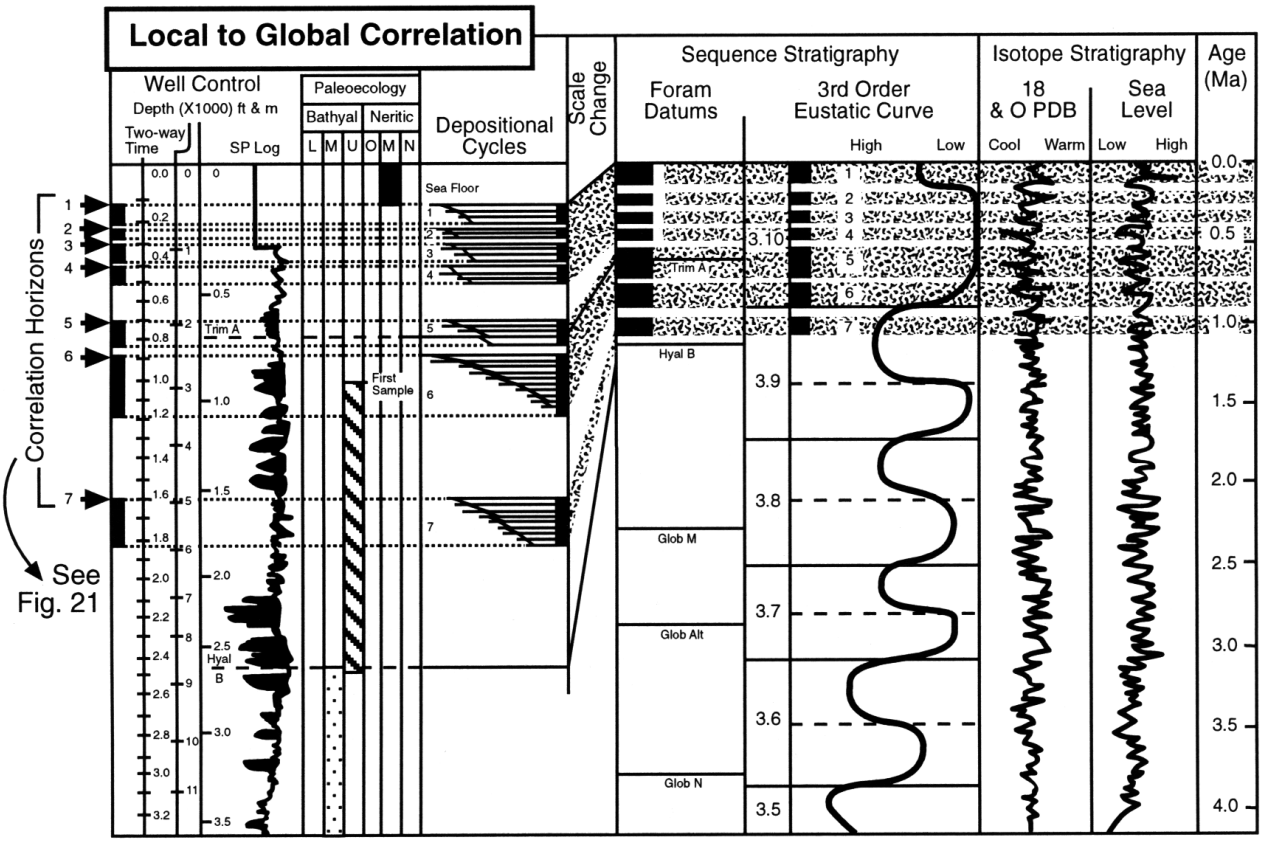

Figure 4–25. From Armentrout (1993); courtesy Gulf Coast SEPM.

Sea Level Cycle Phase and Systems Tracts

Phases of a sea level cycle

Each cycle can be subdivided into four phases of relative sea level change:

- Rising
- Highstand
- Falling
- Lowstand

The interpretation methodology of sequence stratigraphy helps us recognize each cycle phase and provides a nomenclature to describe each element (Vail, 1987; Jervey, 1988; Posamentier and Vail, 1988; Armentrout, 1991, 1996).

Cycle phase & sedimentation

Deposition or erosion of sediments depends on the interaction of cycle phase and the creation of accommodation space. The sediments comprising a depositional sequence are deposited during falling, lowstand, rising, and highstand phases of a sea level cycle. Erosion, which forms a critical element of the boundaries of a depositional sequence, generally occurs during falling sea level and lowstands (Vail, 1987). Within the basin depocenter, the sequence boundary consists of a conformity that correlates with the erosional unconformity along the basin margin.

Systems tracts

Systems tracts are composed of all deposits accumulating during one phase of relative sea level cycle and preserved between specific primary chronostratigraphic surfaces (Brown and Fisher, 1977). Erosion usually dominates the falling phase of a sea level cycle, and the deposited sediments are most often assigned to the lowstand systems tract.

Lowstand systems tracts

The lowstand systems tract occurs between the basal sequence boundary and the transgressive surface. Lowstand systems are thickest toward basin centers because much of the basin margin is undergoing erosion. Lowstand systems with shelf-to-slope geometries may have basin center gravity-flow deposits due to sediment bypass of the slope and thick shelf-edge deltaic systems prograding into deep water. Fluvially dominated depositional systems are common.

Transgressive systems tracts

The transgressive systems tract encompasses those deposits between the transgressive surface and maximum flooding surface. Transgressive systems tracts show landward-stepping depositional patterns and basin margin onlap due to relative rise in sea level, forcing sediment accumulation toward the basin margin. The basin center is likely to become progressively more sediment starved, and coastal depositional systems may show a strong tidal influence.

Highstand systems tracts

The highstand systems tract is between the maximum flooding surface and the overlying sequence boundary. Highstand systems tracts show a progradational stacking pattern due to sediment supply exceeding the accommodation space. Progradation results in basinward downlapping onto the maximum flooding surface. Basin centers may still be sediment starved if shelves are broad. Coastal depositional systems tend to be wave to fluvially dominated, thin, and widespread. Definition and further discussion on identifying characteristics of each of the surface types and systems tracts can be found in Posamentier and Vail (1988), Loutit et al. (1988), Van Wagoner et al. (1990), and Armentrout (1991, 1996).

Identifying Systems Tracts

Introduction

Certain types of hydrocarbon traps are more commonly associated with a particular depositional systems tract. Identifying the highstand, lowstand, or transgressive systems tract and the specific depositional environments within each lets us predict possible reservoir, seal, and charge system for each potential trap.

Methods

Identifying a depositional systems tract can be achieved by analyzing seismic geometries (Figures 4–19 and 4–21), wireline logs motif (Figure 4–22), and biostratigraphic data (Figures 4–20 and 4–23). Carefully integrating multiple data sets increases the probability of a correct interpretation (see Armentrout, 1991, 1996; Armentrout et al., 1993; Vail and Wornardt, 1990).

Stratal pattern simulation

The figure below shows the computer-simulated stacking pattern of stratal units within an unconformity-bound depositional sequence. [For computer modeling, see Jervey (1988).] The simulation forces all sediment to be deposited within the 2-D plain of the diagram. In the natural world, the depositional thicks associated with each systems tract are likely to occur lateral to each other, and their recognition requires a 3-D data set. Additionally, postdepositional deformation and erosion significantly modify the idealized geometry shown in Figures 4–18 and 4–26.

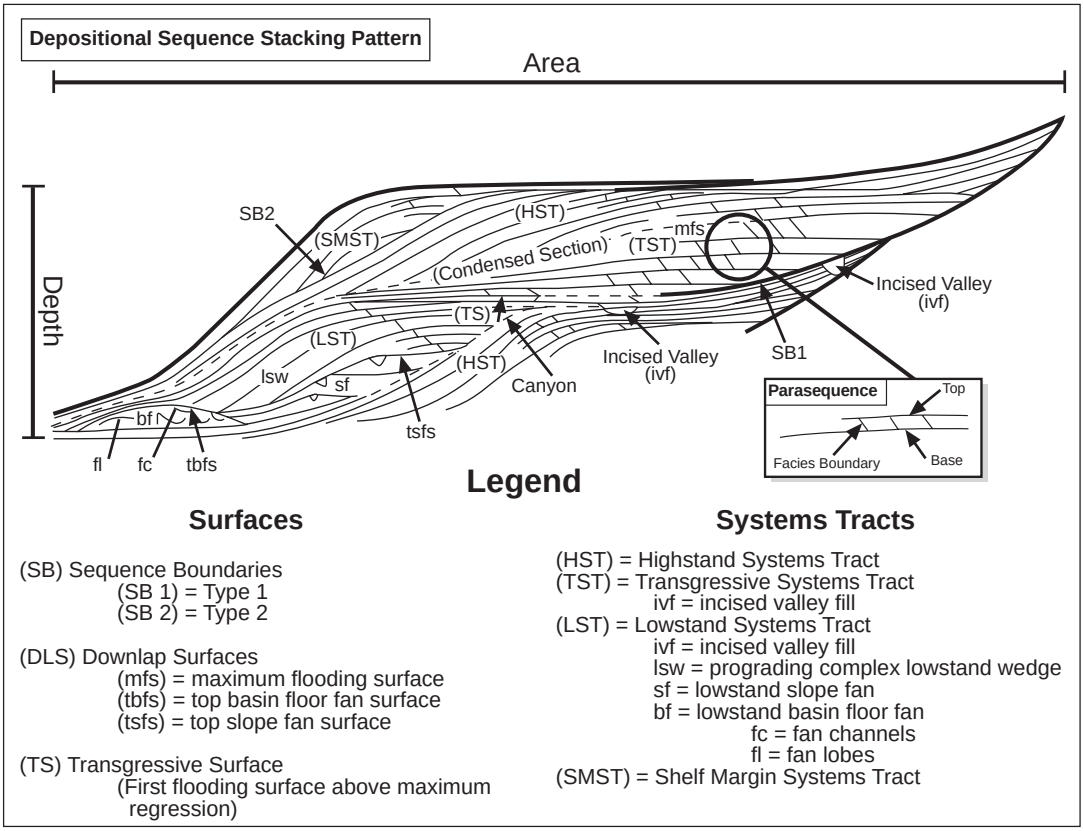

Figure 4–26. Modified from Haq et al. (1988); courtesy SEPM.

Identifying Systems Tracts, continued

Parasequences

For transgressive and regressive shallow-water facies, each of the depositional layers is called a parasequence; they stack into parasequence sets (Van Wagoner et al., 1990). More basinal facies deposited well below wave influence reflect gravity-flow processes and are not called parasequences (Van Wagoner et al., 1990; Vail and Wornardt, 1990). The depositional sequence lithofacies diagram is presented in Posamentier and Vail (1988) for siliciclastics and in Sarg (1988) for carbonate rocks.

Interpreting parasequence sets

Stratal geometries that show parasequences stacked into sets that forestep progressively toward the basin center reflect progradation from the sediment supply exceeding the accommodation space; those that stack into sets that backstep progressively toward the basin margin reflect transgression from an increase in accommodation space that exceeds the sediment supply (Figure 4–22). Progradation of parasequence sets basinward of their age-equivalent shelf edge are, by definition, the lowstand prograding complex; parasequence sets prograding from the basin margin to the age-equivalent shelf margin may be either highstand prograding complexes or shelf margin systems tracts. The absence of a well-defined shelf/slope break complicates recognition of highstand vs. lowstand systems tracts.

Interpretation of stratal patterns example

Relative changes in sea level can also be inferred from detailed analysis of local depositional geometries on seismic reflection profiles. On the seismic reflection profile schematic below (from Armentrout, 1987), clinoforms 1–5 pinch out with toplap against a common horizon, suggesting oblique clinoforms (Mitchum et al., 1977). These oblique clinoforms can be interpreted as forming when sediment supply exceeds the accommodation space and causes shelf-margin progradation; sea level falls at the same rate as subsidence, completely bypassing the shelf with no accumulation of seismic-scale topset beds. Clinoforms 6 and 7 are sigmoidal (Mitchum et al., 1977). These can be interpreted as sediment supply exceeding accommodation space, forcing progradation but with subsidence exceeding the relative change in sea level and consequent accumulation of topset beds. The change from no topset beds to aggradational topset beds indicates a turnaround from apparent stillstand to apparent rise in sea level at the site of deposition.

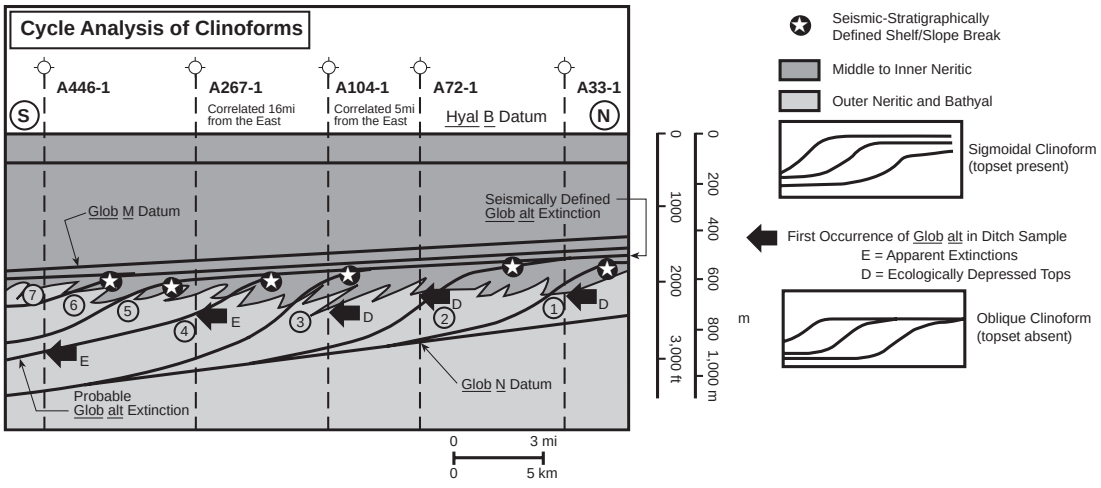

Figure 4–27. From Armentrout (1987); courtesy Gulf Coast SEPM.

Time significance of seismic reflections

Using seismic reflection geometries to suggest relative sea level phase requires confidence in the coeval character of seismic reflections. The first downhole occurrence of *Glob alt (Globoquadrina altispira,* bold arrows) in Figure 4–27 suggests a correlation cross-cutting the seismically imaged clinoforms. If the *Glob alt* occurrences are coeval, the seismic reflections are time transgressive.

Note that the first downhole well-cutting sample occurrence of the bioevent *Glob alt* is at the interface of outer neritic and upper bathyal biofacies, except in the two southern wells, A446-1 and A267-1, where the first occurrences occur within stratigraphic intervals containing bathyal biofacies. *Glob alt* is a planktonic foraminifer normally found associated with open marine faunas and floras interpreted as upper bathyal assemblages. The occurrences of *Glob alt* coincident with the first upper bathyal biofacies assemblage suggests a facies-controlled top, depressed below the true extinction top by environmental factors. The two occurrences within upper bathyal biofacies are interpreted as true extinction events. These true extinction events correlate with a seismic reflection, suggesting that specific reflection approximates a time line and can be used to extend the *Glob alt* extinction event datum (2.8 Ma) northward toward the basin margin (see Armentrout and Clement, 1990).

This type of bioevent analysis is essential when identifying chronostratigraphically useful bioevents and demonstrating that seismic reflections approximate time lines (Vail et al., 1977).

Systems Tracts and Trap Types

Introduction

Each systems tract—highstand, lowstand, and transgressive—has a different trapping potential based on the vertical and lateral distribution of lithofacies deposited within specific depositional environments. White (1980) presents an excellent review of trap types within facies-cycle wedges, which are related to transgressive-regressive cycles and can be related most specifically to the transgressive systems tract and the highstand systems tract. In White's classification, prograding lithofacies of the lowstand systems tract might occur as subunconformity traps or might be mistakenly identified as highstand systems tract deposits. Gravity-flow deposits of slope and basin-floor fan systems are most often placed into the lowstand systems tract because they are deposited basinward of the shelf/slope inflection.

White (1980) discusses both siliciclastic and carbonate systems. Sarg (1988) provides an excellent discussion of carbonate systems. Only siliciclastic systems, similar to those of the Cenozoic of the central and western Gulf of Mexico, are discussed here.

Lowstand systems tract traps

Lowstand gravity-flow, sand-prone reservoirs occur in basin-floor and slope systems. They are most often encased within marine hemipelagic mudstones, which serve as seal and sometimes potential source rock. Traps are often stratigraphic, but postdepositional deformation that places the gravity-flow sand deposit in a structurally high position enhances the potential for focused migration of hydrocarbon fluids to the reservoir facies (Mitchum, 1985).

Lowstand prograding complex traps

Siliciclastic lowstand prograding complexes, imaged on seismic reflection profiles as clinoforms, are often fluvial-deltaic complexes with abundant sand in the depositional topsets (Figures 4–19 and 4–21). As the relative sea level cycle turns around from low to rising, the coarse-grained sediment supply decreases. The fine-grained sediments of the transgressive systems tract overlie the lowstand systems tract–prograding complex sand-prone facies, providing excellent top seal to the underlying sandy reservoir. If the transgressive shales are organic rich and buried in the thermal regime for kerogen cracking, hydrocarbons will be generated. If the lithofacies forming the preceding shelf edge can provide lateral seal, the prograding complex reservoir facies may become charged with hydrocarbons even without structural enhancement of the trap (Armentrout et al., 1997).

Transgressive systems tract traps

Transgressive systems tracts step toward the basin margin, with mud-prone facies overlying most of the sand-prone deposits, providing good top seal and often potential source rock to the underlying sands. However, because of the landward-stepping character of this systems tract, the sand-prone depositional facies are not likely to be very thick, resulting in volumetrically smaller reservoirs. Traps can be purely stratigraphic or enhanced with postdepositional structuring that focuses migration (White, 1980). However, the landward-stepping sand-prone facies may prevent adequate lateral seal for stratigraphic traps.

Systems Tracts and Trap Types, continued

Highstand systems tract traps

Highstand systems tracts step toward the basin center and often prograde at the expense of the preceding parasequence due to erosion during relative fall of sea level. The falling sea level also decreases the space into which the sediment can accumulate, resulting in potentially rapid lateral shifting of the prograding deltaic lobes. This results in relatively thin but widespread sand-prone facies. An effective top seal for such a highstand system would require a very major transgression well landward of the updip end of the sandy facies of the prograding coastal plain (White, 1980). Such a transgression could be eustatic or tectonic in nature, as in a rapidly subsiding foreland basin setting. Postdepositional deformation forming anticlines enhances the potential for entrapping hydrocarbons in sheet-like highstand systems tract reservoirs.

Shelf margin systems tract traps

Shelf-margin systems tracts are the lowstand deposits of a type 2 sequence. Type 2 sequences are deposited when relative sea level falls but not below the preceding depositional inflection. Type 1 sequences are deposited when relative sea level falls below the preceding depositional systems tract (Van Wagoner et al., 1990). The subsequent transgression may provide effective top seal, but the lateral seal of shelf margin systems tracts shares the same limitations as the highstand systems tract.

Early sequence stratigraphic studies, based largely on seismic reflection profiles, used the shelf edge as the depositional inflection reference point (Vail and Todd, 1981; Vail et al., 1984). Subsequent work on outcrops and high-resolution seismic reflection profiles redefined the deposition inflection as the shoreline break (Van Wagoner et al., 1990). The shoreline break is generally coincident with the seaward end of the stream mouth bar in a delta or the upper shoreface in a beach environment. This change in depositional inflection scale results in nearly all seismically recognized lowstand deposits being attributed to type 1 sequences. Because the GOM basin analysis relies largely on seismic reflection profiles, all lowstand deposits are referenced to shelf-edge inflection points.

Systems tracts with greatest trapping potential

White (1980) compiles data on the depositional setting of more than 2000 major oil and gas fields in 200 transgressive and regressive wedges within 80 basins. With clearly stated qualifications, White shows that most hydrocarbons found in siliciclastic reservoirs occur in the base to middle of the wedge in generally lowstand to transgressive depositional facies. This can be attributed to the greater probability of effective top seal in contrast to the highstand systems tract. By using the stratal stacking pattern, supplemented by lithofacies and biofacies data, depositional environments can be properly identified and paleogeographic maps constructed for each systems tract to predict between and beyond data points.

Identifying Sea Level Cycle Phase with Biostratigraphy

Introduction

In basin depocenters, much of the stratigraphic record consists of deposits accumulated during relative lowstand of sea level. These lowstand deposits are separated by condensed intervals containing the distal aspects of the transgressive and highstand systems tracts. Because most of the section is claystone and silty claystone, fossil abundance patterns provide regionally applicable criteria for recognizing systems tracts within a depositional sequence. Upward-increasing fossil abundance suggests rising relative sea level with consequent fossil concentration due to decreasing sediment input. Upward-decreasing fossil abundance suggests falling relative sea level with consequent fossil dilution due to increasing sediment input. Because these strata are largely basinal depocenter deposits of lowstand and condensed section sedimentation, the falling and rising phase of relative sea level changes are correlated to the early phase of lowstand fall and the late phase of lowstand to transgressive rise, respectively.

Example

Within the GOM basin study area, sediment-starved highstand and transgressive deposits merge into the condensed interval. Thick transgressive and highstand deposits occur to the north and in the upper strata of the study area due to the regionally progradational section (Armentrout, 1991). The figure below is a spontaneous potential (SP) well log illustrating the subdivision of the *Glob alt* depositional cycle into the mapping intervals for slope and basin facies. The upper and lower data correlate with locally significant condensed sections at 2.8 and 3.1 Ma (Figure 4–31). The strata between these two condensed sections are divided into presandstone, sandstone, and postsandstone intervals, based on the dominant rock type and the pattern of fossil abundance and biofacies.

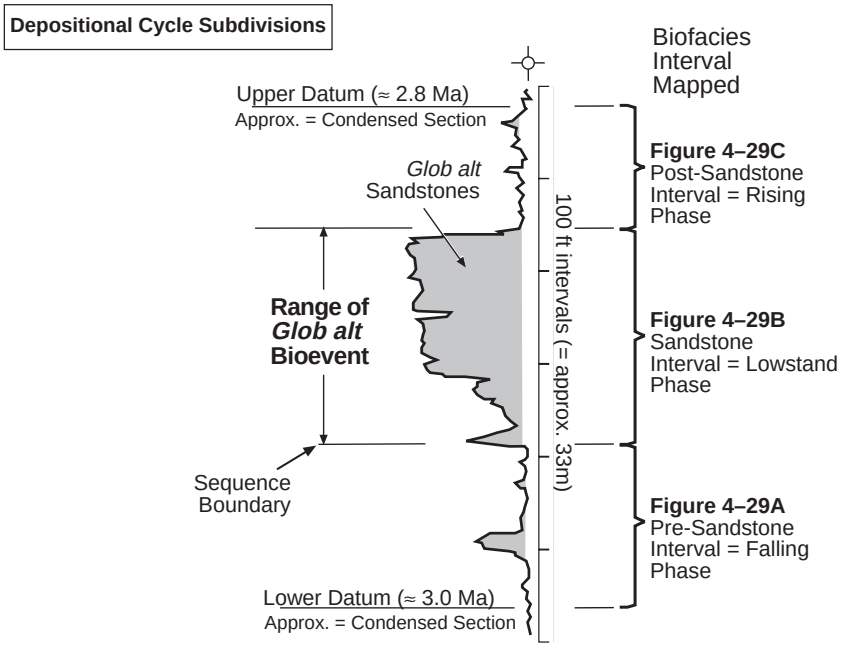

Figure 4–28. After Armentrout (1991, 1996); courtesy Springer-Verlag, Geological Society of London.

Identifying Sea Level Cycle Phase with Biostratigraphy, continued

Interpretation of example

Because of the basinal location of the *Glob alt* depositional thick, the biofacies are typically bathyal. In this setting, the presandstone interval has upward-decreasing fossil abundance away from the fossil abundance peak in the underlying condensed section. This pattern suggests increased rates of sediment accumulation vs. biotic productivity, interpreted as signals of falling sea level. Conversely, the postsandstone interval typically has upward-increasing fossil abundance toward the overlying condensed section. This pattern suggests decreased rates of sediment accumulation vs. biotic productivity and is interpreted as a signal of rising sea level and consequent sediment starvation at the sample site. The sandstone interval typically has few fossils, and those few may reflect very shallow water depths due to downslope transport of the sand by gravity-flow processes. Data from shelf environments have a different set of interpretation criteria (see Armentrout et al., 1990; Armentrout, 1996).

Example of mapping systems tracts

Patterns of biofacies distribution reinforce other lines of evidence for variations in relative sea level, such as those illustrated by the distribution of clinoforms (Figure 4–27). When overlain on maps of lithofacies and seismic facies, biofacies patterns that complement other environmental interpretations increase confidence in reconstructions of the geologic history of the study area, including depositional cycle definition and subdivision and facies distribution of potential reservoir and seal rocks (see Armentrout et al., 1999).

Biofacies assemblage

Fossil biofacies, calibrated by similarity to modern assemblages, provide information on the type of environment in which specific strata were deposited. Biofacies maps are one type of paleogeographic reconstruction.

Example biofacies maps

The following figure shows biofacies maps of the study area in the Gulf of Mexico. They are based on the subdivision of the *Glob alt* depositional cycle into presandstone, sandstone, and postsandstone intervals. The importance of these maps is their relationship to lithofacies distribution for potential reservoir rock, seal rock, and source rock. Part A is a presandstone interval map, showing a basinward excursion of outer neritic and upper bathyal biofacies forced basinward by falling sea level Part B is a sandstone interval map in which the biofacies excursion is less pronounced, reflecting maximum lowstand at the turnaround from falling to rising sea level. Part C is the postsandstone interval in which the biofacies excursion is absent due to relative rise of sea level.

Example biofacies maps (continued)

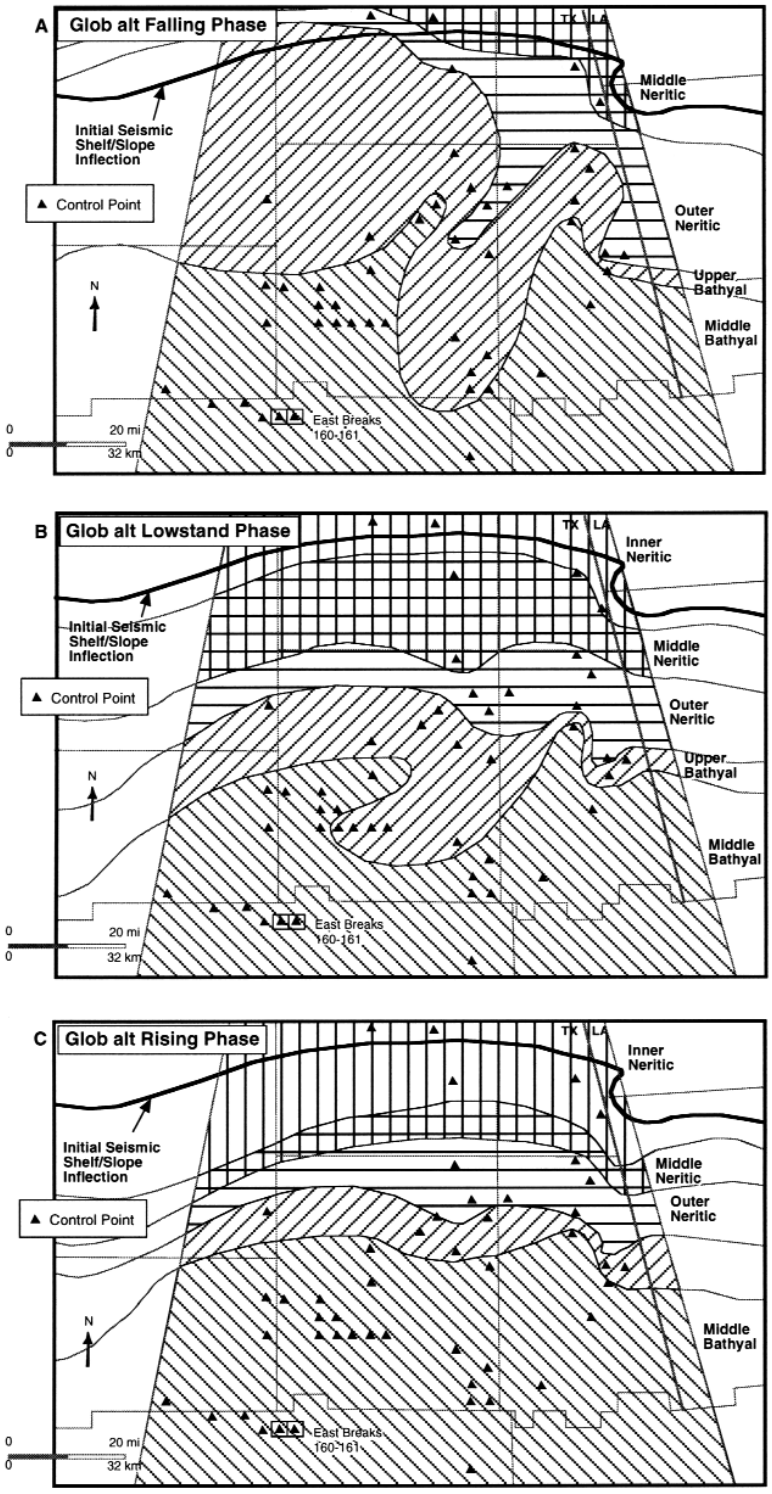

Figure 4–29. After Armentrout (1991, 1996); courtesy Springer-Verlag, Geological Society of London.

Interpreting the maps

Biofacies map patterns are defined by distribution of benthic foraminiferal biofacies (Armentrout, 1991, 1996). Figure 4–29 shows the biofacies distribution below, within, and above the *Glob alt* sandstone interval. In upward stratigraphic order, these intervals are interpreted as the sediment accumulated during (1) falling, (2) low, and (3) rising phases of sea level, respectively. A scenario to explain biofacies and sediment patterns in the example is as follows.

1. During the lowering of sea level, the biofacies distributions and sites of maximum sediment accumulation move seaward (Figure 4–29A) where they are deposited on top of the preceding condensed section and associated maximum flooding surface (Figure 4–18). Within the initial lowering phase, the rate of slope and intraslope basin sediment accumulation increases, with fine-grained deposits above the underlying condensed section. As lowering progresses, the river systems bypass sediment across the shelf, depositing it directly on the upper slope. Remobilized sand and sand supplied directly from rivers during floods may be transported downslope by gravity-flow processes, depositing potential reservoirs (Prior et al., 1987). These sands accumulate at changes in the depositional gradient as slope fan and basin-floor fan deposits within the intraslope basins (minibasins) (Bouma, 1982).
2. The biofacies associated with this lowstand depositional phase, the sandstone interval (Figure 4–29B), show similar basinward excursion in outer neritic and upper bathyal biofacies as deposited during the presandstone phase. The inner and middle neritic shallow-water biofacies of the sandstone interval show a seaward shift, relative to the seismic stratigraphically defined shelf/slope break—interpreted as an indication of coastal progradation associated with lowered sea level.
3. Once sea level begins to rise, the supply of sand-rich sediment to the basinal slope area is rapidly cut off. Mud accumulates during this postsandstone interval, culminating with the overlying upper condensed section. These mudstones and those of the presandstone interval provide a seal for the interbedded lowstand sandstones. The biofacies pattern for this postsandstone interval shows a northward shift toward the basin margin as the coastline regresses across the shelf during transgression (Figure 4–29C). The occurrences of neritic biofacies of the postsandstone interval do not shift northward as far as their position during the presandstone interval. This is interpreted as sediment accumulation rate exceeding the rate of accommodation space formation by sea level rise plus basin subsidence. The consequence is coastal progradation, as suggested by comparing the mapped patterns of presandstone and postsandstone biofacies in the High Island–East Addition area just west of the seaward extension of the Texas/Louisiana border.

Biofacies and Changing Sea Level

Introduction

Biofacies are identified by an assemblage of fossils and are interpreted to reflect a specific environment. The mapped distribution of the biofacies assemblage reflects the distribution of the interpreted environment. Biofacies are especially useful in mudstone-dominated facies such as the GOM basin Cenozoic strata.

Traditional biofacies model

The traditional biofacies model is based on the modern distribution of organisms (Hedgpeth, 1957). This is a good model for a relative highstand of sea level (see figure below), in which neritic biofacies occur mostly on the shelf and bathyal biofacies occur mostly on the slope.

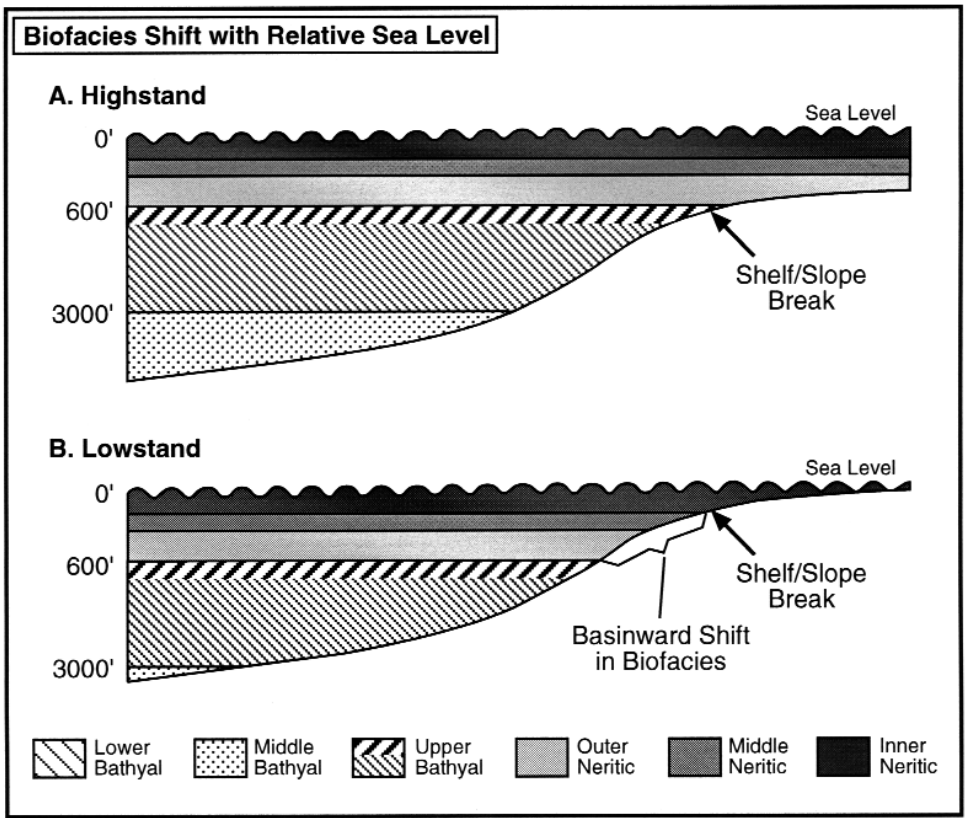

Figure 4–30. After Armentrout (1991, 1996); courtesy Springer-Verlag, Geological Society of London.

Biofacies distribution during lowstand

The lowering of sea level moves the water mass- and substrate-linked biofacies assemblages seaward—possibly far enough to place the inner neritic biofacies at the physiographic shelf/slope break. This movement causes the middle to outer neritic biofacies to shift basinward onto the upper slope of the clinoform (Figure 4–30B). The magnitude of relative sea level fluctuation, as well as the angle of the basin slope, controls how far the biofacies move across the physiographic profile. This pattern of low sea level biofacies distribution is confusing because the commonly used biofacies nomenclature is based on high sea level patterns where, by convention, the neritic biofacies are on the shelf (Figure 4–30A). During a lowstand, neritic biofacies may occur in situ on the physiographic slope.

Biofacies and Changing Sea Level, continued

Holocene GOM basin example

On the Gulf of Mexico shelf, elements of the foraminiferal fauna also move in the seaward direction due to the modification of the environment by the Mississippi River (Poag, 1981). High rates of deltaic sedimentation with coarser sediment grains, abundant terrigenous organic matter, and modified salinity and temperature greatly affect the local environment. Biofacies distribution responds to these environmental modifications. [See Pflum and Freichs (1976) for a discussion of the delta-depressed fauna.]

Lowstand fluvial influence on biofacies

At times of low sea level, when the river systems discharge their sediment load directly on the upper slope, the inclined depositional surface may help sustain downslope transport of the terrigenous material and associated fluids. The modification of the local slope environment near the sediment input point could result in seaward excursions in ecological patterns similar to those caused on the shelf by the modern Mississippi River (Pflum and Freichs, 1976; Poag, 1981). These seaward ecological excursions could extend to bathyal depths where downslope transport is sustained by the inclined surface and gravity-flow processes (see Figure 4–29).

Biofacies mixing

The downslope transport of shallow-water faunas by sediment gravity-flow processes may result in the mixing of biofacies assemblages from different environments (Woodbury et al., 1973). The further mixing of stratigraphically separate assemblages by rotary drilling complicates the identification of mixed assemblages. Such problems can be overcome in three ways:

1. Careful sample analysis, specifically looking for mixed assemblages
2. Use of closely spaced sidewall cores that may sample unmixed in situ assemblages occurring in beds interbedded with displaced assemblages
3. Evaluation of the mapped pattern of age-equivalent interpretations from a large number of wells

Armentrout (1991, 1996) carefully reexamines rapid changes of biofacies and patterns of rapid biofacies variations within age-equivalent intervals between wells. Once these local patterns were reevaluated and accepted as reliable, the interpretations were mapped for each depositional sequence. Figure 4–29 is the results of this analysis and further supports the biofacies models of Figure 4–30.

Constructing Age Model Charts

What is an age model?

Detailed correlation of depositional sequences and the calculation of maturation and timing of generation vs. trap formation requires an age model for the stratigraphy of a study area. An age model is a chart showing the chronostratigraphic relationship of different depositional sequences and associated formations within a study area. Integration of biostratigraphy and depositional sequences and their correlation to a global geologic time scale provides such an age model. Using this age model to calibrate each depositional sequence lets us calculate geologic rates, such as rates of rock accumulation and burial and thermal heating rates of the stratigraphic section.

Procedure

The chart below outlines the procedure for constructing an age model.

Step	Action
1	Construct a depositional sequence chart for the study area. Use all available depositional sequence and biostratigraphic data.
2	Normalize all available sequence charts for the basin, including the study area sequence chart, to the same time scale using the bioevent marker taxa or zonal assemblages.
3	Make a sum of sequences curve by integrating the depositional sequence chart for the study area with the other sequence charts for the basin.
4	Calibrate the sum of sequences curve to a global time scale using global biostratigraphic zones, magnetostratigraphic polarity scales, oxygen isotope chronology, and global sea level cycle charts.

Example

Constructing depositional cycle charts for the GOM basin extends back to at least Kolb and Van Lopik (1958) and Frasier (1974), with Beard et al. (1982) demonstrating the link between depositional sequences and glacial eustasy. The following figure is a composite chronostratigraphic chart that serves as an age model for the GOM basin Pliocene and Pleistocene, summarizing nine studies published between 1982 and 1993. The local cycle charts from each of these studies have been calibrated to the same time scale using the same bioevent marker taxa and are in turn correlated to the global foraminiferal zones and magnetostratigraphic polarity scale as defined by Berggren et al. (1985) and the oxygen isotope chronology of Joyce et al. (1990). The resulting sum of the depositional sequences and their associated condensed sections (Schaffer, 1987a,b, 1990) are illustrated.

The composite of all the local studies appears under the column Sum of Sequences, three of which occur in only one or two studies and are considered to be local and possibly autocyclic events (locally forced redistribution of sediments). The youngest six cycles of the chart occur between the *Pseudoemiliani lacunosa* bioevent (0.8 Ma) and the sea floor (0.0 Ma) and average 130,000 years in duration. The ten older cycles were deposited between *Globigerinoides mitra* (4.15 Ma) and *P. lacunosa* (0.8 Ma) bioevents and average 330,000 years duration. These 16 cycles are interpreted as regionally significant and allocyclic (forced by changes external to the sedimentary unit). They are probably glacioeustatic cycles. (See Figure 4–25 and accompanying discussion.)

Constructing Age Model Charts, continued

Example
(continued)

Age Model, GOM Pliocene–Pleistocene

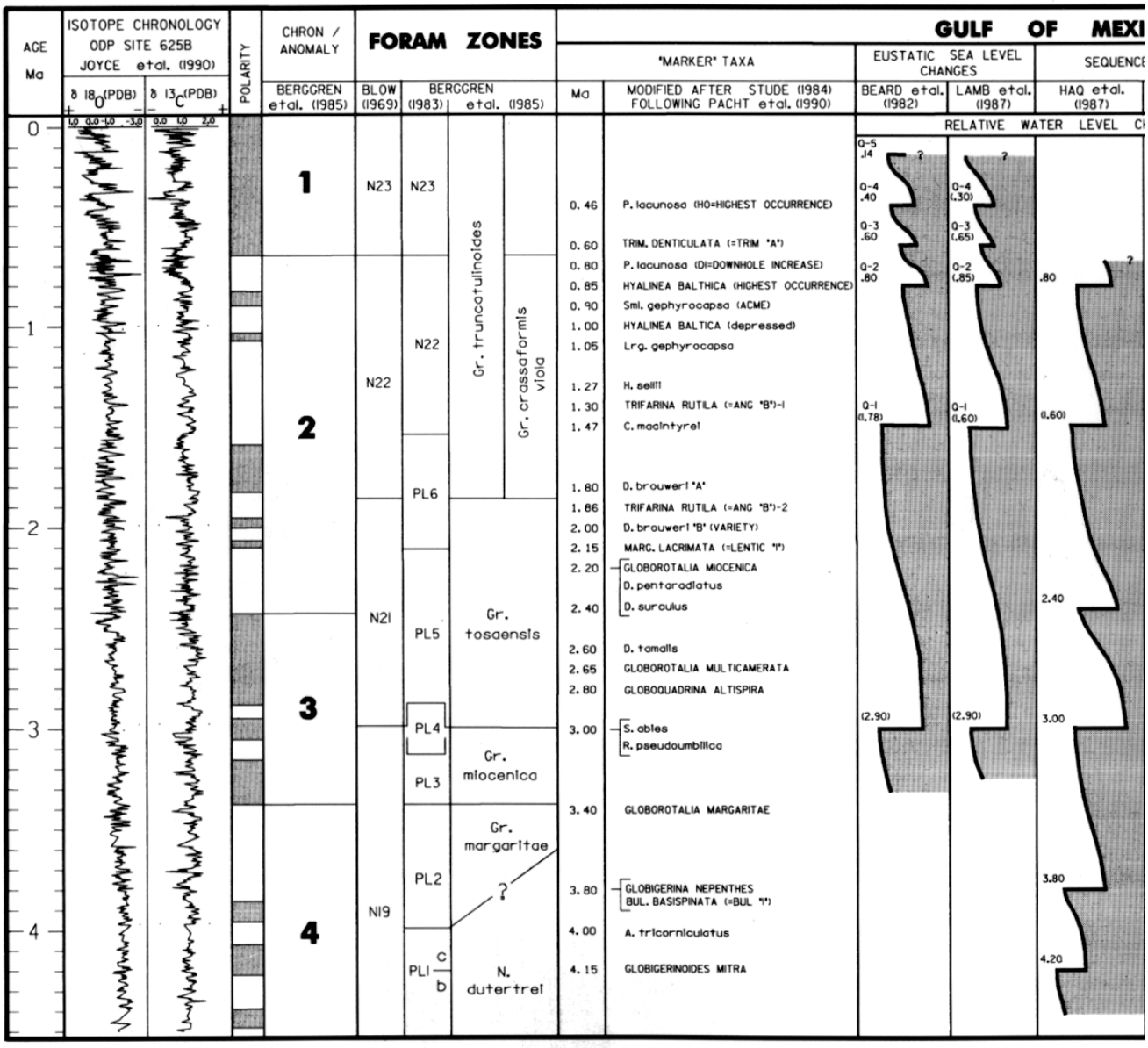

Global Record

GOMB Bioevents

GOMB Exploration Well Sequence Patterns

Figure 4–31. From Armentrout (1996); courtesy The Geological Society, London.

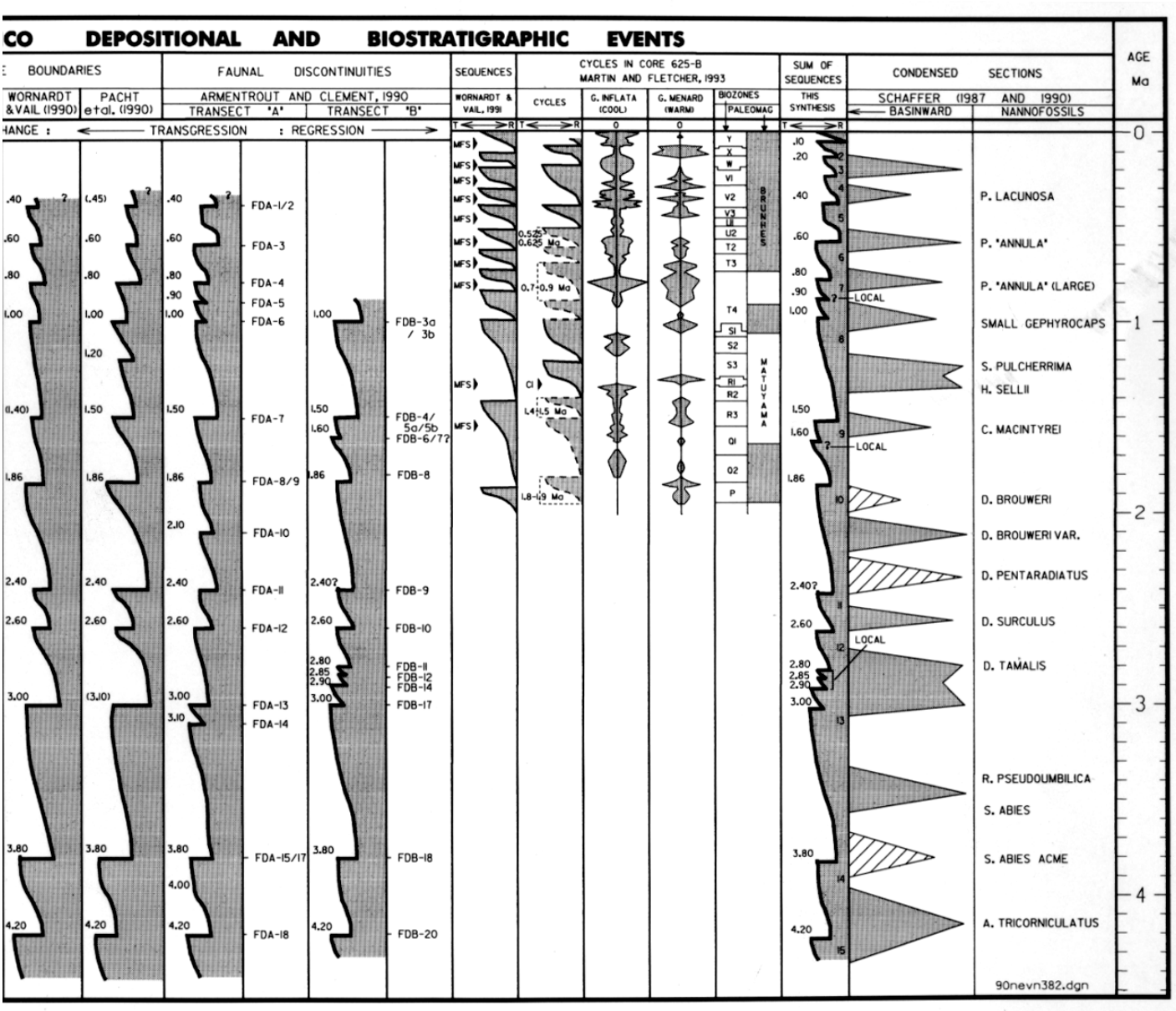

GOMB ODP-Core Sequence Patterns

GOMB "Sum of Sequences"

Constructing Age Model Charts, continued

Example (continued)

Using this age model to calibrate each depositional cycle helps us calculate geologic rates, such as rates of rock accumulation and burial and thermal heating rates of the stratigraphic section.

The following figure shows a rock thickness vs. time plot for nine key wells south of eastern Louisiana within the area of the 6–4 Ma depocenter (Figure 4–13; see also Fiduk and Behrens, 1993). Each major depositional interval is characterized by changes in depositional rates from oldest to youngest, in large part due to the geographic shifting of depositional centers. Dating within the wells is based on key biostratigraphic marker species for the deep-water environments of the GOM basin. Interval B is characterized by high rates of sedimentation associated with abundant gravity-flow sand deposition. It is followed by interval C, characterized by slow sedimentation and deposition of regionally effective top seal.

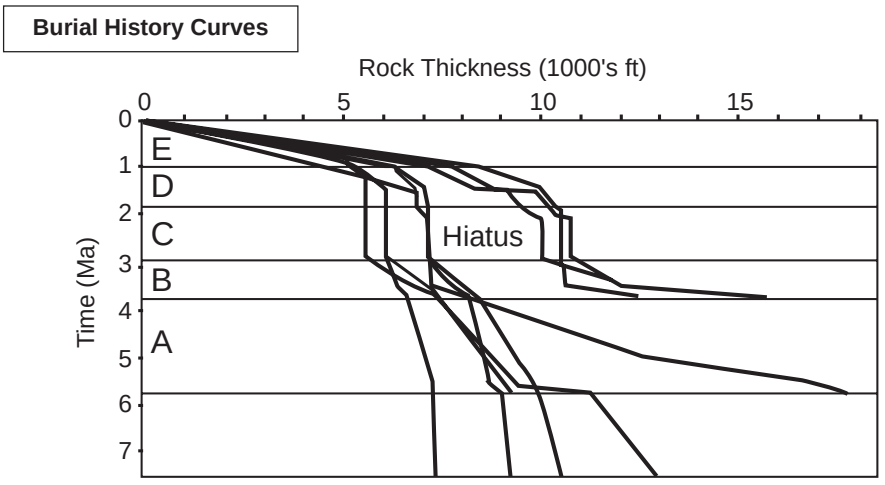

Figure 4–32. After Piggott and Pulham (1993); courtesy Gulf Coast SEPM

Example of modeling oil generation

The figure on the following page shows the rock accumulation rates for the Green Canyon 166 No. 1 well as a histogram (lower graph) and as a set of burial history curves (upper graph). Using temperature data from exploration wells, Piggott and Pulham (1993) calculated temperature thresholds for the accumulated stratigraphic section. Burial of potential marine source rock above a temperature of approximately 100°C could initiate generation of oil.

Example of modeling oil generation (continued)

The dominant hydrocarbon type in the Green Canyon area is associated with hydrocarbon family 6 (Figure 4–5), suggesting a Jurassic source rock. This source rock is indicated by the diamond labeled S and the shaded stratigraphic intervals. Based on the calculation of Piggott and Pulham (1993), using BP Exploration's Theta Modeling, generation of significant oil from a Jurassic source rock may have begun approximately 6 Ma in the Green Canyon 166 No. 1 well area when the Jurassic source rock was buried below 5000 m and above a temperature of 120°C, the threshold for significant oil generation (see "Petroleum Systems").

These calculations of rock accumulation and source rock maturation rates are dependent on good age models. Biostratigraphic data are the primary correlation tools in the GOM basin, as in most basins. Considerable care must be used in correlating basin bioevents to the global geologic time scale. The methodology for and problem of such correlations are discussed in Armentrout and Clement (1990) and Armentrout (1991, 1996).

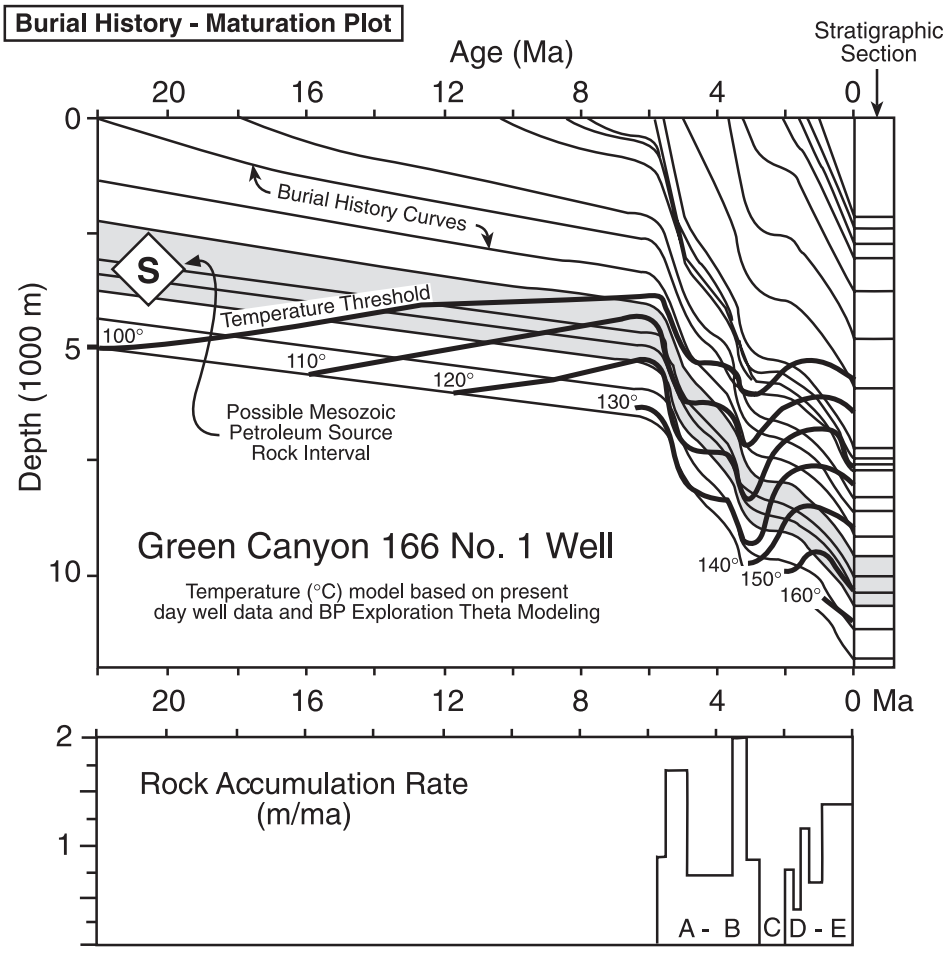

Figure 4–33. After Piggott and Pulham (1993); courtesy Gulf Coast SEPM.

Superimposed Sea Level Cycles

Cycle phase

Cycle phase is the position of relative sea level along a cycle curve at any moment in time. There are at least five or six orders of sea level cycles. Each order can be in phase or out of phase with the other orders. When two successive orders are in phase, i.e., fourth-order transgressions are in phase with third-order transgressions, the impact that each has on deposition or erosion is enhanced (Mitchum and Van Wagoner, 1990). Understanding this phenomenon can help in stratigraphic prediction and lead to the discovery of new fields.

Superimposition of phases

When each scale of cyclicity is convolved with or superimposed onto the next higher order, the patterns of transgression vs. regression either amplify or dampen the transgressions and regressions of the next higher order(s) of cyclicity. The right side of the following schematic illustrates cycle stacking of three orders of symmetrical cyclicity of short (narrow curve), intermediate, and long duration (wide curve), analogous to the fourth, third, and second orders of Haq et al. (1988). Transgressive phases (darker shading) of the short-duration cycles are amplified when coincident with the transgressive phase of the intermediate-duration cycle—even more so if coincident with the transgressive phase of the long-duration cycle.

The same pattern of amplification occurs for coincident regressive cycle phases (lighter shading). When short-duration transgressive phases occur on the regressive phase of the intermediate cycle, the short-duration transgressive phase is dampened and will be even more so if it occurs during the long-duration regressive phase. Regressive phases are similarly dampened if they occur on long-duration transgressions.

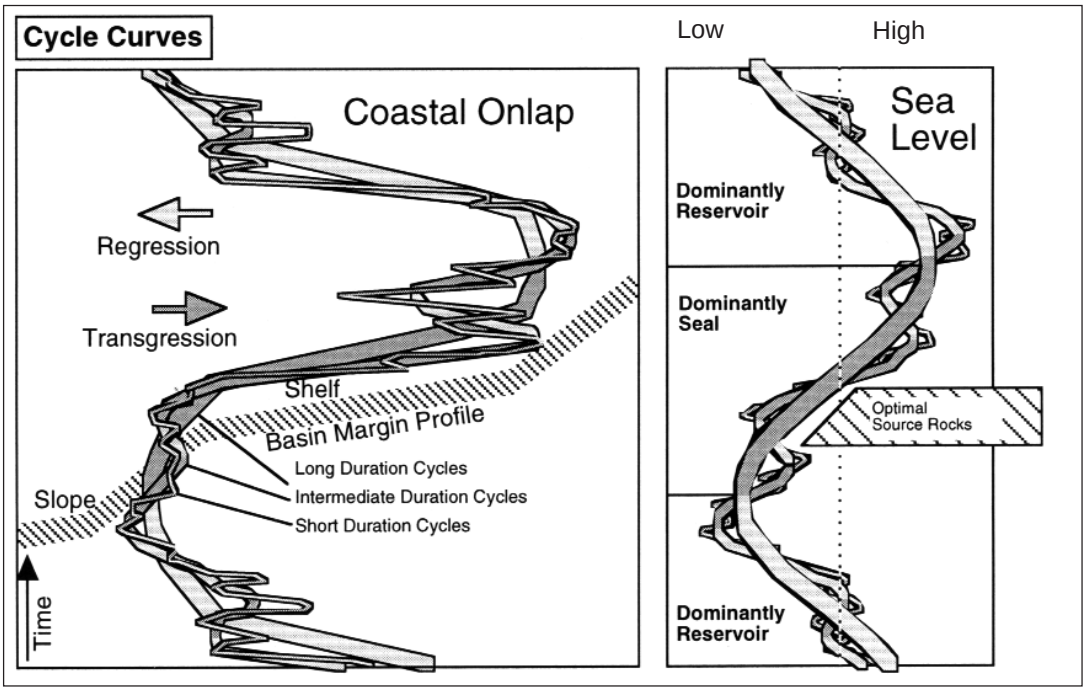

Figure 4–34. From Haq et al. (1988); courtesy SEPM.

Superimposed Sea Level Cycles, continued

Superimposition of phases (continued)

The left side of Figure 4–34 shows the amplification of transgressive and regressive cyclicity when superimposed across a continental margin. Relative sea level rise and fall results in rapid transgressive or regressive deposition across a relatively low-gradient shelf area, slowed and vertically stacked if deposition occurs against a relatively steep gradient slope or basin margin. Regressive phases of siliciclastic deposition are likely to transport significant volumes of sand into the basin, depositing potential reservoir facies. Transgressive phases of siliciclastic deposition are likely to deposit regionally extensive muds, forming potential top seal for underlying regressive sands. During the dominantly transgressive phases of stacked long-to-short transgressive sequences, organic matter can become concentrated in marine muds, forming potential hydrocarbon source rocks (Creaney and Passey, 1993; Herbin et al., 1995).

Depositional geometry of superimposed cycles

The following figure shows the depositional geometry of third-order cycles stacked into a second-order transgressive/regressive cycle. Each third-order cycle is represented by a depositional sequence composed of three phases (Figure 4–18). The lowstand phase may consist of basinal sand-prone mounds (basin-floor fans) and shelf-edge deltas. The transgressive phase is usually dominated by regional mudstones. The highstand most often consists of prograding fluvial and deltaic sediments forming broad coastal plains with potential sandstone reservoir facies.

In carbonate-prone depositional settings, the transgressive-to-highstand phases may be dominated by regionally extensive carbonate platforms. The mudstone-dominated transgressive deposits can provide potential hydrocarbon source rocks, especially in the third-order transgressive phases composited within the second-order transgressive phase. In contrast, the dominance of third-order regressive phases within the second-order regression brings more potential reservoir sand progressively further into the basin. Optimal hydrocarbon traps form where the regressive sandstones are in close proximity to organic-rich transgressive mudstones and are overlain by effective top seal.

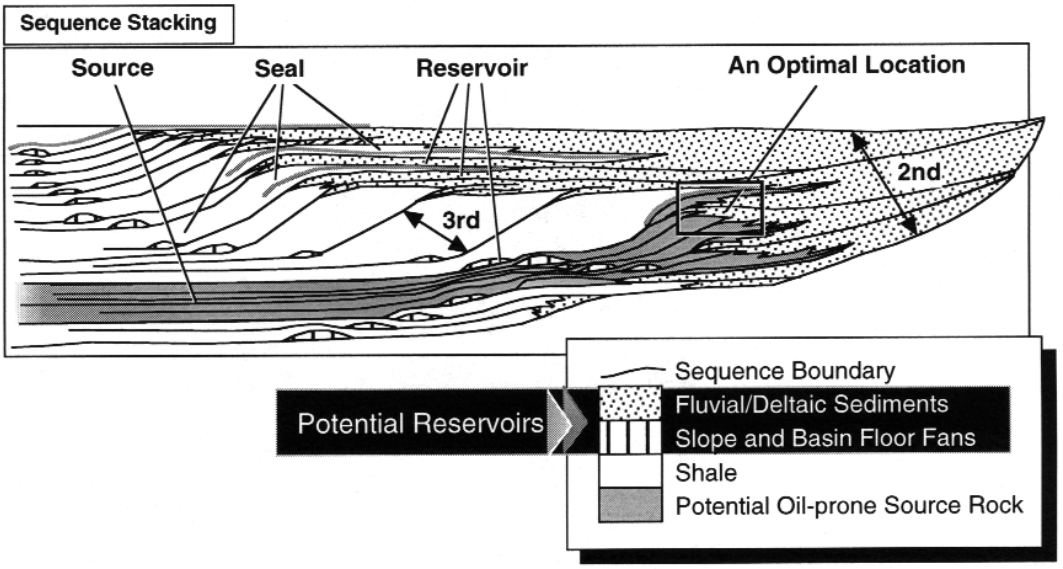

Figure 4–35. After Bartec et al. (1991); courtesy Journal of Geophysical Research.

Superimposed Sea Level Cycles, continued

Effect on reservoir deposition

The lowstand phase of the *Glob alt* depositional sequence is sand prone (Figure 4–29) and produces hydrocarbons from at least 23 fields within the High Island–East Breaks depocenter (Figure 4–40). The sandstone reservoirs were deposited within slope valleys by gravity-flow processes (Armentrout, 1991). The abundance of *Glob alt* sandstone is interpreted to be the consequence of a major fall in relative sea level. The falling sea level resulted in enhanced bypass of sand across the shelf and into the slope basins and deposition of a lowstand systems tract.

The *Glob alt* sequence mapped on Figure 4–29 represents the lowstand depositional phase of the Haq et al. (1988) third-order 3.7 cycle (Figure 4–25). Cycle 3.7 begins with the most significant relative fall in sea level of the Tejas B-3 supersequence after the second-order highstand (cycles 3.4 and 3.5). This significant fall in sea level resulted in transport of large volumes of sand from the paleo-Mississippi River system into the slope basins of the High Island and East Breaks areas of offshore Texas (Figures 4–29 and 4–33), depositing numerous potential reservoirs of gravity-flow sands during maximum amplification of falling sea level. Following lowstand deposition, relative rise in sea level cut off the sand supply and resulted in deposition of hemipelagic mudstones, forming a regional top seal to the *Glob alt* sandstones (Figures 4–29 and 4–33). The top seal is a condensed section that correlates laterally with the transgressive and early highstand systems tracts.

Subsection D2

Paleogeography

Introduction

Basin paleogeographic maps are useful prospecting tools. They help us locate and predict the occurrence of reservoir, seal, or source lithofacies by establishing the location of major geographic features, such as deltas, shorelines, barrier reefs, and slope breaks. Once an isochronous surface or coeval interval is identified, paleogeography can be reconstructed by integrating maps of age-equivalent lithofacies, seismic facies, biofacies, and thickness of reservoir-quality rocks.

In this subsection

This subsection discusses the following topics.

Applying Paleogeography to Prospect Identification

Introduction

Basin paleogeography is defined by picking an isochronous surface or coeval interval and mapping the associated seismic facies and lithofacies. For example, the location of sandy lithofacies vs. clayey lithofacies or mounded vs. tabular seismic reflection configurations may delineate the position of shorelines or reefs. Mapping thickness of reservoir-quality rocks is also useful for establishing paleogeography; thick, linear, dip-oriented trends of sandstone may indicate paleochannel complexes.

Procedure

The table below outlines a suggested procedure for defining paleogeography and applying it to prospect identification.

Step	Action
1	Identify the stratigraphic interval of a single depositional phase that has potential for containing reservoir rocks, i.e., lowstand or highstand, using biostratigraphic markers and regional correlation surfaces.
2	Map depositional facies such as biofacies, net reservoir thickness (lithology or porosity), and seismic facies (i.e., clinoforms, parallel reflections, chaotic reflections within a single depositional phase).
3	Integrate the interpreted seismic facies and biostratigraphic data into a grid of stratigraphic well-log cross sections if wells are available.
4	Map the location of fields producing from reservoirs in the interval of interest with respect to net reservoir thickness; define the type of trap(s) each field contains.
5	Using the seismic interpretations and the geology of the fields mapped in step 4, interpret the deposition of reservoir, seal, and source facies and the formation of stratigraphic or combination traps with respect to sea level cycle phase. Was the reservoir deposited during lowstand, rising, or highstand phases of sea level cycles? What about the seal facies? Is the trap the result of facies relationships that formed during a particular sea level phase or postdepositional deformation?
6	Using information gained in step 5, identify areas that may contain overlooked reservoir, seal, and source rocks in the same isochronous interval or in isochronous intervals with similar character. Also, consider possible migration avenues along which fluids could move from the source rock to the reservoir, from higher to lower pressure regimes. Such avenues might include sand-prone pathways, faults, salt walls, and unconformities.

Constructing a Facies Map

Purpose and procedure

The purpose of a facies map is to reconstruct paleogeography, from which we can predict reservoir, seal, and source-rock distribution. Facies maps are made at an isochronous surface or within a coeval interval (Tearpock and Bischke, 1991; Visher, 1984). We map reservoir system thickness (1) to compare the distribution of reservoir-system thickness and field location and (2) to identify or predict locations with thick reservoirs and trapping conditions that are undrilled. A procedure for mapping facies is outlined in the table below.

Step	Action
1	Identify and correlate significant isochronous surfaces throughout the depocenter, integrating well data, bioevents, and seismic reflection profile grids.
2	Map areas of potential reservoir and seal facies that occur between two isochronous surfaces.
3	Map seismic facies associated with that interval.
4	Plot important physiographic features, such as the shelf-slope break or structurally controlled bathymetric highs.
5	Integrate all data into a depositional facies map.

Seismic facies profile

The figure below is the interpreted seismic facies pattern for part of one seismic reflection profile down the axis of the High Island–East Breaks depocenter (Armentrout, 1991). This is the same seismic profile discussed in Figure 4–27.

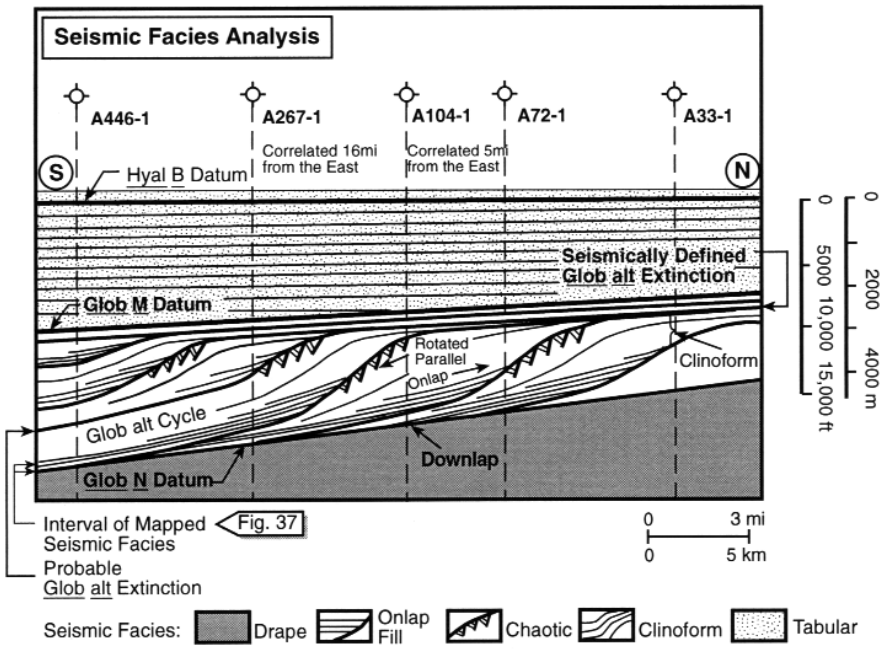

Figure 4–36. After Armentrout (1987); courtesy Gulf Coast SEPM.

Seismic facies profile (continued)

Each prograding clinoform contains a rotated package of chaotic facies within the upper and steepest part of the clinoform facies and basinward of the tabular facies. The clinoform facies is onlapped by parallel, moderate-amplitude, onlapping reflections of the onlap-fill facies, which are subsequently downlapped onto by the next overlying prograding clinoform. In a broader sense, the drape facies below these clinoforms and the *Glob N* datum represent basinal deposits; the clinoform and onlapping-fill facies represent slope deposits; and the overlying tabular facies above the clinoforms and the *Glob M* datum represent shelf deposits—all part of a basin-filling succession.

Associated foraminiferal biofacies shown in Figures 4–27 and 4–29 support this analysis. The *Glob alt* sequence is the fourth clinoform from the right, the fourth-most basinward of five oblique clinoforms that toplap along a common horizon. Superjacent clinoforms show progressively more topset deposition forming sigmoidal clinoforms, suggesting relative rise of sea level (with consistent widespread increase in accommodation space). Observations of seismic facies from a single phase of deposition, such as lowstand or highstand, are recorded on a map and contoured to convey the distribution of each seismic facies (Figures 4–37 and 4–38).

Seismic facies map

Following is a map of the seismic facies of the *Glob alt* lowstand interval (Figures 4–28 and 4–29). The mapped facies are observed in the interval immediately above the sequence boundary at the base of the *Glob alt* sequence in Figure 4–36. In the basin setting, the sequence boundary is, at seismic scale, essentially coincident with the underlying condensed section. The mapped facies are within the lowstand systems tract. Each

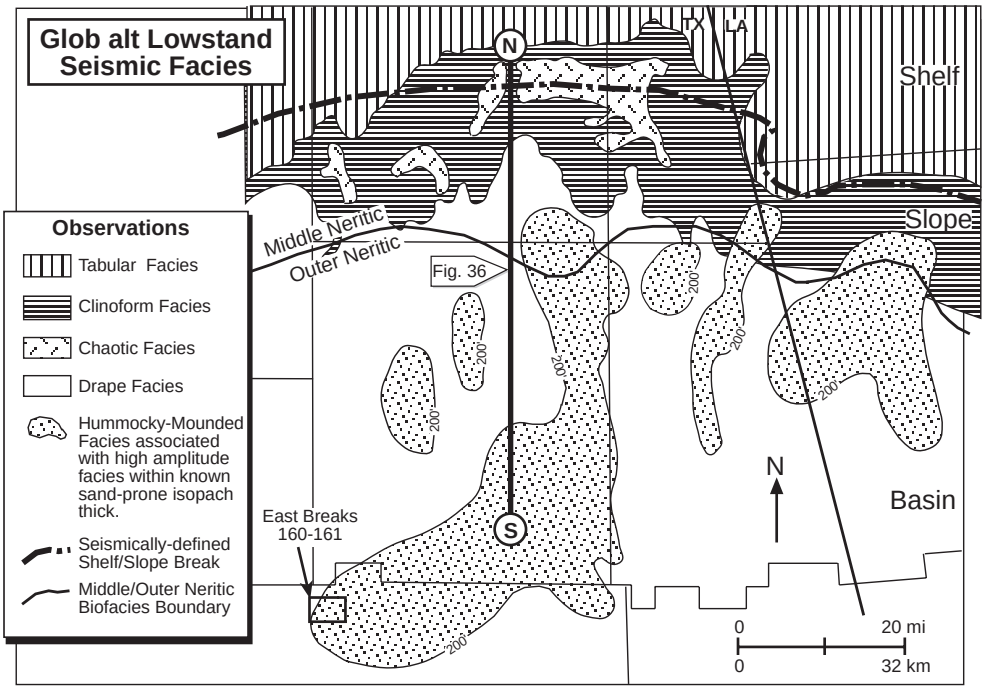

Figure 4–37.

Seismic facies map (continued)

observed facies is plotted along the transect of the seismic reflection profile, profile by profile. The area of shelf/slope inflection is plotted, based on the location of the inflection point between foreset and topset elements of the clinoform. Biofacies information (Figure 4–29) and sediment type (Figure 4–38) can then be overlain on the seismic facies map to provide an integrated data base for interpreting depositional environments (Figure 4–39).

Net sand map

Of the 240 wells used in the study area, 147 penetrated the *Glob alt* interval and provided information on the distribution of the net sand deposited within that interval. Using the net-sand values from the wells, we integrate the data with seismic facies maps within the *Glob alt* lowstand isochron and contour a net-sand isopach map (figure below). Contours are for areas with at least 200 ft (60 m) of net sand. The sandstones occur mostly seaward of the age-equivalent physiographic shelf/slope break identified on the seismic-reflection profiles. Because most of the wells penetrated the *Glob alt* sequence basinward of the *Glob alt* shelf edge, the sandstones penetrated were most likely transported by gravity-flow processes and deposited in environments on the slope and within intraslope basins.

The resulting map shows the net-sand distribution of shelf areas contoured parallel to the shelf edge and slope areas contoured parallel to the depositional dip of the slope valleys down which the sand was transported. The distribution of sand within the depositional dip-oriented isopachs is consistent with the regional pattern of downslope-oriented salt withdrawal valleys bounded by salt-cored anticlines (Figures 4–6 and 4–41). Note the lowstand position of the middle-to-outer neritic biofacies boundary, below which few waves reach the sea floor. This results in downslope sand distribution being controlled by bottom currents alone.

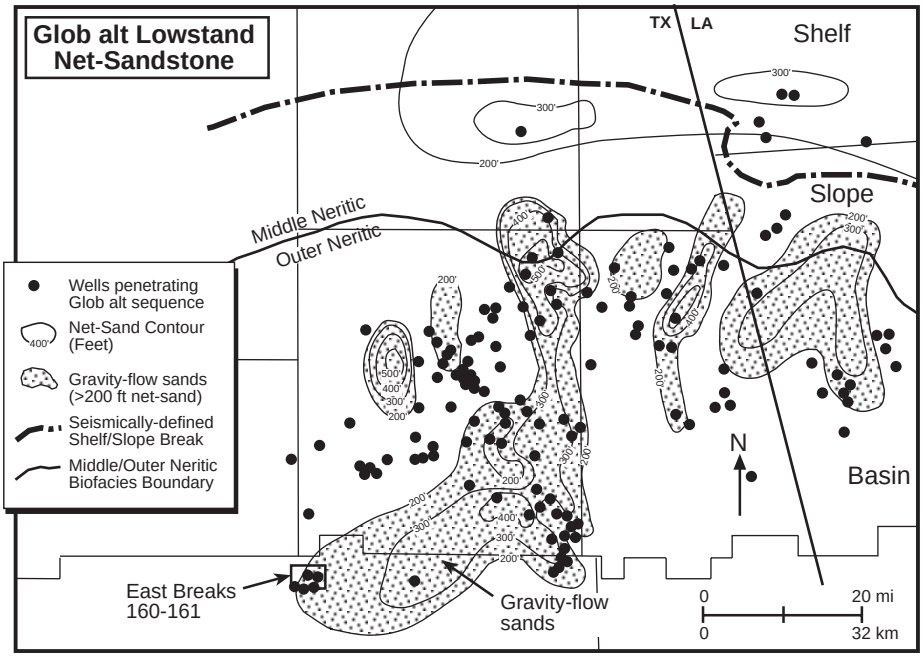

Figure 4–38.

Depositional facies map

The figure below is a depositional facies map for the *Glob alt* interval's basal sequence boundary, constructed by integrating the biofacies map, the net sandstone map, and the seismic facies map (Figures 4–29, 4–38, and 4–37, respectively).

The upper slope deposits consist of the clinoform facies and numerous areas of chaotic facies, including rotated-block packages deposited in middle neritic to upper bathyal water depths (Figures 4–36, 4–37). The shelf facies consist of a thin interval of tabular facies representing a mixed system of inner-to-middle neritic deposits, nonmarine coastal-plain deposits, and the erosional surface at the *Glob alt* sequence boundary. The basinal deposits consist of the drape and onlap-fill facies of bathyal hemipelagic mudstone that encase the sandstone-prone mounded facies of sediment gravity flow origin, indicated here by the > 200 ft (> 60 m) sandstone isopach. The gravity-flow sandstones were deposited within slope valleys basinward of the physiographic shelf/slope break in deep middle neritic and deeper-water environments during falling and lowstand of sea level. The physiographic shelf/slope break is identified by the inflection point between the foreset and the topset reflections of the clinoform.

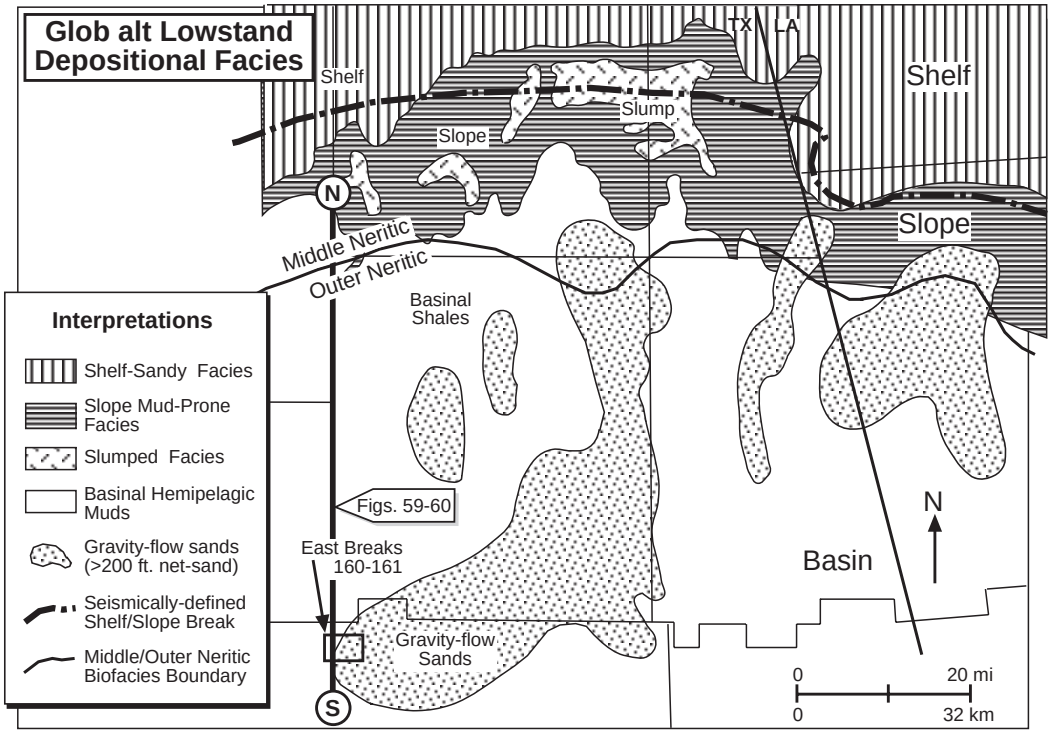

Figure 4–39. After Armentrout (1991); courtesy Springer-Verlag.

Relating Traps to Paleogeography

Introduction

A paleogeography map of a reservoir interval, reservoir thickness, and fields (producing from the same reservoir interval) shows relationships between production and geology that may be used to locate prospects in untested areas.

Procedure

The table below suggests a procedure for relating fields to paleogeography and reservoir thickness.

Step	Action
1	Plot paleogeography, reservoir thickness, and field location on the same map.
2	Relate paleogeographic features (axis of canyons, shelf/slope break, shorelines, etc.), reservoir thickness, and field locations to trap development.

Example

The following figure shows the relationship between 23 fields in the High Island–East Breaks depocenter that produce from the *Glob alt* sandstones and the *Glob alt* sandstone 200-ft (60-m) isopach. Most of the fields with *Glob alt* reservoirs occur around the perimeter of the maximum thickness of net sandstone, near the 200-ft (60-m) isopach. Nearly all of the *Glob alt* reservoirs occur basinward of the lowstand middle-to-outer neritic biofacies boundary [approximately 600 ft (200 m) water depth]. Thus, they are downslope from the shelf/slope inflection and below normal wave base where sedimentation is dominated by gravity-flow processes.

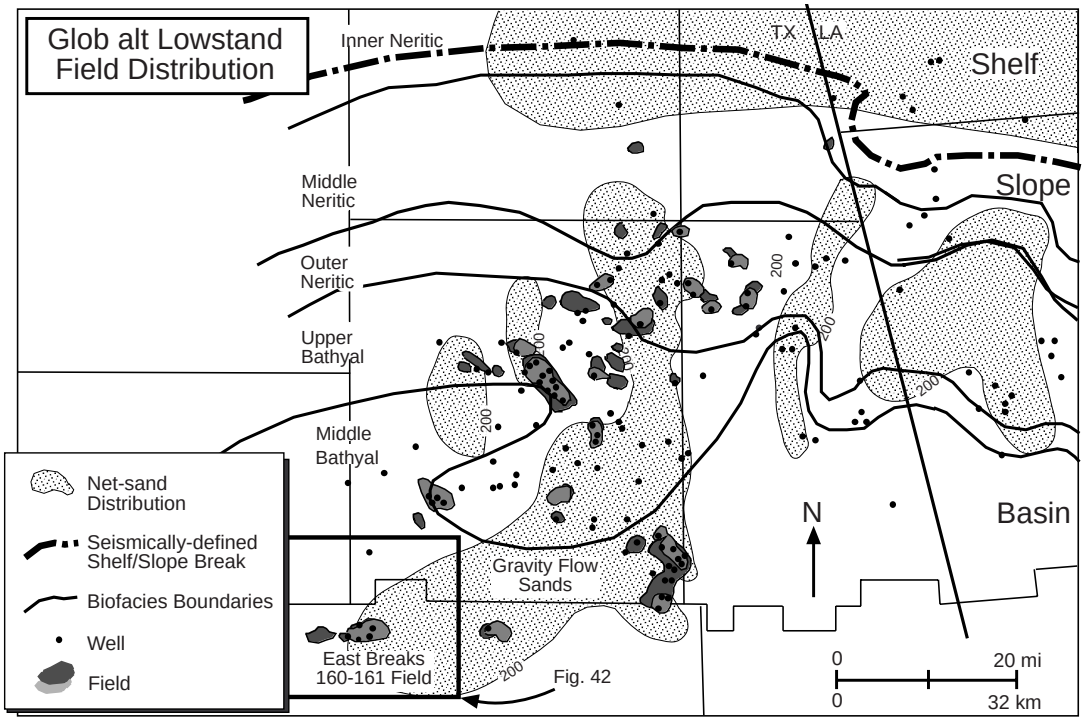

Figure 4–40.

Relating Traps to Paleogeography, continued

Example (continued)

Deposition by gravity-flow processes occurs within physiographic lows (Kneller, 1995; Kneller and McCaffrey, 1995). Although each field occurs within a local structural high, most have a major stratigraphic component related to their transport through slope channels and deposition as a gravity-flow deposit within the axis of a salt-withdrawal valley (see Figures 4–42, 4–43, and 4–56 for the East Breaks 160-161 field). The sands within these valleys were deposited with a slope-parallel orientation. The trapping structure develops after reservoir deposition as the dip-oriented sand bodies are tilted along the flanks of the salt-cored anticlines (Figure 4–41). The anticlines continue to grow, and the tilt of the sand body becomes progressively more accentuated as each successive cycle of synclinal fill accumulates and displaces the underlying salt.

This process accelerates during relative lowstand of sea level when the river systems discharge their loads near to or into the heads of the slope valleys (Anderson et al., 1996; Winker, 1996).

Explanation of example

In Figure 4–40, producing fields are along the 200-ft (60-m) net sand contour or beyond rather than in the axial thick. This is because of gravity-flow sands accumulating within the synclinal valley axes, which continue to subside through time.

The following figure shows a depositional strike seismic reflection profile across one of these valleys. The high-amplitude, more continuous reflections correlate with condensed-section claystones and often bracket pressure compartments due to their very low perme-

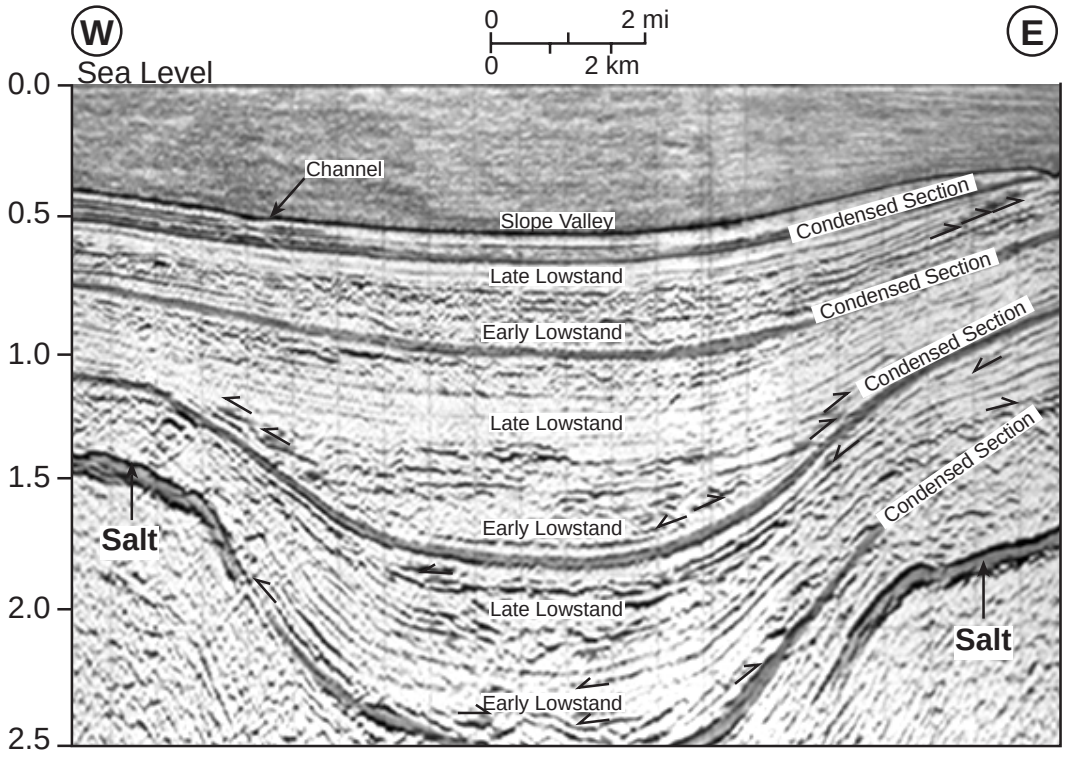

Figure 4–41.

Relating Traps to Paleogeography, continued

Explanation of example (continued)

ability. Between the condensed sections are the sand-prone early lowstand systems tract, sometimes with hummocky-mounded facies suggesting channel complexes, overlain by silt-prone late lowstand deposits. The differential loading of salt by sediment accumulation along the synclinal valley axis results in differential rotation of each depositional sequence. This rotation along the synclinal flanks results in the early lowstand gravity-flow sands pinching-out structurally upward, providing potential hydrocarbon traps along the valley margins (Armentrout et al., 1996; Bilinski et al, 1995; McGee et al., 1994; *see also* Weimer and Bouma, 1995).

The isochron thick of the *Glob alt* sands in the figure represents the sand-prone slope/valley fill of the *Glob alt* sequence. Understanding the interplay of depositional processes and tectonic deformation is essential to hydrocarbon exploration in GOM minibasins.

Basin slope exploration plays

Gravity-flow events, such as slumps and slides, can initiate transport of sediment downslope. Transport by debris flows and turbidites moving downslope may be confined to narrow valleys or spread outward into the less-confining minibasin of the Gulf of Mexico slope (Kneller, 1995; Kneller and McCaffrey, 1995). These sedimentary systems consist of channel elements through which sediment is transported to lobe-and-sheet depositional elements within the minibasins (Armentrout et al., 1991). Confined flow elements are typically channels with levees resulting from sediment fallout from overbanking turbulent flow. The channel-levee complexes are elongate but may stack into thick successions of potential reservoir facies (Armentrout, 1996). The less-confined lobe-and-sheet facies may spread out within the minibasins, forming large-volume reservoir packages (Bilinski et al., 1995). Winn and Armentrout (1996) have compiled examples of this spectrum of gravity-flow exploration targets, which are critical elements of minibasin petroleum systems.

Section E
Minibasins and Petroleum Systems

Introduction

In the northern Gulf of Mexico, the understanding of minibasins—achieved through the integration of stratigraphic, structural, biostratigraphic, and geochemical data—is the critical scale of basin analysis for petroleum system identification and prospect evaluation. Petroleum system analysis is the identification of the origin of the entrapped oil and the reconstruction of the generation-migration-entrapment history. This information provides a template for further exploration for subtle traps along the migration avenue.

Minibasins are a critical scale for Gulf of Mexico petroleum systems evaluation. Basins of other tectonic styles differ, requiring a somewhat different approach to petroleum systems analysis. For example, stratigraphic entrapment along foreland basin limbs adjacent to foredeep hydrocarbon charge areas is an important aspect of foreland basins (Macqueen and Leckie, 1992: Van Wagoner and Bertram, 1995).

In this section

This section contains the following subsections.

Subsection E1

Minibasins and Petroleum Systems

Introduction

Minibasins are subdivisions of depocenters primarily defined on the basis of structural elements. These elements isolate the petroleum system of a minibasin from the petroleum systems of other minibasins within a depocenter.

In this subsection

This subsection contains the following topics.

Minibasins

Definition

A minibasin is a subdivision of a depocenter that in turn is a subdivision of a basin. Sediment thickness is the primary basis for subdividing basins into depocenters. Structural elements separate one minibasin from another within a depocenter. The figure below shows the structural elements that define the East Breaks 160-161 minibasin, which is bound on the north by fault A, on the east by faults B and C, and on the south by a salt-cored high.

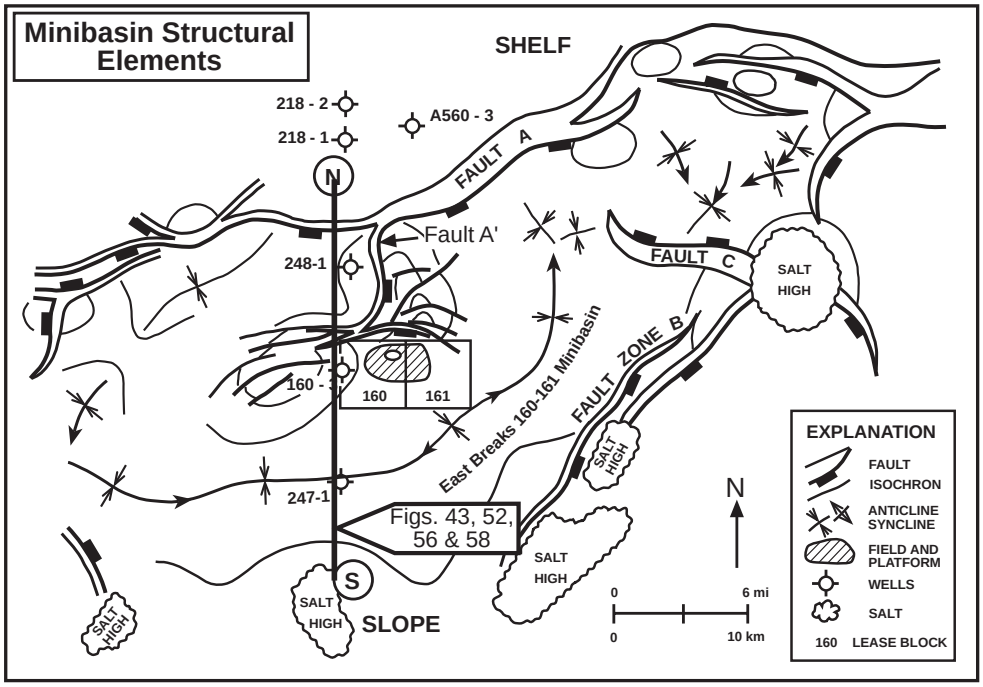

Figure 4–42. From Armentrout et al. (1991); courtesy Springer-Verlag.

Minibasins, continued

Seismic expression

The following figure is a north–south seismic section through the East Breaks 160-161 intraslope minibasin, showing the location of the East Breaks 160-161 field. Production is from the *Trim A* and *Glob alt* reservoirs within the rollover anticline downthrown to the north bounding fault A'. Fault A' splays southwest off regional fault A (Figure 4–42) (see also Schanck et al., 1988; Armentrout et al., 1991).

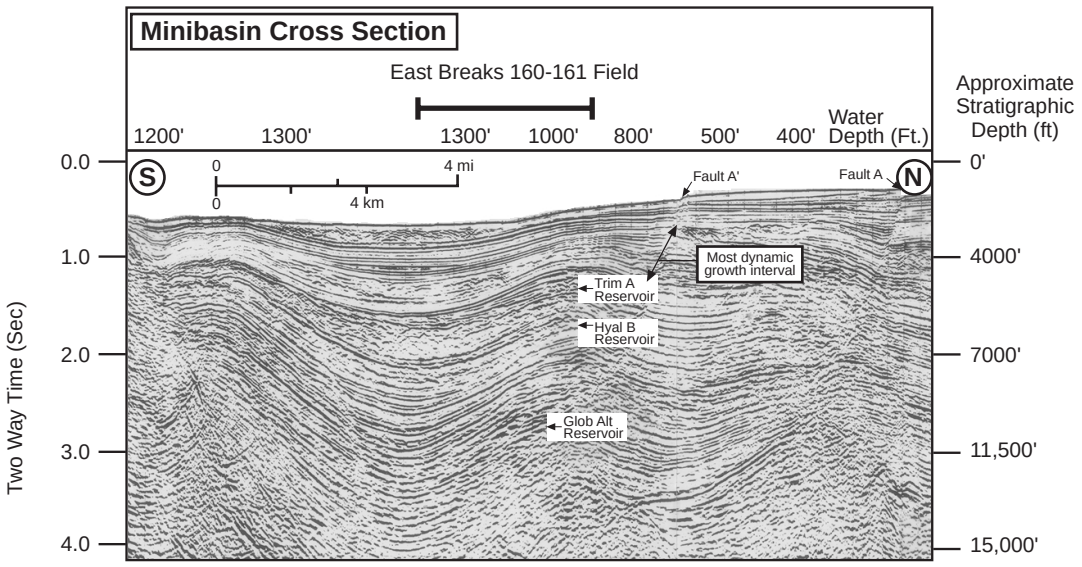

Figure 4–43.

Age of minibasin formation

The age of minibasin formation is determined by looking for relationships between sedimentation and deformation, like faulting or folding. Figure 4–44 is a schematic diagram of the seismic reflection profile along the west side of the East Breaks 160-161 field (Figure 4–42). That reflection profile is nearly coincident with the boundary between the Galveston and High Island exploration areas (Figure 4–17). The diagram depicts salt-cored anticlines and growth faults separating the progradational basin-filling cycles into distinct minibasins. The stratigraphic pattern shows composite depositional sequences, numbered 1 through 4, prograding into and across progressively younger growth-fault and salt-withdrawal basins. The stratigraphic boundaries outline seismic-stratigraphically defined depositional cycles calibrated by bioevents from several wells along the section (Armentrout and Clement, 1990). Scales are approximate.

Age of minibasin formation (continued)

The age of formation of each minibasin can be interpreted from the relative age of expanded sedimentary section downthrown to each major growth fault or salt high. Along the cross section, the expanded section occurs in progressively younger strata. In the northernmost diagrammed minibasin, the expanded section occurs in cycles 1 and 2. In the middle minibasin, the expanded section is in cycles 2 and 3. In the southernmost minibasin (the East Breaks 160-161), the expanded section formed during cycles 3 and 4. A new minibasin has begun to form in cycle 4 sediments basinward of the steep salt-cored upper slope.

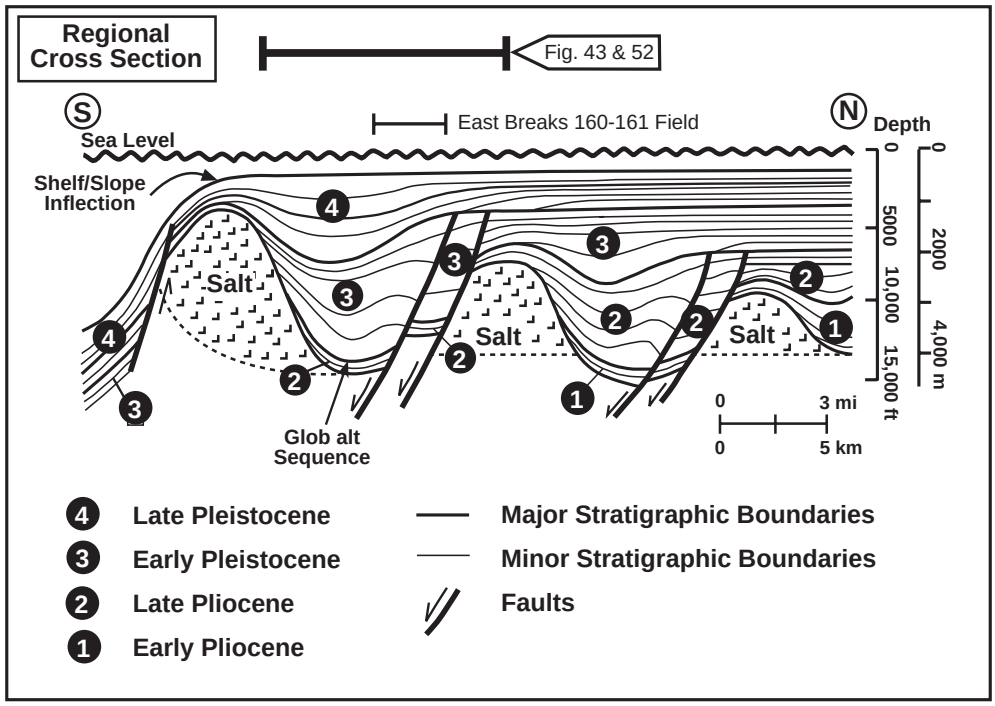

Figure 4–44. From Armentrout and Clement (1990); courtesy Gulf Coast SEPM.

Formation of the East Breaks minibasin

Each of these minibasins formed as sea level fell and the sediment supply system prograded to the shelf edge where it oversteepened and differentially loaded slope muds. Growth faults developed within this unstable sediment prism and displaced mobile salt to accommodate the downbuilding sediment (Winker and Edwards, 1983). This process continued until the salt was completely displaced and the downbuilding sediments welded with the sediments underlying the displaced salt (West, 1989). Once the sediment-on-sediment welding occurred, the fault system either propagated downward or locked up, resulting in the basin filling to the equilibrium profile of the sea floor. The next cycle of minibasin downloading, growth fault development, and salt withdrawal stepped basinward to the next deformable site. That site could be either at the shelf/slope break or within an upper slope valley.

Petroleum Systems

Definitions

Magoon and Dow (1994) define a petroleum system as the essential geologic elements and processes related to those hydrocarbons generated from a single pod of active source rock. The geologic elements are the source rock, reservoir rock, seal rock, and overburden rock. The processes are trap formation, hydrocarbon generation, expulsion, secondary migration, and accumulation. Aspects of preservation, degradation, and destruction of petroleum are omitted as processes because they generally occur after a petroleum system is formed, but these aspects must still be evaluated in assessing the petroleum system potential of a play or prospect.

Events chart

The development of a petroleum system can be summarized using an events chart. The petroleum system events chart plots the timing of each element and process and helps us understand critical moments in the history of the petroleum system under study. Magoon and Dow (1994) define the critical moment as the time that best depicts the generation-migration-accumulation of hydrocarbons in the petroleum system. The critical moment is often an interval of time encompassing the major pulse of hydrocarbon expulsion and accumulation within an existing trap. There can be several critical moments if there is an episodic history for a trap or if there are more than one source rock interval. The figure below is the events chart for the petroleum systems in the East Breaks 160-161 minibasin.

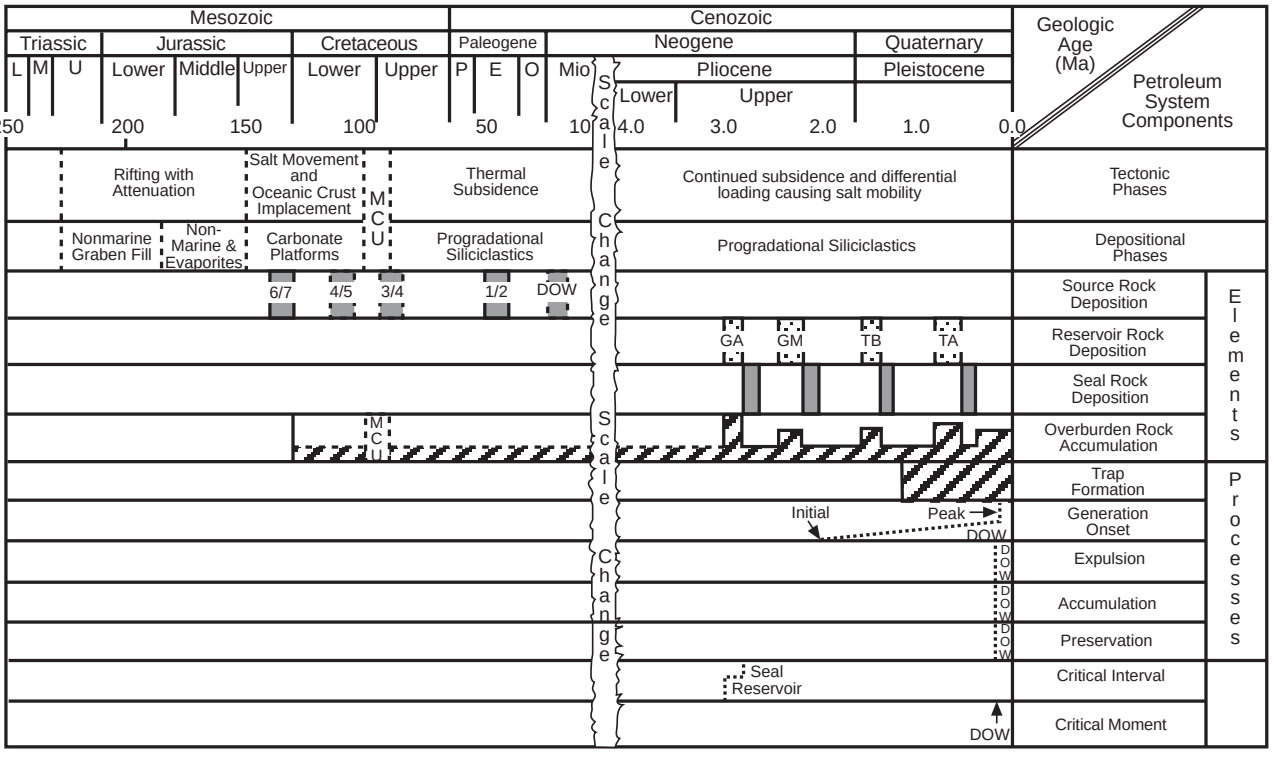

Figure 4–45. Time scale from Haq et al. (1988); DOW represents source rock, generation, and critical moment estimates (Dow et al., 1990).

Events of East Breaks minibasins

Included on the chart for the East Breaks 160-161 minibasin petroleum system is the timing of each tectonic phase and primary facies depositional phase that have had major impact on the local petroleum system. As discussed earlier, the rifting of continental crust formed the proto-GOM basin with local depocenters in which Late Jurassic salt was deposited. As the basin continued to rift, oceanic crust was emplaced and transitional crust became the site of prograding continental margin siliciclastic and carbonate complexes. The prograding sediments differentially loaded the salt, and a progression of salt-withdrawal and growth-fault-bound minibasins formed. It is in the context of these minibasins that petroleum systems developed within the northern GOM basin.

Phases, elements, and processes

As shown in Figure 4–45, twelve critical petroleum system components can be grouped into phases, elements, and processes. Also included are critical interval and critical moment. Other items could be added if needed, such as reservoir diagenesis. The table below summarizes the main components of petroleum system analysis.

Phases	Elements	Processes
• Tectonic • Depositional	• Source • Reservoir • Seal • Overburden	• Trap formation • Hydrocarbon generation • Hydrocarbon expulsion and migration • Hydrocarbon accumulation • Preservation of traps

East Breaks events chart details

Figure 4–45 shows the relationship between the essential elements and processes of the petroleum system of the East Breaks 160-161 minibasin. Also charted are important tectonic phases and primary depositional phases. Numbers on source-rock intervals are for the mapped source rocks of Figure 4–5 and the middle Miocene speculative source interval of Dow et al. (1990). The following abbreviations are used: GA = *Globoquadrina altispira;* GM = *Globorotalia miocenica;* HB = *Hyalinea balthica;* TA = *Trimosina denticulata;* MCU (on overburden accumulation) = *Mid-Cretaceous Unconformity*.

East Breaks source

Magoon and Dow (1994) define a petroleum system as all aspects of hydrocarbons generated from a single pod of active source rock. Five potential source rocks are recognized on Figure 4–45. Dow et al. (1990) consider the middle Miocene as the probable source of East Breaks 160-161 oil. Other workers suggest the East Breaks 160-161 field hydrocarbons are from a mixture of Late Jurassic (numbers 6 and 7) and early Paleogene (numbers 1 and 2) source horizons (see Figure 4–5). Thus, more than one petroleum system is probably active within the East Breaks 160-161 minibasin, and a different critical moment would exist for each system.

Subsection E2

East Breaks Petroleum System Elements

Introduction

The East Breaks 160-161 minibasin is an example of where more than one petroleum system can charge the same trap. It contains all the components required for generation, migration, and accumulation of hydrocarbons. This subsection describes the main elements of the petroleum systems in the East Breaks 160-161 minibasin.

In this subsection

This subsection contains the following topics.

Reservoir Rock

Introduction

Four reservoir intervals are productive in the East Breaks 160-161 minibasin: *Glob alt, Glob M, Hyal B,* and *Trim A* horizons. Reservoir intervals are named for the regionally useful bioevent species stratigraphically above the reservoir. These bioevents most often occur within condensed sections. All four reservoir intervals are interpreted to be gravity-flow sand deposits (Armentrout et al., 1991). Only the *Glob alt* reservoir is considered here.

Glob alt sequence deposition

The *Glob alt* depositional sequence of Late Pliocene age (mapped below) is part of depositional cycle 2 in Figure 4–44. The sequence, deposited on a relatively open slope with only slightly undulating sea-floor topography, thins rapidly basinward due to sediment starvation in the most distal areas of the High Island–East Breaks depocenter (Figure 4–47). Subsequent progradation resulted in differential loading of the allochthonous salt and formation of local depocenters between downloaded growth fault sediment prisms and differentially displaced salt-cored anticlines.

Glob alt isochron and seismic facies map

Glob alt sandstones of the East Breaks 160-161 field occur within an isochron thick where hummocky seismic facies downlap toward and are buried by parallel low-amplitude seismic facies indicative of hemipelagic mudstone drape (Armentrout et al., 1991). The following figure shows an isochron and seismic facies map of the *Glob alt* reservoir interval. The internal reflections of the mounded facies (1) downlap away from the isochron thick and toward the parallel seismic facies (2). Neither the isochron nor the seismic facies is mapped north of the fault due to poor data quality.

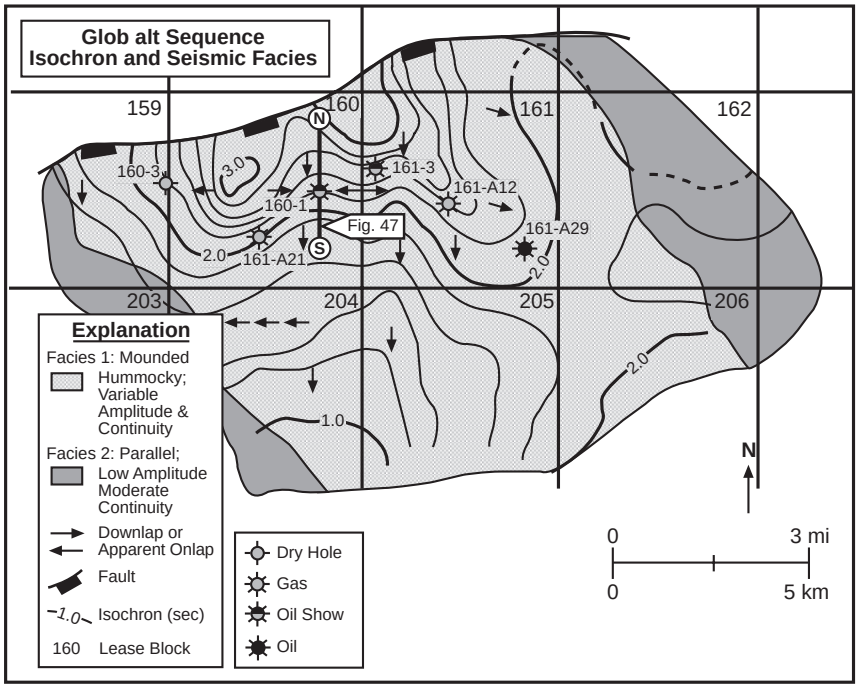

Figure 4–46. After Armentrout et al. (1991); courtesy Springer-Verlag. Original map by Charles R. Beeman, Mobil Oil, 1987.

Seismic profile

The figure below is a seismic reflection profile showing the *Glob alt* reservoir interval. Section A is uninterpreted; section B is interpreted. The reservoir thins southward between the top seal at the *Glob alt* condensed section datum and the underlying, unlabeled datum (thick black lines). The reservoir is penetrated by the 160-1 well in the faulted anticlinal trap formed by the rollover into the growth-fault complex bounding the north side of the minibasin (Figures 4–42 through 4–44). The 160-1 electric log pattern is spontaneous potential.

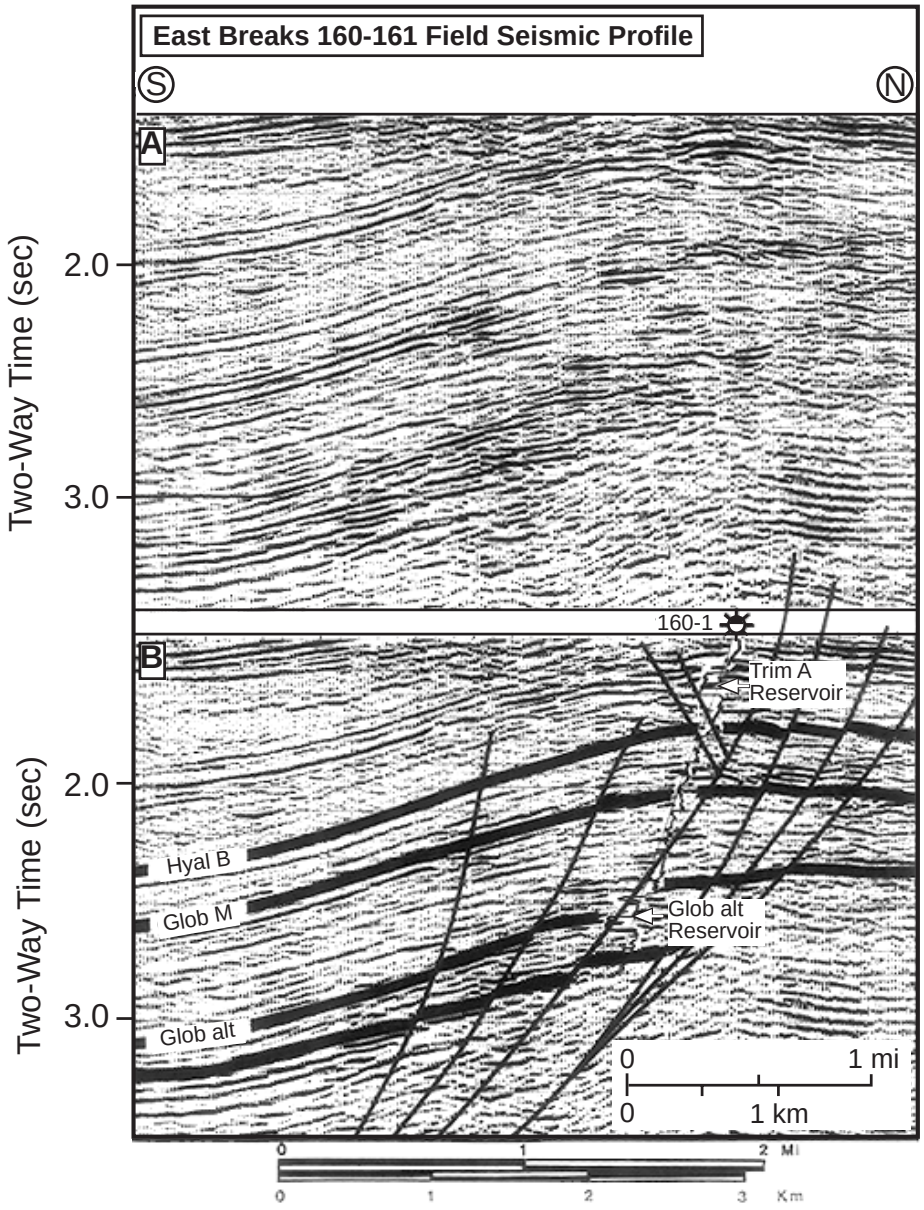

Figure 4–47. After Armentrout et al. (1991); courtesy Springer-Verlag.

Well-log cross section

The following figure is a well-log cross section of the *Glob alt* reservoir interval; datum is a mudstone within the GA-2 sandstone (well locations are shown on Figure 4–46). All logs are spontaneous potential with true vertical depth displays. The GA-4 reservoir sand is below the displayed interval. Log profiles are annotated: arrow C = funnel-shaped, coarsening-upward sandstone; arrow F = bell-shaped, fining-upward sandstone; parallel lines B = blocky profile of relatively thick sandstones and thin mudstone interbeds.

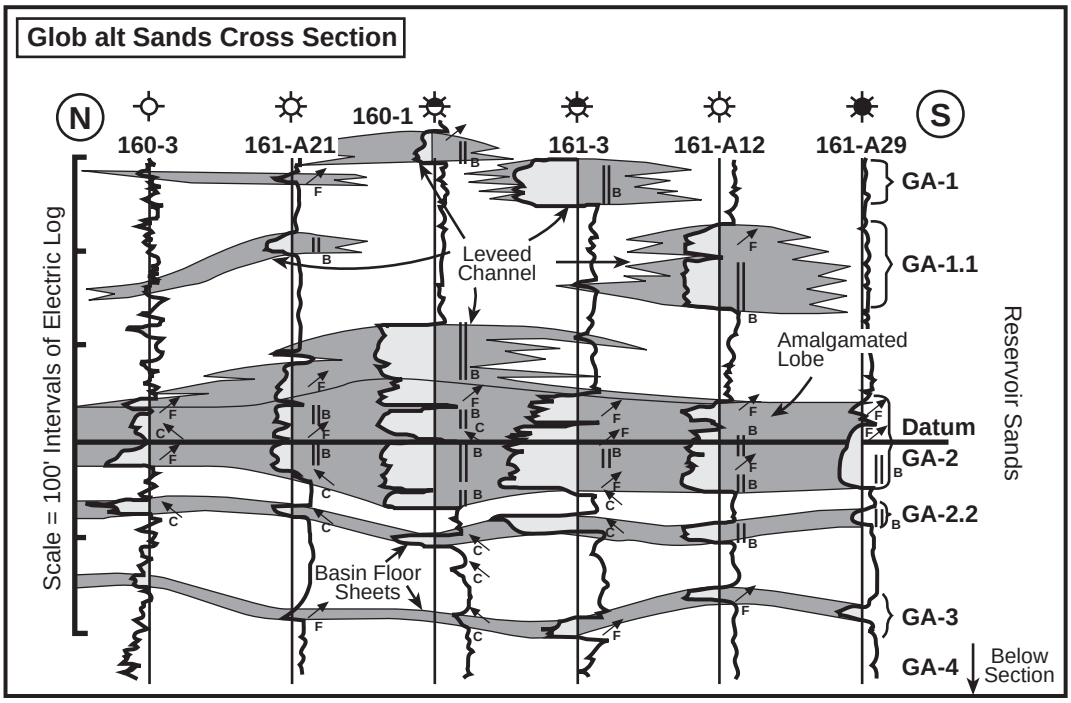

Figure 4–48. After Armentrout et al. (1991); courtesy Springer-Verlag.

Net sandstone isopachs

Well-log correlations within the *Glob alt* isochron thick show a succession of aggrading sandstone bodies (Figure 4–48). Figure 4–49 shows net sandstone isopachs for reservoir units of the *Glob alt* sandstone interval. The stratigraphic succession from top to bottom reservoir sandstone is 1, 1.1, 2, 2.2, 3, and 4. Maps of each sandstone interval document lobate deposition within the minibasin. Individual lobe development shows compensation lobe switching as progressively younger deposits infill the mud-rich/sand-poor intralobe areas of the preceding lobe.

The patterns mapped on the figure suggest lower thin lobate sheets (GA-4, GA-3, and GA-2.2), an intermediate thick lobe of amalgamated blocky sandstones (GA-2), and an upper moderately thick, bilobed leveed-channel system (GA-1.1 and GA-1). Net sandstone isopach contours are 10 ft (3 m); the scale bar is 3000 ft (1000 m).

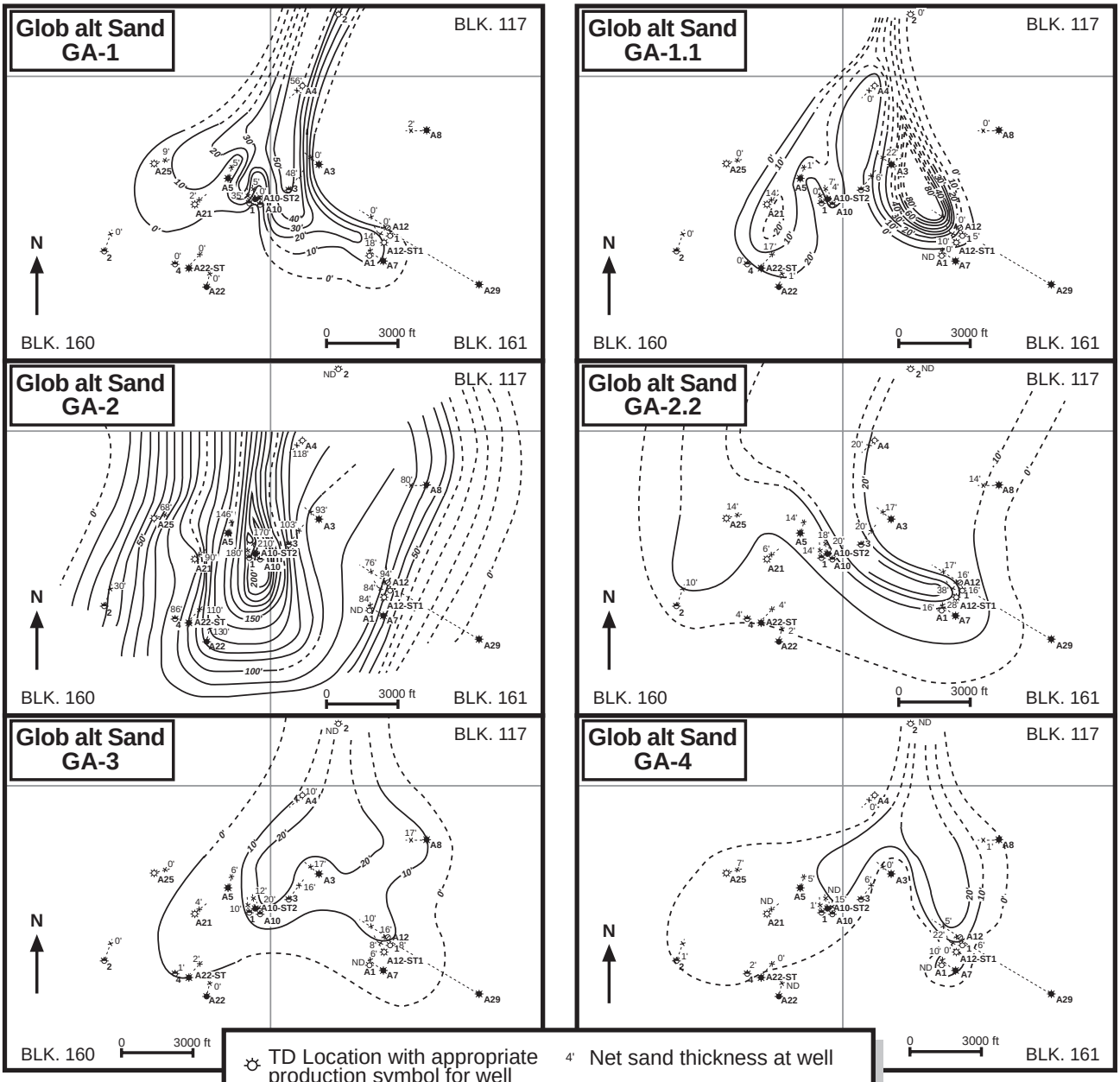

Figure 4–49. From Armentrout et al. (1991); courtesy Springer-Verlag.

Reservoir Rock, continued

Depositional model summary

All the observations made from seismic profiles, isochron maps, seismic facies maps, well-log cross sections, cuttings, biofacies, and cores have been used to construct a depositional model for the *Glob alt* cycle of the High Island–East Breaks 160-161 minibasin. This model incorporates far-traveled gravity-flow sands that accumulated in a depositional thick, filling an upper-slope salt-withdrawal sea-floor low. Laterally shifting fan lobes resulted in a complex architectural framework (Figure 4–48). The profile pattern (Figure 4–47), combined with the mapped isochron and seismic facies pattern of Figure 4–46 and the net sandstone patterns of Figure 4–49, have been interpreted as minibasin basin-floor sheet sandstones, amalgamated-lobe sandstones, and leveed-channel sandstones by Armentrout et al. (1991) (see Figure 4–48).

Depositional model diagram

The following figure is a block diagram of the depositional model for the *Glob alt* reservoir interval. The model shows a 40–50-mi-long (60–80 km) transport system from a shelf-edge delta basinward to the East Breaks 160-161 minibasin. Depositional water depths exceeded 1000 ft (320 m) (upper bathyal), suggesting transport was by gravity-flow processes. Sandstone deposition in the minibasin may have resulted from subtle variations of sea-floor topography, perhaps related to early salt withdrawal (Kneller and McCaffrey, 1995). Mass-wasting processes occurred on the slope well to the north of the field, as shown by slump facies on Figure 4–39. The areal extent of the basin-floor sheet is restricted by the areal extent of the East Breaks 160-161 intraslope minibasin.

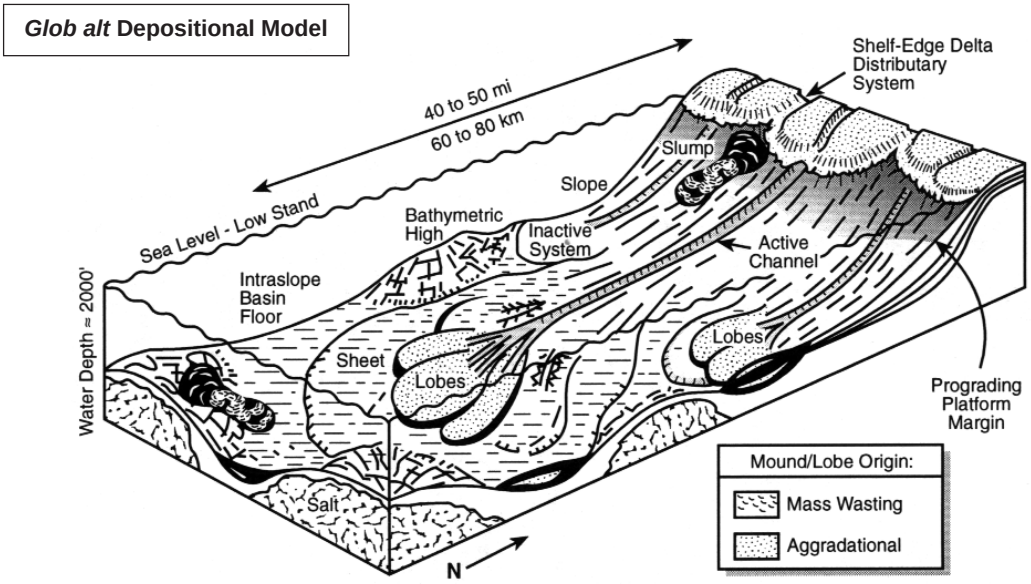

Figure 4–50. From Armentrout et al. (1991); courtesy Springer-Verlag.

Reservoir Rock, continued

Accommodation space

Differential loading of the mobile salt resulted in some syndepositional subsidence and accommodation of the *Glob alt* sand-prone isochron thick. The apparent thickening into the north-bounding growth fault is due to the maximum differential subsidence and isochron thickening being coincident with the fault trace of a much younger growth fault phase. Biostratigraphic calibration of the fault system indicates most, if not all, of the fault offset occurred during middle Pleistocene time, after the *Trifarina rutila bioevent* (= *Ang B*) dated at 1.30 Ma (Figure 4–31). This is more than 1.5 m.y. after deposition of the *Glob alt* sands.

Structural trap formation

Structural trap formation is related to differential rotation of the *Glob alt* sand-prone interval. This rotation occurred between 1.3 Ma and the present. The result was the development of the rollover anticline downthrown to fault A', which is a splay off regional fault A (Figures 4–42 and 4–43). (See Apps et al., 1994; Armentrout et al., 1996; Kneller and McCaffrey, 1995; and Weimer and Bouma, 1995, for discussions on structural control of deepwater deposition.)

Seal Rock

Description

The deepwater sands of the *Glob alt* reservoir are encased in hemipelagic mudstones and have a top seal associated with the condensed section of the *Glob alt* depositional cycle (Armentrout et al., 1991). The well-log cross section in Figure 4–48 shows the correlation of the *Glob alt* sandstones. The top seal, which occurs above the log cross section, is a major mudstone condensed interval coincident with the *Glob alt* datum labeled on Figure 4–47. Precondensed section mudstones encasing the *Glob alt* sandstones provide local top seal and lateral seal.

Effectiveness

The top seal of the *Glob alt* reservoir is especially effective because it is thick and has a regional extent as a consequence of its position at a third-order turnaround from regression to transgression. This turnaround is from regressive cycles 3.4–3.5–3.6 to transgressive cycles 3.7–3.8 on the Haq et al. (1988) cycle chart (see Figure 4–25).

Despite its regional extent and thickness, hydrocarbons have leaked upward into the *Hyal B* and *Trim A* reservoirs, most probably along faults during intervals of fault movement with consequent dilation of fracture networks along the fault

Carrier beds and seal evaluation

Impermeable rocks also affect migration pathways. Porous and permeable beds bounded above and below by impermeable rocks can provide highly effective hydrocarbon carrier beds.

Overburden Rock

Introduction

Overburden rock is the total stratigraphic section above the source rock (Magoon and Dow, 1994). The thickness and age of overburden rock provides a history of the rate of burial of a source rock toward and through the increasing temperature domains of the basin. This includes the range of temperatures necessary for cracking kerogens into hydrocarbons.

Because the depth to the probable source rocks of the East Breaks 160-161 field hydrocarbons is unknown, multiple working hypotheses must be considered. Four intervals of identified source rock are reported by Gross et al. (1995) (Figure 4–5) and are plotted on Figure 4–45. Also plotted is the speculated middle Miocene source rock of Dow et al. (1990). Gross et al. (1995) consider the petroleum of the East Breaks area to have been sourced by Jurassic marine mudstones for the oil and Paleogene marine mudstones for the gas. Alternatively, Dow et al. (1990) suggest middle Miocene marine mudstones as the probable source rock, although Taylor and Armentrout (1990) believe the source rock facies to be older than the Miocene slope mudstones.

Rate of accumulation

Accumulation of overburden above these five potential source rocks is shown by a dashed line on the events chart (Figure 4–45), indicating no specific rate of accumulation until the interval of late Pliocene to Recent sedimentation where rate variation is shown as defined by Piggott and Pulham (1993). Figures 4–32 and 4–33 indicate a major increase in rate of sediment accumulation occurred 6 Ma, which would accelerate burial of potential source rocks into the thermal zone for hydrocarbon generation.

Amount

Drilling has documented that the East Breaks depocenter in the vicinity of the 160-161 field contains at least 15,000 ft (5000 m) of late Miocene to Recent sediment (Figure 4–43). Dow et al. (1990) use this thickness in calculating maturation and generation models. The thickness of overburden rock for any one of the older potential source rock intervals will be greater than 15,000 ft (5000 m), but the exact amount is highly speculative.

Source Rock

Identification problem

Geochemical typing of an oil in a reservoir rock and its correlation to a probable source rock are used to determine the level of certainty or the confidence that an oil originated from a specific source. Oils from the East Breaks 160-161 field have been analyzed by Dow et al. (1990). Those oils, one each from the *Glob alt* GA-3 reservoir and the *Hyal B* HB-2 reservoir, are very similar geochemically and closely resemble continental shelf oils of Louisiana and Texas. The East Breaks 160-161 *Glob alt* and *Hyal B* oils do not correlate with the Type 1-B oils (Thompson et al., 1990) of shelf-edge and continental slope reservoirs (Dow et al., 1990).

Miocene source?

Dow et al. (1990) present a case for a Miocene source rock for the East Breaks 160-161 field, based primarily on the interpretation that the East Breaks 160-161 minibasin is a self-contained petroleum system enclosed by a salt floor and walls, and thus the hydrocarbons must have been generated from within (see Figure 4–8). Those workers present analyses of kerogens from late Miocene gravity-flow-deposited mudstones, suggesting some potential for oil generation, and speculate that more deeply buried, more organic-rich middle Miocene mudstones may be the source of the hydrocarbons. Taylor and Armentrout (1990) analyzed oils and kerogens in turbidite facies at the High Island A-537 field. They speculate that kerogens in Neogene turbidite facies are unlikely to be the source of oils in the A-537 field and further speculate that deeper source rocks with a strong marine algal fingerprint were more likely sources for the oils.

Early Tertiary source?

Gross et al. (1995) suggest that the oil of the East Breaks–High Island area originated from either lower Tertiary mudstones or uppermost Jurassic mudstones (Figure 4–5). Philippi (1974) and Sassen et al. (1988) present evidence for source potential for crude oil in the upper Paleocene to lower Eocene Wilcox Formation. If lower Tertiary Wilcox equivalent or uppermost Jurassic mudstones are the source for hydrocarbons in the East Breaks 160-161 field, then a migration avenue must exist through the salt that underlies the minibasin and generation-migration-accumulation must have been delayed until the trap formed approximately 1.2 Ma. In fact, alternative interpretations of salt distribution at the East Breaks 160-161 field suggest a salt weld with sediment-on-sediment below the minibasin rather than a salt floor (compare Figures 4–8 and 4–9). This suggests migration could have occurred from even older, more deeply buried source rocks.

Migration pathways

Data currently available preclude a precise correlation of the East Breaks 160-161 field oils with a specific source rock. Therefore, the petroleum system(s) charging the *Glob alt* reservoirs is speculative. However, the data do suggest that the hydrocarbons originate from more deeply buried thermally mature rocks than those encasing the reservoir and therefore vertical migration has occurred.

Future work

Detailed biomarker analysis of the East Breaks oils and comparison to detailed analyses of potential source rocks are necessary for a precise correlation and resolution of relatively shallow middle Miocene vs. much deeper lower Tertiary source rocks for the East Breaks 160-161 field hydrocarbons. If this exercise is successful, then the level of certainty for these petroleum systems could be raised to known.

Subsection E3

East Breaks Petroleum System Processes

Introduction

Petroleum system processes include trap formation; source-rock maturation; and generation, expulsion, secondary migration, and accumulation of hydrocarbons within a trap. Modeling of oil generation within the East Breaks 160-161 minibasin suggests that middle Miocene strata would have begun to generate hydrocarbons only 200,000 years ago and would still be active today. If older strata are the source of the petroleum, then generation must have been delayed until the late Pleistocene.

An alternative is that the petroleum has migrated after 1.2 Ma from older traps into the East Breaks 160-161 *Glob alt* through *Trim A* anticlinal traps. Periodic vertical migration of oil probably took place along growth faults between overpressured source beds and more normally pressured reservoirs. Oil accumulated in faulted rollover anticlinal traps with slightly overpressured mudstone seals. Biodegradation of oils reflects shallow accumulation prior to burial of the reservoirs below 140°F (60°C).

This subsection details aspects of this generation-migration-accumulation model.

In this subsection

This subsection contains the following topics.

Trap Formation

Minibasin structural–stratigraphic development

The structural/stratigraphic configuration of the East Breaks 160-161 minibasin formed well after *Glob alt* time. As discussed earlier, the High Island–East Breaks basin was a late Pliocene/early Pleistocene slope basin through which gravity flow sands flowed southward. Progradation overloaded the underlying salt and minibasins formed as a succession of southward-stepping growth-fault/salt-withdrawal sediment thicks (Figure 4–44).

Structural traps

Within these minibasins, structural traps of gravity-flow sandstones formed

- as fault-dependent closure at growth faults,
- as anticlinal closure formed by rollover into growth faults, or
- by postdepositional tilting of sandstones that shale-out upstructure due to syndepositional pinching-out against sea-floor valley margins (Bouma, 1982; Kneller and McCaffrey, 1995).

Stratigraphic traps

Pure stratigraphic traps occur where basinal sandstones completely bypassed updip areas subsequently filled by mud, providing both top seal and updip lateral seal (Bouma, 1982; Galloway and McGilvery, 1995).

Timing of fault movement

Fault movement timing is critical for trap formation timing. Growth-fault rollover anticlines develop by updip expansion and sediment entrapment on the downthrown side of the fault and consequent downdip sediment starvation and continued subsidence within the intraslope basin (see Figure 4–43 for geometries above the *Trim A* interval along fault A'). Thus, the updip trap for gravity-flow sandstone is the rollover into the fault, formed during the dynamic phase of fault movement.

Fault A'

In the East Breaks 160-161 minibasin, the fault splay fault A' forms the northern boundary to the field (Figures 4–42 and 4–43). The dynamic phase of this fault is recorded by the wedge-shaped sediment thickening into the fault, deposited between pre-*Hyal B* (ca. 1.00 Ma) time and late *Trim A* (ca. 0.56 Ma) time (Figure 4–31). Its growth phase began about 1.20 Ma (Armentrout in Dow et al., 1990; Armentrout et al., 1991). Sea-floor expression of this fault clearly indicates offset of Holocene sediments, showing that the fault is currently active (Figure 4–43).

Geochemistry of Two Oils from East Breaks

Introduction

Two oil samples (*Glob alt* = GA-3 and *Hyal B* = HB-2) from two different reservoirs in the East Breaks 160-161 field provide data for modeling the history of hydrocarbon generation and migration within this minibasin. Dow et al. (1990) report that the East Breaks oils are biodegraded and mixed lower molecular weight, thermally mature oil. The C_{10} through C_{30} alkanes of the GA-3 oil are better preserved than those of the HB-2 oil. This is demonstrated by the higher peaks of C_{10} through C_{30} alkanes on the gas chromatograms below, suggesting that the stratigraphically deeper GA-3 oil is less degraded and slightly more mature than the stratigraphically shallower HB-2 oil. Neither oil exhibits evidence of evaporative fractionation reported by Thompson (1987) in over 75% of Gulf Coast Tertiary oils.

Oil preservation pattern

The oil preservation pattern is attributed to the history of generation, expulsion, secondary migration, and accumulation (Dow et al., 1990). The better preserved C_{10} to C_{30} alkanes in the GA-3 oil occur where the reservoir temperature is about 160°F (71°C). The more poorly preserved alkanes in the HB-2 oil occur where the reservoir temperature is about 130°F (Figure 4–52). Microbial activity responsible for biodegradation occurs at temperatures below 140°F (60°C). The earliest migration fluids would have been the least mature and potentially most biodegraded due to the shallow level of accumulation. With increasing burial of the source rock, more mature oil and condensate would have been generated and better preserved in deeper reservoirs below the depth of microbial activity. These observations suggest sequential expulsion and migration of progressively more mature products as the source(s) passed through the oil window. Alternative interpretations are offered in Dow et al. (1990).

The figure below shows whole oil chromatograms of crude oils from two reservoirs in the East Breaks 160-161 field. Oil 1 is from the HB-2 reservoir; oil 2 is from the *Glob alt* GA-3 reservoir. Both are interpreted as biodegraded and mixed with fresh oil, suggesting multiple pulses of accumulation.

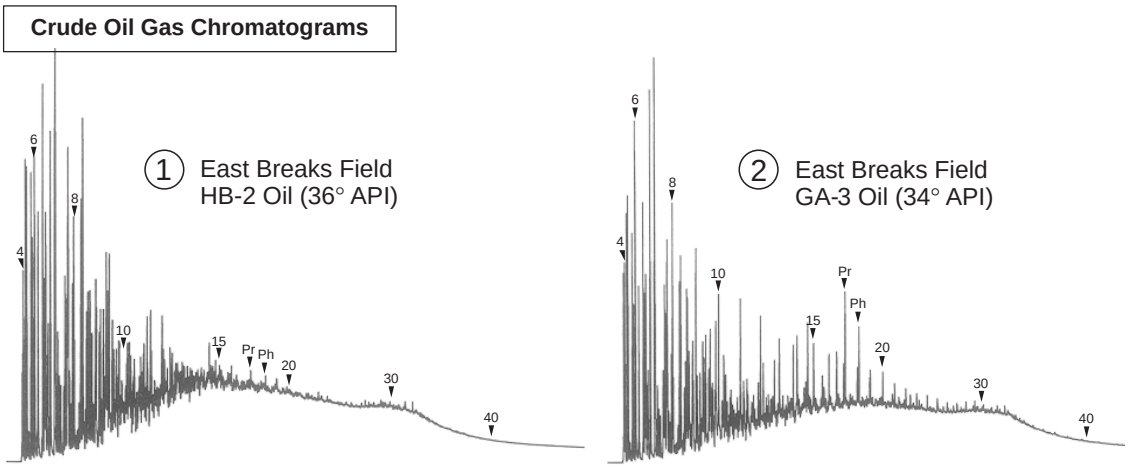

Figure 4–51. From Dow et al. (1990); courtesy Gulf Coast SEPM.

Hydrocarbon Generation Model

Method

A 32-layer, 1-D mathematical model (Figure 4–53) was constructed for the East Breaks 160-161 minibasin. The No. A-29 well in block 160 was used for stratigraphic and thermal control, including borehole temperature surveys and vitrinite reflectance data. Modeling was extended 3,000 ft (1000 m) below true vertical drilling depth (12,000 ft, 4000 m) to evaluate the underlying speculated source potential of the middle and lower Miocene section. The figure is a north–south seismic reflection profile across the East Breaks 160-161 intraslope minibasin (see Figures 4–42 and 4–44). The deviated wellbore of the East Breaks well 160 No. A-29 is marked with a white dashed line. Reservoirs for analyzed oils are indicated for the *Hyal B* HB-2 reservoir and for the *Glob alt* GA-3 reservoir. Rock cutting samples from intervals indicated by A and B were used by Dow et al. (1990) to calibrate kerogen type for kinetic modeling.

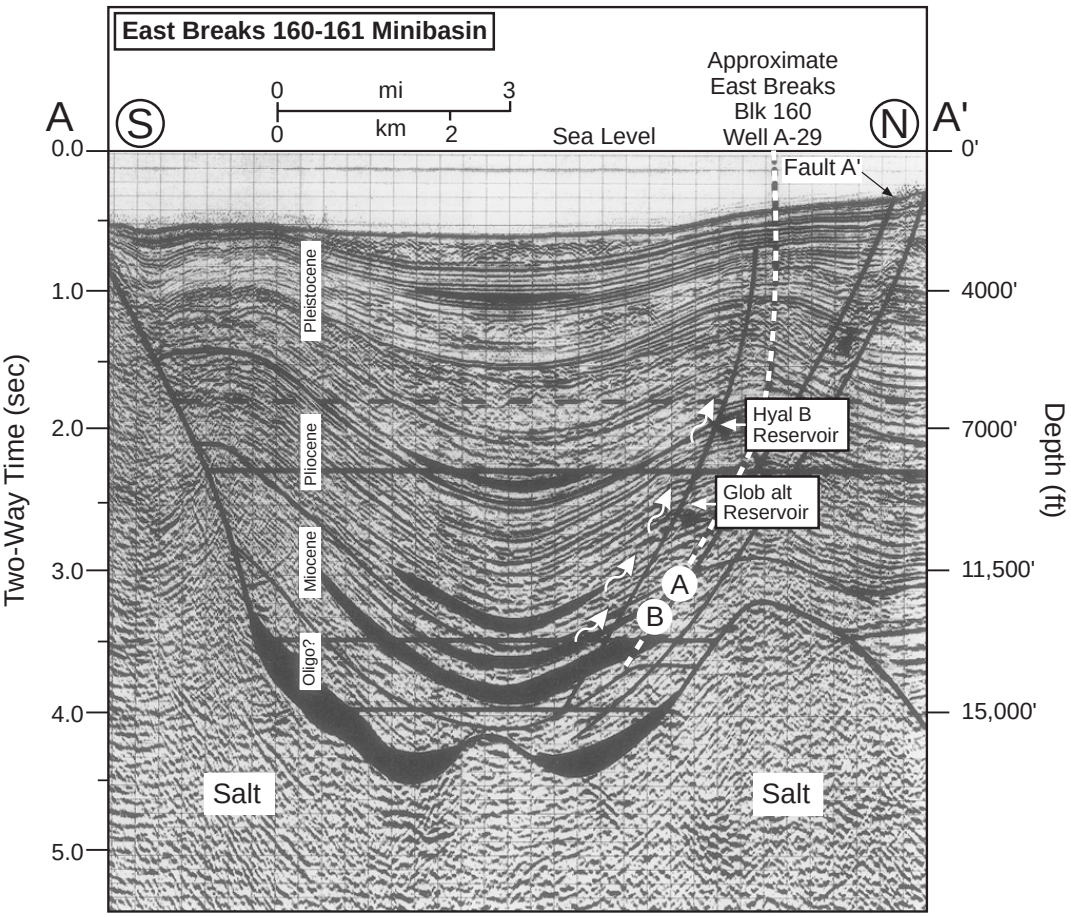

Figure 4–52. After Dow et al. (1990); courtesy Gulf Coast SEPM.

Hydrocarbon Generation Model, continued

Generation and expulsion timing

A burial history plot with computed hydrocarbon generation history shows that peak oil generation in the A-29 well began at the inferred base of the lower Miocene when buried below 11,000 ft (3000 m) about 1.2 Ma, at the base of the inferred middle Miocene when it too passed below 11,000 ft (3000 m) burial about 0.2 Ma.

Miocene source beds, if present, would be actively generating and expelling oil and gas at the present time. Dow et al. (1990) interpret this to account for the biodegraded East Breaks 160-161 field oils being recharged with fresh oil during a later migration phase. The relatively low maturity of the inferred Miocene section should also result in only minor thermogenic gas generation and might explain the absence of evaporative fractionation in the produced crudes of this field in contrast to approximately 75% of Gulf Coast Tertiary crudes (Thompson et al., 1990).

Burial history

The following figure is a 1-D burial history/maturation plot showing the critical moment (2.0 Ma) and the time of oil generation (2.0 Ma to present) for the East Breaks 160-161 minibasin petroleum system, assuming that lower Miocene rocks have sourced the hydrocarbons. Alternative burial history plots could be constructed using the assumed burial depths for each potential source horizon. For these deeply buried potential source horizons, generation must have been delayed until very recently or secondary migration from older, deeper reservoirs provides the hydrocarbons trapped at the East Breaks 160-161 field. Additionally, basins are 3-D entities, and either 2-D models throughout the basin or a 3-D model of the entire basin is essential to understanding the maturation history of a basin.

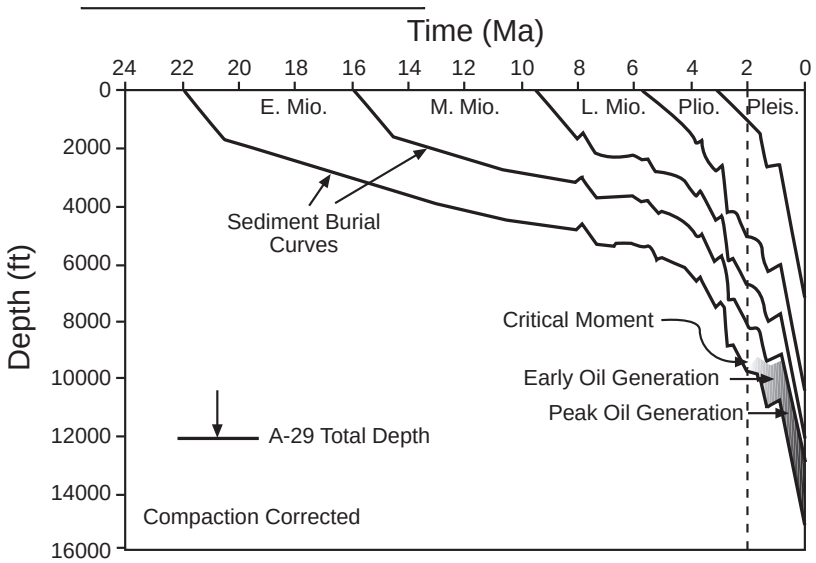

Figure 4–53. After Dow et al. (1990); courtesy Gulf Coast SEPM.

Hydrocarbon Migration Model

Vertical migration path

Petroleum generated at depth, either from the middle Miocene as suggested by Dow et al. (1990) or the lower Tertiary or upper Jurassic as suggested by Gross et al. (1995), had to move vertically within the East Breaks 160-161 minibasin to charge the known gravity-flow sandstone reservoirs. The deepwater lowstand gravity-flow reservoir sandstones are separated by hemipelagic mudstones deposited during condensed sedimentation of each cycle. Migration through matrix porosity of these effective top-seal mudstones is highly unlikely. Thus, vertical migration along faults is the most probable avenue. Episodic movement on the faults would result in multiple phases of migration and could account for the observed mix of oils of different maturities within the same structure (Schanck et al., 1988) and the mix of biodegraded and nonbiodegraded oil in the same reservoir (Dow et al., 1990; see also Anderson, 1993, and Anderson et al., 1994, for migration model).

Lateral migration path

Once the petroleum has migrated up the fault to the porous and permeable sandstone, it could move laterally up-structure within the continuous sand beds until it accumulated within structural closure. The driving force behind the migration is most likely a combination of several factors, including fluid buoyancy, formation pressure trends, and salinity gradients. Similar migration patterns have been suggested by Hanor and Sassen (1990).

Southern Louisiana model

Hanor and Sassen (1990) present data from Cretaceous and Tertiary strata in southern Louisiana for aqueous fluid flow from deep, geopressured sediments vertically upward to normally hydropressured zones. This migration is interpreted to occur through fractures and faults rather than through matrix porosity.

The following figure is a regional cross section summarizing in a qualitative, conceptual way the regional hydraulic flow regimes of the Louisiana Gulf Coast above a depth of 20,000 ft (6096 m). The uppermost regime consists of low-salinity, meteoric water driven gulfward by differences in topographic elevation. The deepest regime consists of moderately saline water driven upward and laterally by excess fluid pressures. In between is a hydraulic regime in which lateral and vertical flow of saline brines is taking place—in part in response to differences in fluid density caused by spatial variations in temperature and salinity. The dissolution of salt plays a critical role in driving fluid flow in this region. Arrows show possible pathways of fluid flow.

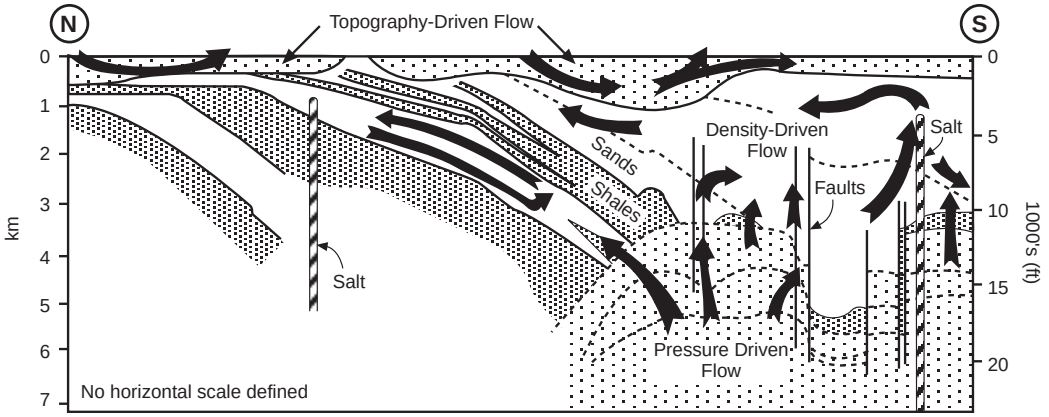

Figure 4–54. From Hanor and Sassen (1990); courtesy Gulf Coast SEPM).

Hydrocarbon Migration Model, continued

GOM Neogene model

Patterns of migration in the offshore Gulf of Mexico Neogene strata suggest migration avenues similar to the southern Louisiana model. Lovely and Ruggiero (personal communication, 1995) integrated multiple data sets, including geochemical analysis of cores and sea-floor acoustic impedance patterns and orthocontouring of structure maps, and formulated a hypothesis for petroleum migration.

The figure below is a north–south 3-D seismic reflection profile illustrating three possible hydrocarbon migration pathways and related sea-bed features. They concluded that the primary migration pathway involves migration up from geopressured source rocks along the sediment/salt interface with sea-floor seepage forming hydrates and providing nutrients to carbonate producing organisms (1). A secondary pathway involves redirection of some of the petroleum from the sediment/salt interface laterally into sand-rich carrier beds (2). Pathway 3 consists of a fault intersection of either pathway 1 or 2 and the vertical migration along fault-associated fracture conduits with possible formation of fault scarp amplitude halos at intersected reservoirs and sea-floor hydrate/carbonate mounds.

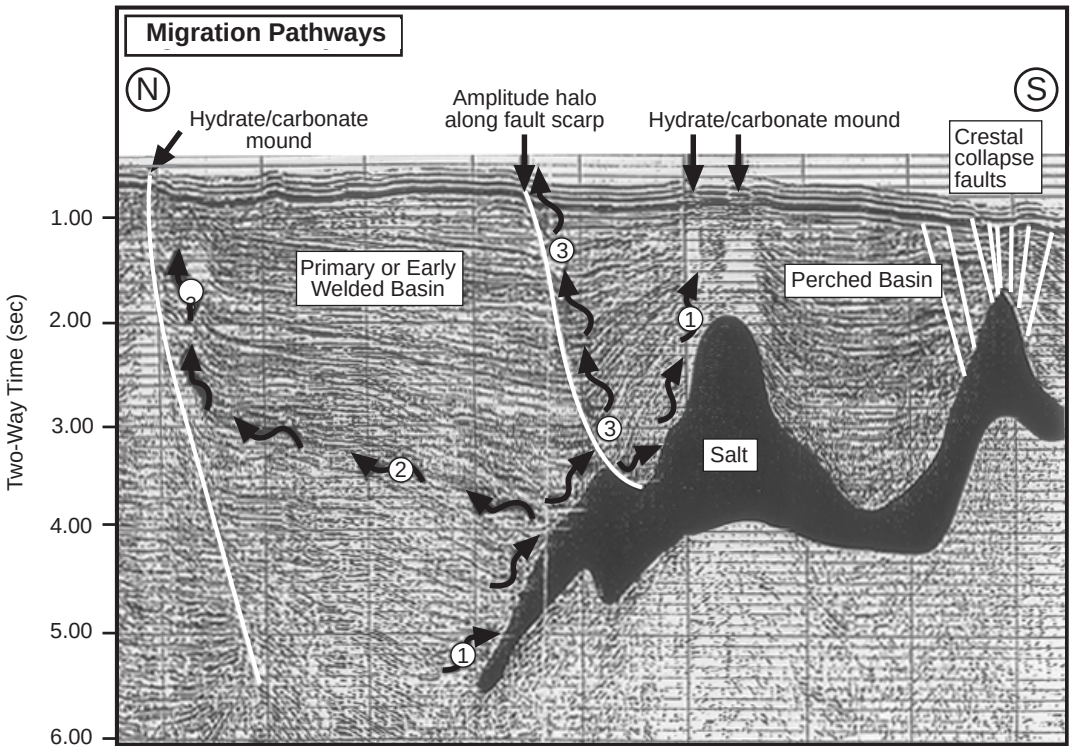

Figure 4–55. Based on data from Lovely and Ruggiero (1995, personal communication).

Hydrocarbon Migration Model, continued

East Breaks migration model

Using these hypothetical migration avenues, a migration pathway model has been constructed for the East Breaks 160-161 minibasin. Dow et al. (1990) present temperature information, indicating an elevated thermal gradient in the block 160-A-29 well where it is in close proximity to salt. Additionally, the A-29 borehole mud weight of 13.5 lb below 5,000 ft (1524 m) and 15.7 lb below 7,000 ft (2134 m) and mathematical modeling suggest probable overpressure and undercompacted sediments below a depth of 10,000 ft (3048 m). The consequent thermal and geopressure gradient would drive fluid flow from depth up migration pathways into available reservoirs.

The figure below is a north–south seismic section showing the hypothetical model for migration pathways within the East Breaks 160-161 field (see Figure 4–42 for location). Fault conduits allow upward migration from high-pressure, thermally mature probable source rocks into the intersected gravity-flow sandstone reservoirs at the *Glob alt, Hyal B,* and *Trim A* horizons. The *Glob M* horizon between the *Glob alt* and *Hyal B* horizons is productive from sands in the East Breaks 158-159 field 6 mi (about 10 km) to the west within the same minibasin.

The probable fault-plane migration pathway of the East Breaks 160-161 field offsets the sea floor and locally has associated mud volcanoes along the fault scarp. Despite these observations of recent and/or current fault movement and fluid discharge, the absence of hydrates and biogenic carbonate buildups suggests that hydrocarbons are not reaching the shallowest section.

Seal rocks consist of condensed-section mudstones that provide effective top seal for each lowstand gravity-flow sandstone. These condensed-section mudstones are often thick enough to provide effective lateral seal except where faults offset juxtaposed sandstones.

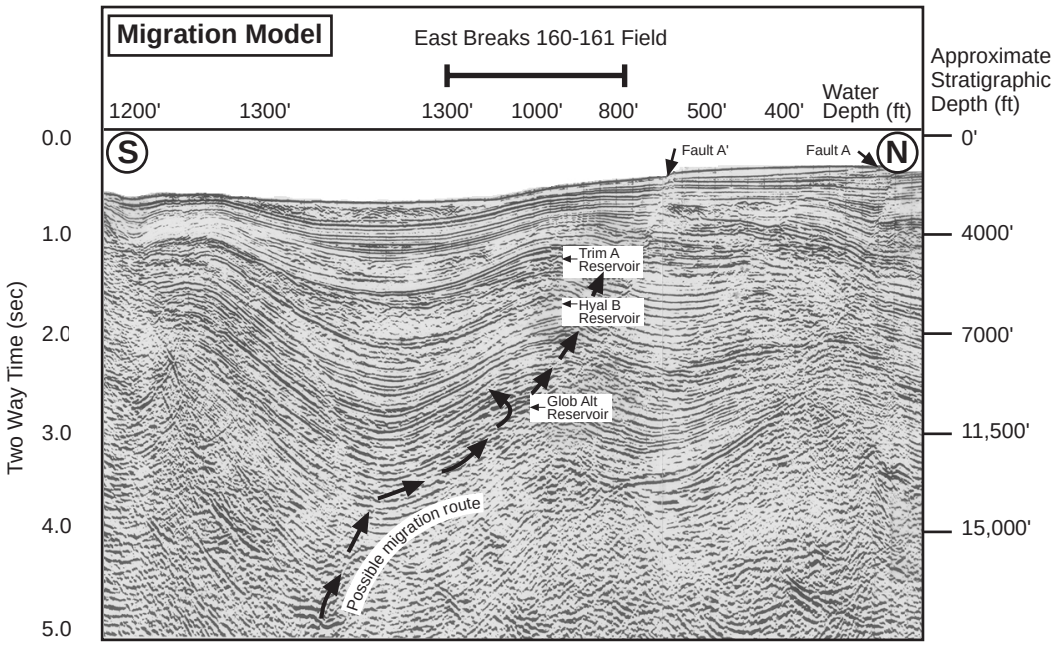

Figure 4–56. From Dow et al. (1990); courtesy Gulf Coast SEPM.

Hydrocarbon Accumulation Model

Impact of growth-fault movement

The multiple phases of petroleum charging the East Breaks 160-161 reservoirs and their accumulation within the anticlinal trap is interpreted to be controlled by the timing of growth-fault movement. Fault movement and fault-associated fracturing in the adjacent rocks could enhance the migration conduit. Migration up the fault would have provided petroleum charge into the intersected reservoir sandstones.

Fault movement and trap formation

Rollover into the growth-fault-initiated trap formation occurred between about 1.2 Ma and the present. Fault movement occurred during each lowstand of sea level when differential loading from shelf-edge deltaic sedimentation and consequent salt withdrawal destabilized the upper slope system (Armentrout, 1993). Given the sea-level fluctuation cycles documented within the East Breaks 160-161 minibasin (Armentrout and Clement, 1990; Armentrout, 1993), at least five and potentially nine lowstand events may have caused episodic movement of the north-bounding growth fault of the East Breaks 160-161 field (Figure 4–31, nine cycles between 1.2 Ma and the present).

Sandbody geometries

The gravity-flow sandstone reservoirs within the field were transported from the north, southward into the East Breaks 160-161 minibasin (Figure 4–40), where the mapped pattern of the *Glob alt* sandstones show elongate and lobate north-to-south geometries (Figure 4–49). These north-to-south depositional geometries are draped over the east–west down-to-the-north rollover anticline, resulting in a seismic reflection amplitude pattern that shows north-to-south flank structural downdip termination (Figure 4–57C). East-to-west reflection amplitude termination is stratigraphically controlled by sand distribution. This petroleum-associated reflection amplitude pattern is in contrast to that for sheet sands that would drape over the entire structure and show four-way downdip structural termination of seismic reflection (Figure 4–57D).

Hydrocarbon Accumulation Model, continued

Tying seismic to well data

The figure below is a seismic reflection profile across the East Breaks 160-161 field, showing the 160 No. 1 well SP log and synthetic seismogram and two schematic diagrams for interpreting possible seismic reflection amplitude anomaly maps, which could indicate hydrocarbon-charged sands. Bioevent horizons correlate with the top seal above each reservoir interval. Only the lower *Trim A* and *Glob alt* reservoir sandstones are well developed in this well. The depositional model for a delta-front sheet sand extending over the entire postdepositional anticline is likely to have four-way downdip termination of petroleum-associated seismic reflection amplitude anomalies (view C). The depositional model for a depositional dip-oriented gravity-flow sandstone draped over the postdepositional anticline is likely to have two-way structural termination of a petroleum-associated seismic reflection amplitude anomaly, with stratigraphic termination of reflectors along both depositional-strike directions (view D). The mapped amplitude pattern in both the *Trim A* and *Glob alt* intervals agrees with a channel-fed gravity-flow depositional system.

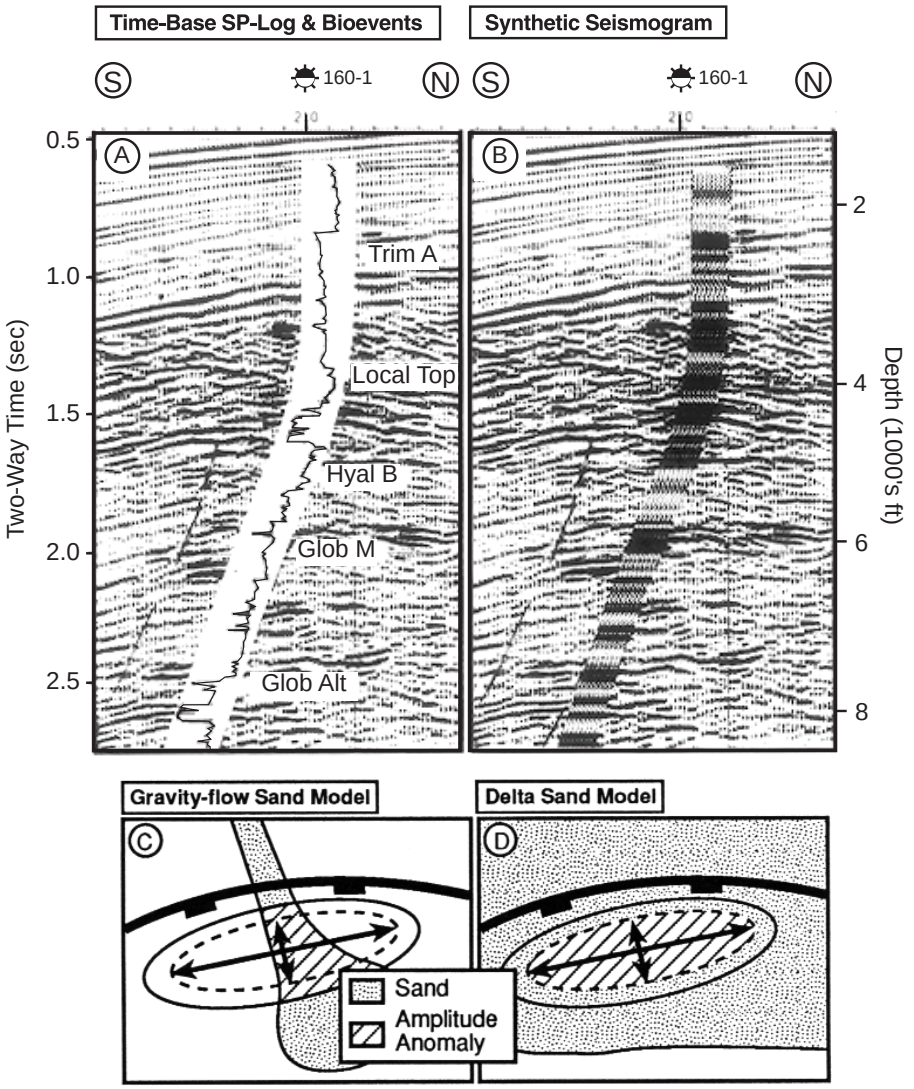

Figure 4–57.

Hydrocarbon Accumulation Model, continued

Recharging of reservoirs

Preserving these petroleum resources has been discussed in reference to biodegradation, which has produced much of the gas in the reservoirs—especially at the *Trim A* horizon. Burial of the reservoirs to depths with temperatures in excess of 140°F (60°C) prevents further microbial degradation of the oil. Late episodes of fault movement facilitates recharging the reservoirs with higher maturity oil, migrating upward from the deeply buried active source rock that is not yet specifically identified (see Anderson, 1993; Anderson et al., 1994).

Critical Moment (or Interval)

Introduction

Magoon and Dow (1994) define the critical moment as the time that best depicts the generation-migration-accumulation of most hydrocarbons in a petroleum system. The East Breaks 160-161 field began to accumulate no earlier than 1.2 Ma when the trap began forming, and accumulation is inferred to continue to the present (Dow et al., 1990). The structural configuration has changed little since initial formation, so that the present-day map (Figure 4–42) and cross-sectional geometry (Figure 4–43) accurately depict the trapping aspects of the petroleum system.

Possible critical moments

According to the maturation model for a middle Miocene source rock, peak oil generation would have begun 0.2 Ma (Dow et al., 1990), and the critical moment for the East Breaks 160-161 petroleum system would be 0.20 Ma (Figures 4–45 and 4–53). If a stratigraphically deeper lower Paleocene or upper Jurassic source rock is the origin of the East Breaks oils, an earlier onset of significant generation could have occurred with migration, continuing to today and supplying the petroleum that has charged the field.

Summary

The critical moment will be different for the middle Miocene, lower Paleocene, and lower Tertiary source rock. The critical interval encompasses the composite of all critical moments. The critical interval for the East Breaks 160-161 petroleum system is 2.8 Ma to the present. It is that time period after deposition of the reservoir and seal during which subsequent growth fault movement formed the anticlinal trap and accumulation of migrating hydrocarbons occurred.

Section F
Summary and Exploration Strategy for Deepwater Sands

Introduction

Synthesis of the regional basin analysis, depocenter, and depositional sequence history and the geologic setting of local minibasins provides geologic constraints on petroleum system formation. The East Breaks 160-161 minibasin contains all the elements required for generation, migration, and accumulation of hydrocarbons and is a true petroleum system. Understanding this petroleum system provides a template for exploration of depositionally similar areas.

In this subsection

This section contains the following topics.

Summary of the Petroleum Geology of the East Breaks Minibasin

Introduction

Field development, including step-out drilling, and exploration are enhanced by the understanding of the petroleum system—especially the occurrence of probable source rock, migration pathways, and reservoir.

Generation–migration–accumulation

Reservoired oils in the East Breaks 160-161 field are more thermally mature than the surrounding sediments, demonstrating that the hydrocarbons were contributed from deeper source rocks. Their generation history is controlled by the thermal gradient and overburden rock accumulation history, interpreted from both regional depocenter patterns and local minibasin history. Fault and salt-wall migration pathways provide vertical avenues for migration. Slope basin gravity-flow sands are the principal reservoir target in the High Island–East Breaks area for all except the most shallow stratigraphic intervals, where wave-dominated deposition of shelf sands produced laterally continuous sheet-like reservoirs subsequently draped over anticlinal structure.

Traps

The gravity-flow sands were transported and deposited within sea-floor physiographic lows between the anticlinal structures and within the isochron thicks of the synclinal sediment fill. Petroleum accumulations occur within traps where these synclinal sandstones are folded over postdepositional anticlines (Armentrout et al., 1991) or within structural-stratigraphic traps where synclinal sandstones pinch-out against sea-floor valley margins (McGee et al., 1994) or completely bypassed valley conduits subsequently filled by mudstone plugs (Galloway and McGilvery, 1995).

Exploration Strategy for Deepwater Sands

Introduction

The lateral shifting of depositional lobes within the stacked sandstones of the *Glob alt* reservoir at the East Breaks 160-161 field clearly demonstrates the need to carefully map the internal seismic facies and amplitude patterns within prospects in order to optimize prediction of sandstone occurrence. In concert with detailed fault-pattern maps, the highly compartmentalized reservoir can be delineated and wells optimally located. Additionally, seismic facies maps may suggest downflank or off-structure potential where faulting may not impose development problems. Construction of detailed seismic facies and fault pattern maps, preferably using 3-D seismic reflection volumes, results in a higher success rate of finding the closely spaced but laterally discontinuous reservoirs of gravity-flow intraslope basin plays.

Procedure

Based on the regional basin analysis as previously discussed, an exploration strategy for the East Breaks area and GOM basin deepwater areas can be defined. The table below lists possible steps to take to implement the strategy.

Step	Action
1	Delineate prospective areas by looking for lowstand sand-prone areas. Use trends of isochron thicks basinward of each depositional cycle's shelf edge as a guide.
2	Map seismic facies and structures of sand-prone intervals to locate prospects.
3	Map amplitude patterns within prospects to optimize prediction of sandstone and hydrocarbon occurrence. Calibrate rock/physics models with local well data.
4	Map deep penetrating fault and salt patterns as possible migration avenues for charging reservoirs of potential traps. Take particular note of the timing of active fault movement vs. the modeled timing of hydrocarbon expulsion from active source-rock volumes in communication with the fault.
5	Calculate the risk of trap existence vs. generation-migration timing using burial history and migration avenue models.
6	Locate exploration wells using detailed fault pattern maps overlain by seismic facies maps of sand-prone facies and structural maps showing closure at the top of the sand-prone seismic facies.
7	Use seismic facies maps to identify downflank or off-structure potential where faulting may not impose development problems.
8	As wells are drilled, place each sandstone unit encountered into its regional depositional context as a means of understanding potential reservoir continuity.
9	Use computer simulations based on empirical data to predict the geology—especially petroleum system elements—beyond control points.

Exploration Strategy for Deepwater Sands, continued

Locating sand-prone areas

Trends of isochron thick synclinal fill basinward of each depositional cycle's shelf edge delineate areas in which to map seismic facies, looking for lowstand sand-prone areas partitioned by regionally correlative condensed sections. The slope facies within the lowstand isochron thicks are most likely to be sandy downslope for sand-prone shelf depocenters formed during the preceding relative highstand of sea level.

Finding prospects

Once areas of potentially sand-prone seismic facies are identified, the trapping potential of each can be assessed through both prospect scale seismic facies mapping and structural mapping of the potentially sand-prone interval. In concert with prospect mapping, mapping of deep penetrating fault and salt patterns as potential migration avenues and the calculation of trap vs. generation-migration models helps us assess the risk of specific prospects.

Drilling prospects

Once drilling has commenced, each sandstone unit encountered should be placed into its regional depositional context so that downslope or upslope reservoir potential can be correctly assessed and subsequent wells optimally located.

Potential of *Glob alt* and *Trim A* sandstones

The figure below contrasts the depositional setting of the *Trim A* (A) and *Glob alt* (B) sandstones of the East Breaks 160-161 field. Drilling at the field encountered only channels in the *Trim A* reservoir, with the channel-fed lobes interpreted to occur further down paleoslope in the age-equivalent hummocky-mounded-to-sheet seismic facies. The *Trim A* shelf edge is mapped at the north boundary of the field. Thus, all *Trim A* associated sand-prone facies are restricted to this minibasin. Drilled *Glob alt* facies include channels and channel-fed lobes nearly 50 mi (80 km) from the mapped *Glob alt* shelf edge and probable deltaic sediment source from which the gravity-flow sands were supplied. Exploration potential within the *Glob alt* depositional sequence exists along the entire sediment transport system, as clearly demonstrated by the known occurrence of *Glob alt* reservoirs in the High Island–East Breaks area (Figure 4–40).

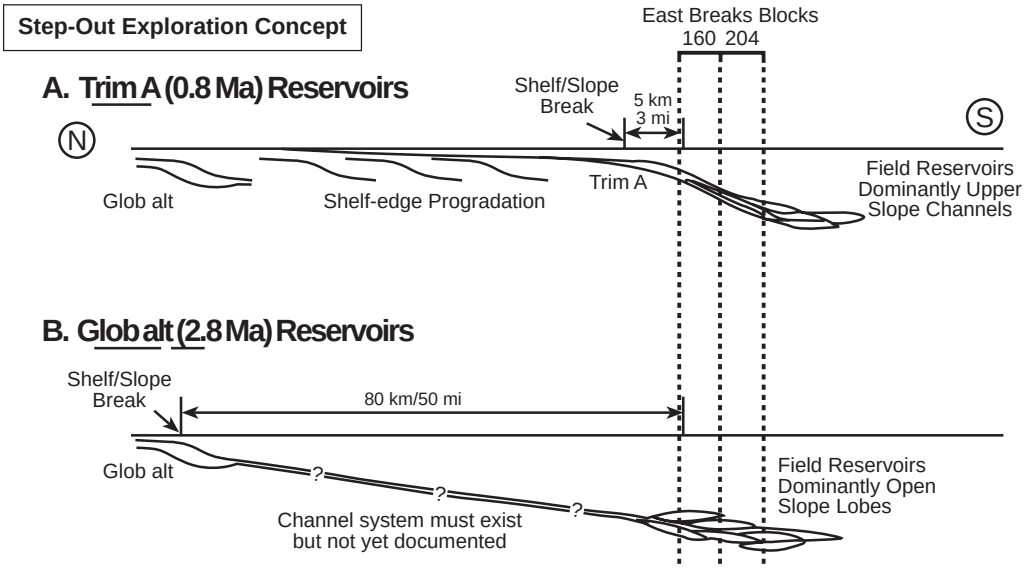

Figure 4–58. After Armentrout et al. (1991); courtesy Springer-Verlag.

Stratigraphic Predictions from Computer Simulation

Introduction

Computer simulation can help us predict lithofacies and hydrocarbon occurrence between and beyond data control. Both 2-D and 3-D simulation programs are available or in development. With high-resolution input of chronostratigraphy, lithofacies, and sedimentary process rates, simulations can be constructed that interpolate and extrapolate distributions of potential organic-rich source rock, seal rock, and reservoir rock.

Sedimentation model

The following figures are from a simulation done by Rouch et al. (1993) for the seismic reflection profile transect in Figure 4–44 (location on Figure 4–39). The detailed calibration of that seismic profile using wireline logs, well-cuttings lithofacies, and biostratigraphic data provides a high-resolution data set.

The data were input in a commercially available simulation package that performs 2-D backstripping and calculates subsidence rates and sediment flux rates across the entire seismic profile. Using a spectrum of input parameters based on regional geology and including those calculated from the backstripping exercise, the simulation fills in each polygon defined by digitized maximum flooding surface horizons with geologically appropriate lithofacies. The digitized horizons and the degree of fit between the simulated sedimentary record and the input data are shown below. Areas where the simulation shows excess sediment accumulation compared to the known record are noted by striped black patterns above the digitized flooding horizon; areas where the simulation shows less sediment accumulation than the known area are noted by solid gray areas below the digitized flooding horizon. The figure is the end result of 24 simulation runs converging toward a best-fit answer (Rouch et al., 1993).

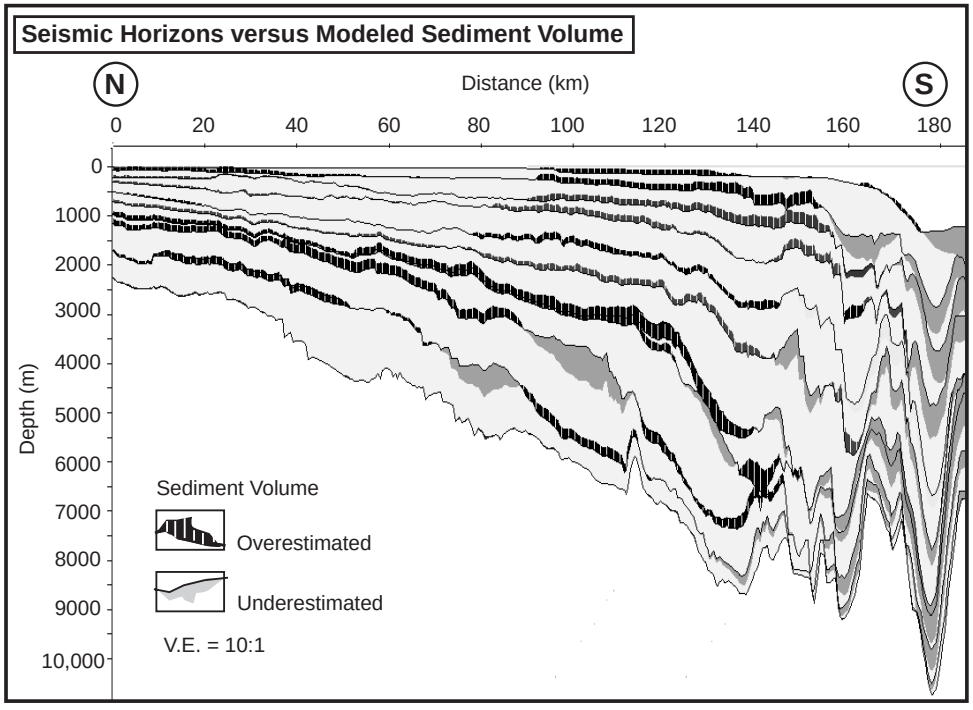

Figure 4–59. After Armentrout (1991); courtesy Springer-Verlag.

Stratigraphic Predictions from Computer Simulation, continued

Model refinement

The difference between the simulation predictions and the known geology lets us focus on specific areas and processes to refine the model. Analysis of subsidence rates, paleobathymetry, fluvial and coastal gradients, volume of sediment bypassing the area (slope stability factor), slumping, and gravity-flow transport must be considered.

Lithofacies simulation

Once the best-fit simulation for most areas is achieved, lithofacies can be simulated. The resulting simulation displays a spectrum of lithofacies types based on the computer program. These predictions can be tested against the well data lithofacies and further fine-tuning performed. Once the best-fit lithofacies simulation is achieved, it can be used to infer the distribution of source, seal, and reservoir rock between well control and beyond into undrilled areas.

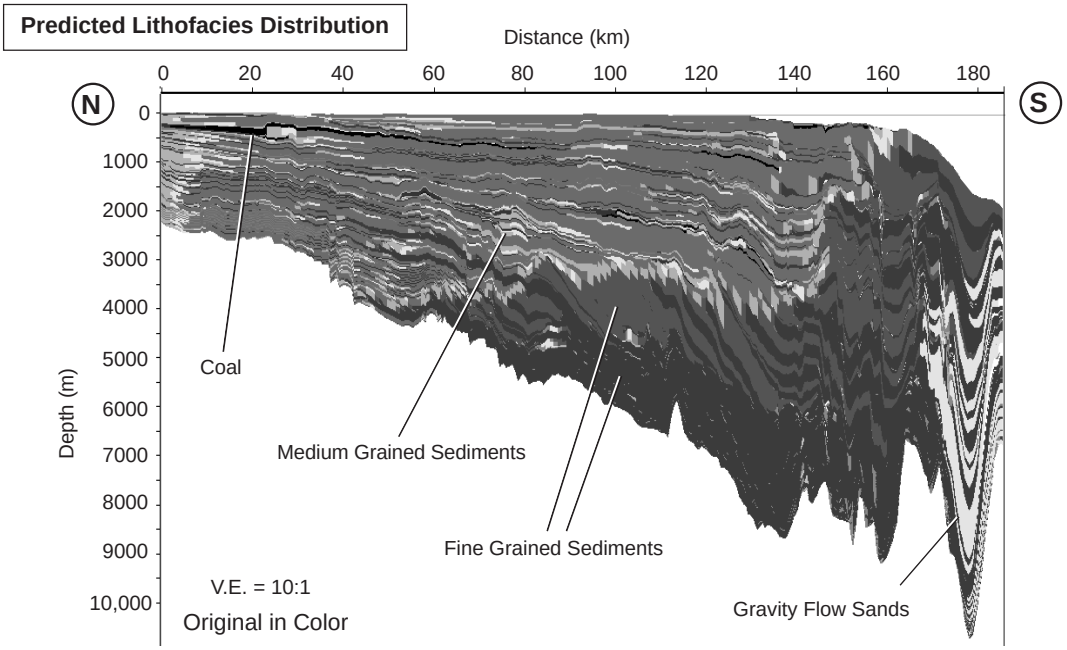

Figure 4–60. After Armentrout (1991); courtesy Springer-Verlag.

Using different computer packages

Continuing development of the simulation package used by Rouch et al. (1993) is focused on predicting organic richness, maturation, porosity, and fluid flow, as well as converting the lithofacies distributions into synthetic seismic reflection profiles that can be compared to profiles generated from field data. Each of the simulations must be checked against available data. Several simulations, each using different computer programs, clarify prediction reproducibility. Development of 3-D simulation programs will further enhance the predictions based on well-constrained data sets.

Integrating basin history

All of these efforts—gathering and integrating empirical data, computer simulation of geologic processes, and prediction of specific lithofacies—must be evaluated within the context of the basin history. The future success of geologic analysis is dependent on our careful and accurate interpretation of basin history from regional to local scales.

Section G
References

Anderson, R.N., 1993, Recovering dynamic Gulf of Mexico reserves and the U.S. energy future: Oil & Gas Journal, 26 April 1993, p. 85–88, 90–92.

_____, P. Flemings, S. Losh, J. Austin, and R. Woodhams, 1994, Gulf of Mexico growth fault drilled, seen as oil, gas migration pathway: Oil & Gas Journal, 6 June 1994, p. 97–104.

_____, K. Abdulah, S. Sarzalejo, F. Siringan, and M.A. Thomas, 1996, Late Quaternary sedimentation and high-resolution sequence stratigraphy of the East Texas shelf, *in* M. DeBatist and P. Jacobs, eds., Geology of Siliciclastic Shelf Seas: Geological Society of London Special Publication 117, p. 94–124.

Antoine, J.W., R.G. Ray, Jr., T.G. Pyle, and W.R. Bryant, 1974, Continental margins of the Gulf of Mexico, *in* C.A. Burk and C.L. Drake, eds., The Geology of Continental Margins: New York, Springer-Verlag, p. 683–693.

Apps, G.M., F.J. Peel, C.J. Travis, and C.A. Yeilding, 1994, Structural controls on Tertiary deep water deposition in the northern Gulf of Mexico: Proceedings, Gulf Coast Section SEPM 15th Annual Research Conference, p. 1–7.

Armentrout, J.M., 1987, Integration of biostratigraphy and seismic stratigraphy: Pliocene–Pleistocene, Gulf of Mexico: Proceedings, Gulf Coast Section SEPM 8th Annual Research Conference, p. 6–14.

_____, 1991, Paleontological constraints on depositional modeling: examples of integration of biostratigraphy and seismic stratigraphy, Pliocene–Pleistocene, Gulf of Mexico, *in* P. Weimer and M.H. Link, eds., Seismic Facies and Sedimentary Processes of Submarine Fans and Turbidite Systems: New York, Springer-Verlag, p. 137–170.

_____, 1993, Relative seal-level variations and fault-salt response: offshore Texas examples: Proceedings, Gulf Coast Section SEPM 14th Annual Research Conference, p. 1–7.

_____, 1996, High-resolution sequence biostratigraphy: examples from the Gulf of Mexico Plio–Pleistocene, *in* J. Howell and J. Aiken, eds., High Resolution Sequence Stratigraphy: Innovations and Applications: The Geological Society of London Special Publication 104, p. 65–86.

_____, and J.F. Clement, 1990, Biostratigraphic calibration of depositional cycles: a case study in High Island–Galveston–East Breaks areas, offshore Texas: Proceedings, Gulf Coast Section SEPM 11th Annual Research Conference, p. 21–51.

_____, R.J. Echols, and T.D. Lee, 1990, Patterns of foraminiferal abundance and diversity: implications for sequence stratigraphic analysis: Expanded Abstracts, Gulf Coast Section 11th Annual Research Conference, p. 53–58.

_____, L.B. Fearn, K. Rodgers, S. Root, W.D. Lyle, D.C. Herrick, R.B. Bloch, J.W. Snedden, and B. Nwankwo, 1999, High-resolution sequence stratigraphy of a low-stand prograding deltaic wedge, Oso field (late Miocene), Nigeria, *in* R.W. Jones and M.D. Simmons, eds., Biostratigraphy in Production and Development Geology: Geological Society, London, Special Publication 152, p. 259–290.

_____, S.J. Malacek, P. Braithwaite, and C.R. Beeman, 1991, Seismic facies of slope basin turbidite reservoirs, East Breaks 160-161 field: Pliocene–Pleistocene, northwestern Gulf of Mexico, *in* P. Weimer and M.J. Link, eds., Seismic Facies and Sedimentary Processes of Submarine Fans and Turbidite Systems: New York, Springer-Verlag, p. 223–239.

_____, _____, L.B. Fearn, C.E. Sheppard, P.H. Naylor, A.W. Miles, R.J. Desmarais, and R.E. Dunay, 1993, Log-motif analysis of Paleogene depositional systems tracts, central and northern North Sea: defined by sequence stratigraphic analysis, *in* J.R. Parker, ed., Petroleum Geology of Northwest Europe: Proceeedings of the 4th Conference, The Geological Society of London, p. 45–57.

_____, _____, V.R. Mathur, G.L. Neuder, and G.M. Ragan, 1996, Intraslope basin reservoirs deposited by gravity-driven processes: south Ship Shoal and Ewing Banks areas, offshore Louisiana, *in* J.A. Pacht, R.E. Sheriff, and B.F. Perkins, eds., Stratigraphic Analysis: Utilizing Advanced Geophysical, Wireline, and Borehole Technology for Petroleum Exploration and Production: Proceedings, Gulf Coast Section SEPM 17th Annual Research Conference, p. 7–18.

_____, B.K. Rodgers, L.B. Fearn, R.B. Block, J.W. Snedden, W.D. Lyle, D.C. Herrick, and B. Nwankwo, 1997, Application of high resolution biostratigraphy, Oso field, Nigeria: Proceedings, Gulf Coast Section SEPM 18th Annual Research Conference, p. 13–20.

Bartek, L.R., P.R. Vail, J.B. Anderson, P.A. Emmet, and S. Wu, 1991, The effect of Cenozoic ice sheet fluctuations on the stratigraphic signature of the Neogene, *in* S. Cloetingh, ed., Long Term Sea Level Changes: Journal of Geophysical Research, vol. 96, 6753–6778.

Beard, J.H., J.B. Sangree, and L.A. Smith, 1982, Quaternary chronology, paleoclimate, depositional sequences, and eustatic cycles: AAPG Bulletin, vol. 66, p. 158–169.

Berggren, W.A., D.V. Kent, and J.A. Van Couvering, 1985, The Neogene: part 2. Neogene geochronology and chronostratigraphy, *in* N.J. Snelling, ed., The Chronology of the Geologic Record: Blackwell Scientific Publishing and Geological Society of London Memoir 10, p. 211–260.

Bilinski, P.W., D.T. McGee, D.S. Pfeiffer, and R.S. Shew, 1995, Reservoir characterization of the “S” sand, Auger field, Garden Banks 426, 427, 470, and 471, *in* R.D. Winn, Jr., and J.M. Armentrout, eds., Turbidites and Associated Deep-water Facies: SEPM (Society for Sedimentary Geology) Core Workshop No. 20, p. 75–93.

References, continued

Blow, W.H., 1969, The late Middle Eocene to Recent Planktonic foraminiferal biostratigraphy: Proceedings, First Planktonic Conference, Geneva, p. 199–422.

Bouma, A.H., 1982, Intraslope basins in northwest Gulf of Mexico: a key to ancient submarine canyons and fans: AAPG Memoir 34, p. 567–581.

Brown, L.F., and W.L. Fisher, 1977, Seismic-stratigraphic interpretation of depositional systems: examples from Brazilian rift and pull-apart basins, *in* C.E. Payton, ed., Seismic Stratigraphy—Applications to Hydrocarbon Exploration: AAPG Memoir 26, p. 213–248.

Bruce, C.H., 1973, Pressured shale and related sediment deformation: mechanism for development of regional contemporaneous faults: AAPG Bulletin, vol. 57, p. 878–886.

Buffler, R.T., 1991, Early evolution of the Gulf of Mexico basin, *in* D. Goldthwaite, ed., An Introduction to Central Gulf Coast Geology: New Orleans Geological Society, p. 1–16.

Coleman, J.M., and H.H. Roberts, 1991, Mississippi River depositional system: model for the Gulf Coast Tertiary, *in* D. Goldthwaite, ed., An Introduction to Central Gulf Coast Geology: New Orleans Geological Society, p. 99–121.

Creaney, S., and Q.R. Passey, 1993, Recurring patterns of total organic carbon and source rock quality within a sequence stratigraphic framework: AAPG Bulletin, vol. 77, p. 386–401.

Culver, S.J., 1988, New foraminiferal depth zonation of the northwestern Gulf of Mexico: Palaios, vol. 3, p. 69–85.

Dow, W.G., M.A. Yukler, J.T. Senftle, M.C. Kennicutt II, and J.M. Armentrout, 1990, Miocene oil source beds in the East Breaks basin, Flex-Trend, offshore Texas: Proceedings, Gulf Coast Section SEPM 9th Annual Research Conference, p. 139–150.

Feng, J.C., and E.W. Behrens, 1993, A comparison of Plio-Pleistocene to Recent sediment accumulation rates in the East Breaks area, northwestern Gulf of Mexico: Proceedings, Gulf Coast Section SEPM 14th Annual Research Conference, p. 115–125.

Fiduk, J.C., and E.W. Behrens, 1993, A comparison of Plio-Pleistocene to Recent sediment accumulation rates in the East Breaks area, northwestern Gulf of Mexico: Proceedings, Gulf Coast Section SEPM 14th Annual Research Conference, p. 41–55.

_____, _____, and R.T. Buffler, 1989, Distribution and movement of salt on the Texas–Louisiana continental slope, Garden Banks and eastern East Breaks areas, Gulf of Mexico: Proceedings, Gulf Coast Section SEPM 10th Annual Research Conference, p. 39–47.

References, continued

Frasier, D.E., 1974, Depositional episodes: their relationship to the Quaternary stratigraphic framework in the north-western portion of the Gulf basin: University of Texas at Austin, Bureau of Economic Geology Circular 74–1.

Galloway, W.E., 1989a, Genetic stratigraphic sequences in basin analysis I: architecture and genesis of flooding-surface bounded depositional units: AAPG Bulletin, vol. 73, p. 125–142.

_____, 1989b, Genetic stratigraphic sequences in basin analysis II: application to northwest Gulf of Mexico Cenozoic basin: AAPG Bulletin, vol. 73, p. 143–154.

_____, and T.A. McGilvery, 1995, Facies of a submarine canyon fill reservoir complex, lower Wilcox Group (Paleocene), central Texas coastal plain, *in* R.D. Winn, Jr., and J.M. Armentrout, eds., Turbidites and Associated Deep-Water Facies: WEPM Core Workshop 20, p. 1–23.

Gary, M., R. McAfee, Jr., and C.L. Wolf, 1974, Glossary of Geology: AGI, 805 p.

Goldthwaite, D., 1991, Central Gulf Coast stratigraphy, *in* D. Goldthwaite, ed., An Introduction to Central Gulf Coast Geology: New Orleans Geological Society, p. 17–30.

Golonka, J., M.I. Ross, and C.R. Scotese, 1993 , Phanerozoic paleogeographic and paleoclimatic modeling maps, *in* A.F. Embry, B. Beauchamp, and D.J. Glass, eds., Pangea—Global Environments and Resources: Canadian Society of Petroleum Geologists Memoir 17, p. 1–47.

Gross, O.P., K.C. Hood, L.M. Wenger, and S.C. Harrison, 1995, Seismic imaging and analysis of source and migration within an integrated hydrocarbon system study, northern Gulf of Mexico basin: Abstracts, 1st Latin American Geophysical Conference, p. 1–4.

Hall, D.J., B.E. Bowen, R.N. Rosen, S. Wu, and A.W. Bally, 1993, Mesozoic and early Cenozoic development of the Texas margin: a new integrated cross-section from the Cretaceous shelf edge to the Perdido fold belt: Selected Papers, Gulf Coast Section SEPM 13th Annual Research Conference, p. 21–31.

Hanor, J.S., and R. Sassen, 1990, Evidence for large-scale vertical and lateral migration of formation waters, dissolved salt, and crude oil in the Louisiana Gulf Coast: Proceedings, Gulf Coast Section SEPM 9th Annual Research Conference, p. 283–296.

Haq, B., J. Hardenbol, and P.R. Vail, 1988, Mesozoic and Cenozoic chronostratigraphy and cycles of sea-level change: SEPM Special Publication 42, p. 71–108.

Hedgpeth, J.W., 1957, Classification of marine environments: Geological Society of America Memoir 67, p. 17–27.

Herbin, J.P., J.L. Fernandez-Martinez, J.R. Geyssant, A.E. Albani, J.F. Deconinck, J.N. Proust, J.P. Colbeaux, and J.P. Vidier, 1995, Sequence stratigraphy of source rocks applied to the study of the Kimmeridgian/Tithonian in the North-West European shelf (Dorset/UK; Yorkshire/UK; Boulonnais/France): Marine and Petroleum Geology, vol. 12, no. 2, p. 177–194.

Ingram, R.J., 1991, Salt tectonics, *in* D. Goldthwaite, ed., An Introduction to Central Gulf Coast Geology: New Orleans Geological Society, p. 31–60.

Jackson, M.P.A., and W.E. Galloway, 1984, Structural and depositional styles of Gulf Coast Tertiary continental margins: applications to hydrocarbon exploration: AAPG Continuing Education Course Note Series 25, 226 p.

_____, D.G. Roberts, and J.S. Snelson, eds., 1995, Salt Tectonics: AAPG Memoir 65, 454 p.

Jervey, M.T., 1988, Quantitative geologic modeling of siliciclastic rock sequences and their seismic expression: SEPM Special Publication 42, p. 47–69.

Jones, J.O., and R.L. Freed, eds., 1996, Structural Framework of the Northern Gulf of Mexico: Gulf Coast Assoc. of Geological Sciences, 112 p.

Joyce, J.E., L.R.C. Tjalsma, and J.M. Prutzman, 1990, High-resolution planktic stable isotope record and spectral analysis for the last 5.35 myr: ODP site 625 northeast Gulf of Mexico: Paleoceanography, vol. 5, p. 507–529.

Kennett, J.P., K. Elmstrom, and N. Penrose, 1985, The last deglaciation in Orca basin, Gulf of Mexico: high-resolution planktonic foraminiferal changes: Palaeogeography, Palaeoclimatology, Palaeoecology, vol. 50, p. 189–216.

Kneller, B., 1995, Beyond the turbidite paradign: physical models for deposition of turbidites and their implications for reservoir prediction, *in* A.J. Hartley and D.J. Prosser, eds., Characterization of Deep Marine Clastic Systems: Geological Society, London, Special Publication 94, p. 31–49.

_____ and B. McCaffrey, 1995, Modelling the effects of salt-induced topography on deposition from turbidity currents, *in* C.J. Travis, H. Harrison, M.R. Hudec, B.C. Vendeville, F.J. Peel, and B.F. Perkins, eds., Salt, Sediment and Hydrocarbons: Gulf Coast Section SEPM Sixteenth Annual Research Conference, p. 137–145.

Kolb, C.R., and J.R. Van Lopik, 1958, Geology of the Mississippi River deltaic plain, southeastern Louisiana: U.S. Army Engineer Waterway Experiment Station, Corps of Engineers, Vicksburg, MS, Technical Report 3-483, 120 p.

Koyi, H., 1993, Modeling of segmentation and emplacement of salt sheets in anisotropic overburden: Selected Papers, Gulf Coast Section SEPM 13th Annual Research Conference, p. 135–142.

References, continued

Lamb, J.L., W.W. Warnardt, T.C. Huang, and T.E. Dube, 1987, Practical application of Pleistocene eustacy in offshore Gulf of Mexico, *in* R.A. Ross and D. Haman, eds., Timing and Depositional History of Eustatic Sequences: Constraints on Seismic Stratigraphy: Cushman Foundation for Foraminiferal Research Special Publication 24, p. 33–39.

Loucks, R.G., and J.F. Sarg, eds., 1993, Carbonate Sequence Stratigraphy: AAPG Memoir 57, 545 p.

Loutit, T.S., J. Hardenbol, P.R. Vail, and G.R. Baum, 1988, Condensed sections: the key to age determination and correlation of continental margin sequences: SEPM Special Publication 42, p. 183–213.

MacQueen, R.W., and D.A. Leckie, eds., 1992, Foreland Basins and Fold Belts: AAPG Memoir 55, 460 p.

Magoon, L.B., and W.G. Dow, 1994, The Petroleum System: AAPG Memoir 60, p. 3–24.

Martin, R.E., and R.R. Fletcher, 1993, Biostratigraphic expression of Plio–Pleistocene sequence boundaries, Gulf of Mexico: Proceedings, Gulf Coast Section SEPM 14th Annual Research Conference, p. 119–126.

_____, E.D. Neff, G.W. Johnson, and D.E. Krantz, 1990, Biostratigraphic expression of sequence boundaries in the Pleistocene: the Ericson and Wollin zonation revisited: Proceedings, Gulf Coast Section SEPM 11th Annual Research Conference, p. 229–236.

Marton, G., and R.T. Buffler, 1993, The southeastern Gulf of Mexico in the framework of the opening of the Gulf of Mexico basin: Selected Papers, Gulf Coast Section SEPM 13th Annual Research Conference, p. 127–139.

McGee, D.T., P.W. Bilinski, P.S. Gary, D.S. Pfeiffer, and J.L. Sheiman, 1994, Geologic models and reservoir geometries of Auger field, deepwater Gulf of Mexico: Proceedings, Gulf Coast Section SEPM 15th Annual Research Conference, p. 245–256.

McGuinness, D.B., and J.R. Hossack, 1993, The development of allochthonous salt sheets as controlled by the rates of extension, sedimentation, and salt supply: Proceedings, Gulf Coast Section SEPM 14th Annual Research Conference, p. 127–139.

Miall, A.D., 1994, Paleocene 16: sequence stratigraphy and chronostratigraphy—problems of definition and precision in correlation, and their implications for global eustasy: Geoscience Canada, vol. 21, no. 1, p. 1–26.

Mitchum, R.M., Jr., 1977, Seismic stratigraphy and global changes in sea level, II: Glossary of terms used in seismic stratigraphy, *in* Seismic Stratigraphy—Applications in Hydrocarbon Exploration: AAPG Memoir 26, p. 205–212.

_____, 1985, Seismic stratigraphic expression of submarine fans: AAPG Memoir 39, p. 117–136.

_____, and J.C. Van Wagoner, 1990, High-frequency sequences and eustatic cycles in the Gulf of Mexico basin: Proceedings, Gulf Coast Section SEPM 11th Annual Research Conference, p. 257–267.

_____, P.R. Vail, and J.B. Sangree, 1977, Stratigraphic interpretation of seismic reflection patterns in depositional sequences, *in* C.E. Payton, ed., Seismic Stratigraphy—Applications to Hydrocarbon Exploration: AAPG Memoir 26, p. 117–143.

Pacht, J.A., B.E. Bowen, J.H. Bearn, and B.L. Schaffer, 1990, Sequence stratigraphy of Plio–Pleistocene depositional facies in the offshore Louisiana south additions: Gulf Coast Assoc. of Geological Societies Transactions, vol. 40, p. 1–18.

Pflum, C.E., and W.E. Freichs, 1976, Gulf of Mexico deep water foraminifers: Cushman Foundation Foraminiferal Research Special Publication 14, 125 p.

Philippi, G.T., 1974, The influence of marine and terrestrial source material on the composition of petroleum: Geochim. Cosmochim. Acta, vol. 38., p. 947–966.

Piggott, N., and A. Pulham, 1993, Sedimentation rate as the control on hydrocarbon sourcing, generation, and migration in the deepwater Gulf of Mexico: Proceedings, Gulf Coast Section SEPM 14th Annual Research Conference, p. 179–191.

Pindell, J.L., 1993, Regional synopsis of Gulf of Mexico and Caribbean evolution: Proceedings, Gulf Coast Section SEPM 13th Annual Research Conference, p. 251–274.

Poag, C.W., 1981, Ecologic Atlas of Benthic Foraminifera of the Gulf of Mexico: Woods Hole Marine Science Institute, 174 p.

Posamentier, H.W., and P. Weimer, 1993, Siliciclastic sequence stratigraphy and petroleum geology: where to from here?: AAPG Bulletin, vol. 77, no. 5, p. 731–742.

_____ and P.R. Vail, 1988, Eustatic controls on clastic deposition II—sequence and systems tract models: SEPM Special Publication 42, p. 125–154.

_____, M.T. Jervey, and P.R. Vail, 1988, Eustatic controls on clastic deposition I—conceptual framework: an integrated approach: SEPM Special Publication 42, p. 109–124.

Prior, D.B., B.D. Bornhold, W.J. Wiseman, Jr., and D.R. Lowe, 1987, Turbidity current activity in a British Columbia fjord: Science, vol. 237, p. 1330–1333.

Prosser, 1993, Rift-related linked depositional systems and their seismic expression, *in* C.D. Williams and A. Dobb, eds., Tectonic and Seismic Sequence Stratigraphy: Geological Society Special Publication 71, p. 35–66.

References, continued

Rouch, L.S., J.M. Armentrout, and S.A. Bowman, 1993, Iterative analysis of depositional sequences: computer simulation of seismically defined geometries, south Galveston and East Breaks areas, Gulf of Mexico: Proceedings, Gulf Coast Section SEPM 14th Annual Research Conference, p. 195–207.

Sarg, J.F., 1988, Carbonate sequence stratigraphy: SEPM Special Publication 42, p. 155–181.

Sassen, R., R.S. Tye, E.W. Chinn, and R.C. Lemoine, 1988, Origin of crude oil in the Wilcox Trend of Louisiana and Mississippi: evidence of long range migration: Gulf Coast Assoc. Geological Societies Transactions, vol. 38, p. 27–34.

Schanck, J.W., C.C. Cobb, and M.L. Ivey, Jr., 1988, East Breaks 160 field on the offshore Texas shelf edge: a model for deepwater exploration and development: Proceedings, 20th Annual Offshore Technology Conference, p. 157–162.

Shaffer, B.L., 1987a, The potential of calcareous nannofossils for recognizing Plio–Pleistocene climatic cycles and sequence boundaries on the shelf: Proceedings, Gulf Coast Section SEPM 8th Annual Research Conference, p. 142–145.

_____, 1987b, The nature and significance of condensed sections in Gulf Coast late Neogene sequence stratigraphy: Gulf Coast Assoc. of Geological Societies and Gulf Coast Section SEPM Transactions, vol. 40, p. 767–776.

_____, 1990, The nature and significance of condensed sections in Gulf Coast late Neogene sequence stratigraphy: Gulf Coast Assoc. of Geological Societies Transactions, vol. 40, p. 186–195.

Simmons, G.R., W.R. Bryant, G. Lee, and C. Fiduk, 1996, Regional distribution of salt and basin architecture in the northwestern Gulf of Mexico, *in* J.O. Jones and R.L. Freed, eds., Structural Framework of the Northern Gulf of Mexico: Gulf Coast Assoc. of Geological Societies Special Publication, p. 93–94.

Steel, R.J., V.L. Felt, E.P. Johannessen, and C. Mathiew, eds., 1995, Sequence Stratigraphy on the Northwest European Margin: Elsevier, 608 p.

Sutter, J.S., and H.L. Berryhill, Jr., 1985, Late Quaternary shelf-margin deltas, northwest Gulf of Mexico: AAPG Bulletin, vol. 69, p. 77–91.

Taylor, G.S., and J.M. Armentrout, 1990, Rock geochemistry and relationships to produced oils from upper Pliocene turbidites, High Island area, Gulf of Mexico: Proceedings, Gulf Coast Section SEPM 9th Annual Research Conference, p. 151–161.

Tearpock, D.J., and R.E. Bischke, 1991, Applied Subsurface Geologic Mapping: Prentice-Hall, 648 p.

Thompson, K.F.M., 1987, Fractionated aromatic petroleums and the generation of gas-condensates: Organic Geochemistry, vol. 11, p. 573–590.

_____, M.C. Kennicutt II, and J.M. Brooks, 1990, Classification of offshore Gulf of Mexico oils and gas condensates: AAPG Bulletin, vol. 74, p. 187–198.

Tipsword, H.L.J., F.M. Setzer, and F.L. Smith, Jr., 1966, Interpretation of depositional environment in Gulf Coast exploration from paleoecology and related stratigraphy: Gulf Coast Assoc. of Geological Societies Transactions, vol. 16, p. 119–130.

Trippet, A.R., 1981, Characteristics of diapirs on the outer continental shelf–upper continental slope boundary, northwest Gulf of Mexico: Gulf Coast Assoc. of Geological Societies Transactions, vol. 31, p. 391–397.

Vail, P.R., 1987, Seismic stratigraphy interpretation procedure, *in* A.W. Bally, ed., Atlas of Seismic Stratigraphy: AAPG, p. 1–10.

_____ and R.G. Todd, 1981, North Sea Jurassic unconformities, chronostratigraphy and seal-level changes from seismic stratigraphy: Proceedings, Petroleum Geology of the Continental Shelf, Northwest Europe, p. 216–235.

_____ and W.W. Wornardt, 1990, Well log seismic stratigraphy: a new tool for exploration in the '90s: Proceedings, Gulf Coast Section SEPM 11th Annual Research Conference, p. 379–388.

_____, J. Hardenbol, and R.G. Todd, 1984, Jurassic unconformities, chronostratigraphy and sea-level changes from seismic stratigraphy and biostratigraphy, *in* J.S. Schlee, ed., Interregional Unconformities and Hydrocarbon Accumulation: AAPG Memoir 36, p. 129–144.

_____, R.G. Todd, and J.B. Sangree, 1977, Chronostratigraphic significance of seismic reflections, *in* C.E. Payton, ed., Seismic Stratigraphy—Applications to Hydrocarbon Exploration: AAPG Memoir 26, p. 99–116.

Van Wagoner, J.C., and G.T. Bertram, eds., 1995, Sequence Stratigraphy of Foreland Basin Deposits: AAPG Memoir 64, 487 p.

_____, R.M. Mitchum, P.R. Vail, J.F. Sarg, T.S. Loutit, and J. Hardenbol, 1990, Siliciclastic Sequence Stratigraphy in Well Logs, Cores, and Outcrops: AAPG Methods in Exporation Series 7, 55 p.

_____, H.W. Posamentier, R.M. Mitchum, P.R. Vail, J.F. Sarg, T.S. Loutit, and J. Hardenbol, 1988, An overview of the fundamentals of sequence stratigraphy and key definitions: an integrated approach: SEPM Special Publication 42, p. 39–45.

Visher, G.S., 1984, Exploration Stratigraphy: Tulsa, PennWell Books, 334 p.

Weimer, P., A.H. Bouma, and B.F. Perkins, eds., 1994, Submarine Fans and Turbidite Systems: Sequence Stratigraphy, Reservoir Architecture and Production Characteristics, Gulf of Mexico and International: Gulf Coast Section SEPM Foundation Fifteenth Annual Resesarch Conference Proceedings, 440 p.

References, continued

Weimer, P., 1990, Sequence stratigraphy, facies geometries, and depositional history of the Mississippi fan, Gulf of Mexico: AAPG Bulletin, vol. 74, p. 425–453.

West, D.B., 1989, Model for salt deformation on deep margin of central Gulf of Mexico basin: AAPG Bulletin, vol. 73, p. 1472–1482.

Wheeler, H.E., 1964, Base level, lithosphere surface, and time stratigraphy: GSA Bulletin, vol. 75, p. 599–610.

White, D.A., 1980, Assessing oil and gas plays in facies-cycles wedges: AAPG Bulletin, vol. 64, p. 1158–1178.

Williams, D.F., and D.M. Trainor, 1987, Integrated chemical stratigraphy of deep-water frontier areas of the northern Gulf of Mexico: Proceedings, Gulf Coast Section SEPM 8th Annual Research Conference, p. 151–158.

Winker, C.D., 1982, Cenozoic shelf margins, northwestern Gulf of mexico: Gulf Coast Assoc. of Geological Societies Transactions, vol. 32, p. 427–448.

_____, 1996, High-resolution seismic stratigraphy of a late Pleistocene submarine fan ponded by salt-withdrawl minibasins on the Gulf of Mexico contentental slope: Proceedings, Offshore Technology Conference, no. 38, vol. 1, p. 619–628.

_____ and R.T. Buffler, 1988, Paleogeographic evolution of the early deep-water Gulf of Mexico and its margins, Jurassic to middle Cretaceous (Comanchean): AAPG Bulletin, vol. 72, p. 318–346.

_____ and M.B. Edwards, 1983, Unstable progradational clastic shelf margins: SEPM Special Publication 33, p. 139–157.

Winn, R.D., and J.M. Armentrout, eds., 1995, Turbidites and Associated Deep-water Facies: SEPM Core Workshop 20, 176 p.

Woodbury, H.O., I.B. Murray, P.J. Pickford, and W.H. Akers, 1973, Pliocene and Pleistocene depocenters, outer continental shelf, Louisiana and Texas: AAPG Bulletin, vol. 57, p. 2428–2439.

Wornardt, W.W., Jr., and P.R. Vail, 1990, Revisions of the Plio–Pleistocene cycles and their application to sequence stratigraphy of shelf and slope sediments in the Gulf of Mexico: Proceedings, Gulf Coast Section SEPM 12th Annual Research Conference, p. 391–397.

References, continued

Acknowledgments The author is indebted to several former and present co-workers at Mobil who shared their insight about the Gulf of Mexico. Tom Crutcher and Gil Taylor provided the initial orientation and demonstrated the power of data integration. Tom Lee, Jerry Ragan, Rick Becker, and Ron Echols helped clarify the utility of the fossil record. And George Gail provided astute observations about the petroleum systems. These people, many of the workers cited, all of the papers cited, and the overwhelming number of papers not cited but used over the years provided the basis for this chapter. The use of that information is entirely the responsibility of the author.

Special thanks is due to Ted Beaumont for the invitation to contribute to the volume and for his patience through three rewrites as we adapted a more traditional text to the information mapping format. The initial draft was reviewed and improved thanks to Ron Echols, Vivian Hussey, and George Gail. This final manuscript benefited significantly from reviews by Les Magoon, George Gail, Ron Echols, Ken Tillman, Arlene Anderson, Kris Meisling, Alan Cunningham, and Ted Beaumont. The figures were drafted by Greg Dill and David Helber. Mobil Exploration and Producing Technical Center Inc. approved publication of the paper, and TGS-Calibre Geophysical Company authorized inclusion of the seismic reflection profiles.